

REPORT DOCUMENTATION PAGE			Form Approved OMB NO. 0704-0188		
<p>The public reporting burden for this collection of information is estimated to average 1 hour per response, including the time for reviewing instructions, searching existing data sources, gathering and maintaining the data needed, and completing and reviewing the collection of information. Send comments regarding this burden estimate or any other aspect of this collection of information, including suggestions for reducing this burden, to Washington Headquarters Services, Directorate for Information Operations and Reports, 1215 Jefferson Davis Highway, Suite 1204, Arlington VA, 22202-4302. Respondents should be aware that notwithstanding any other provision of law, no person shall be subject to any penalty for failing to comply with a collection of information if it does not display a currently valid OMB control number.</p> <p>PLEASE DO NOT RETURN YOUR FORM TO THE ABOVE ADDRESS.</p>					
1. REPORT DATE (DD-MM-YYYY) 02-10-2014		2. REPORT TYPE Ph.D. Dissertation		3. DATES COVERED (From - To) -	
4. TITLE AND SUBTITLE Runtime Systems for Extreme Scale Platforms			5a. CONTRACT NUMBER W911NF-13-1-0098		
			5b. GRANT NUMBER		
			5c. PROGRAM ELEMENT NUMBER		
6. AUTHORS Sanjay Chatterjee			5d. PROJECT NUMBER		
			5e. TASK NUMBER		
			5f. WORK UNIT NUMBER		
7. PERFORMING ORGANIZATION NAMES AND ADDRESSES William Marsh Rice University 6100 Main St., MS-16 Houston, TX 77005 -1827			8. PERFORMING ORGANIZATION REPORT NUMBER		
9. SPONSORING/MONITORING AGENCY NAME(S) AND ADDRESS (ES) U.S. Army Research Office P.O. Box 12211 Research Triangle Park, NC 27709-2211			10. SPONSOR/MONITOR'S ACRONYM(S) ARO		
			11. SPONSOR/MONITOR'S REPORT NUMBER(S) 63302-CS-ACI.2		
12. DISTRIBUTION AVAILABILITY STATEMENT Approved for public release; distribution is unlimited.					
13. SUPPLEMENTARY NOTES The views, opinions and/or findings contained in this report are those of the author(s) and should not be construed as an official Department of the Army position, policy or decision, unless so designated by other documentation.					
14. ABSTRACT Future extreme-scale systems are expected to contain homogeneous and heterogeneous many-core processors, with O(103) cores per node and O(106) nodes overall. Effective combination of inter-node and intra-node parallelism is recognized to be a major software challenge for such systems. Further, applications will have to deal with constrained energy budgets as well as frequent faults and failures. To aid programmers manage these complexities and enhance programmability, much of recent research has focussed on designing state-of-art software runtime systems. Such runtime systems are expected to be a critical component of the software ecosystem for the					
15. SUBJECT TERMS dynamic task parallelism, locality control					
16. SECURITY CLASSIFICATION OF:			17. LIMITATION OF ABSTRACT UU	15. NUMBER OF PAGES	19a. NAME OF RESPONSIBLE PERSON Vivek Sarkar
a. REPORT UU	b. ABSTRACT UU	c. THIS PAGE UU			19b. TELEPHONE NUMBER 713-348-5304

Report Title

Runtime Systems for Extreme Scale Platforms

ABSTRACT

Future extreme-scale systems are expected to contain homogeneous and heterogeneous many-core processors, with $O(10^3)$ cores per node and $O(10^6)$ nodes overall. Effective combination of inter-node and intra-node parallelism is recognized to be a major software challenge for such systems. Further, applications will have to deal with constrained energy budgets as well as frequent faults and failures. To aid programmers manage these complexities and enhance programmability, much of recent research has focussed on designing state-of-art software runtime systems. Such runtime systems are expected to be a critical component of the software ecosystem for the management of parallelism, locality, load balancing, energy and resilience on extreme-scale systems.

In this dissertation, we address three key challenges faced by a runtime system using a dynamic task parallel framework for extreme-scale computing. First, we address the challenge of integrating an intra-node task parallel runtime with a communication system for scalable performance. We present a runtime communication system, called HC-COMM, designed to use dedicated communication cores on a system. We introduce the HCMPI programming model which integrates the Habanero-C asynchronous dynamic task parallel language with the MPI message passing communication model on the HC-COMM runtime. We also introduce the HAPGNS model that enables data flow programming for extreme-scale systems in which the user does not require knowledge of MPI. Second, we address the challenge of separating locality optimizations from a programmer with domain specific knowledge. We present a tuning framework, through which performance experts can optimize existing applications by specifying runtime operations aimed at co-scheduling of affinitized tasks. Finally, we address the challenge of scalable synchronization for long running tasks on a dynamic task parallel runtime. We use the phaser construct to present a generalized tree-based synchronization algorithm and support unified collective operations at both inter-node and intra-node levels. Overcoming these runtime challenges are a first step towards effective programming on extreme-scale systems.

RICE UNIVERSITY

Runtime Systems for Extreme Scale Platforms

by

Sanjay Chatterjee

A THESIS SUBMITTED
IN PARTIAL FULFILLMENT OF THE
REQUIREMENTS FOR THE DEGREE

Doctor of Philosophy

APPROVED, THESIS COMMITTEE:

Vivek Sarkar, Chair
E.D. Butcher Chair in Engineering
Professor of Computer Science

John Mellor-Crummey
Professor of Computer Science

Lin Zhong
Associate Professor of Electrical and
Computer Engineering

Zoran Budimlic
Research Scientist

Houston, Texas

December, 2013

ABSTRACT

Runtime Systems for Extreme Scale Platforms

by

Sanjay Chatterjee

Future extreme-scale systems are expected to contain homogeneous and heterogeneous many-core processors, with $O(10^3)$ cores per node and $O(10^6)$ nodes overall. Effective combination of inter-node and intra-node parallelism is recognized to be a major software challenge for such systems. Further, applications will have to deal with constrained energy budgets as well as frequent faults and failures. To aid programmers manage these complexities and enhance programmability, much of recent research has focussed on designing state-of-art software runtime systems. Such runtime systems are expected to be a critical component of the software ecosystem for the management of parallelism, locality, load balancing, energy and resilience on extreme-scale systems.

In this dissertation, we address three key challenges faced by a runtime system using a dynamic task parallel framework for extreme-scale computing. First, we address the challenge of integrating an intra-node task parallel runtime with a communication system for scalable performance. We present a runtime communication system, called HC-COMM, designed to use dedicated communication cores on a system. We introduce the HCMPI programming model which integrates the Habanero-C asynchronous dynamic task parallel language with the MPI message passing communication model on the HC-COMM runtime. We also introduce the HAPGNS model that enables data

flow programming for extreme-scale systems in which the user does not require knowledge of MPI. Second, we address the challenge of separating locality optimizations from a programmer with domain specific knowledge. We present a *tuning* framework, through which performance experts can optimize existing applications by specifying runtime operations aimed at co-scheduling of affinitized tasks. Finally, we address the challenge of scalable synchronization for long running tasks on a dynamic task parallel runtime. We use the **phaser** construct to present a generalized tree-based synchronization algorithm and support unified collective operations at both inter-node and intra-node levels. Overcoming these runtime challenges are a first step towards effective programming on extreme-scale systems.

Acknowledgments

It was an honor and a gift to have had Prof. Vivek Sarkar as my PhD advisor. Working with him has been a truly great learning experience for me. He is one of most brilliant and knowledgeable researchers I have known, and yet he is a lesson in humility and generosity. He participated in my research with great enthusiasm and his guidance was critical for constructing my dissertation. His faith and confidence in my work encouraged me to pursue exploratory research on diverse topics. He always made himself available for discussions and even patiently sat through many Sunday afternoons providing critical assessment of my blue-sky ideas. I am really thankful for his support throughout my PhD years, through thick and thin, both academic and personal, and when everything just seemed piled higher and deeper. He inspires me to be a better human being, and that, in my eyes, makes him the *complete* advisor.

I would like to express my gratitude to Prof. John Mellor-Crummey for agreeing to be on my thesis committee and supporting my research work by providing access to the Jaguar supercomputer at Oak Ridge National Labs. The experimental results on Jaguar are the cornerstone of my thesis and this dissertation would have been incomplete without his help. I am really thankful for his detailed feedback on my dissertation drafts which helped improve my writeup manyfold. I have also greatly enjoyed being part of two parallel computing courses taught by John. I gained deep insight into the nuances of dealing with concurrency issues and they helped me greatly in constructing the runtime algorithms and data structures in this dissertation.

I would like to sincerely thank Prof. Lin Zhong for agreeing to be on my thesis committee. His insights and feedback were very important in shaping my thesis and helped me to keep the broader picture in mind for my dissertation.

I am grateful to Zoran Budimlić for agreeing to be on my thesis committee. I worked with Zoran almost on a day-to-day basis during my PhD. He is always up for quick chats, hallway discussions and deep dive meetings. I have greatly enjoyed interacting with him and am really thankful for his technical contributions to my research work.

I would like to thank Kath Knobe of Intel for inspiring my work on the *tuning* framework. I remember meeting Kath at Intel during my internship at Hillsboro where she was presenting her ideas on tuning. I spoke to her about similar ideas and we started collaborating after I returned to Rice.

I would like to thank all Habanero group members, both past and present, for helping me with discussions, feedback and insights related my work. Specifically, I would like to thank Max Grossman for our collaboration on numerous topics, and Vincent Cavé for many technical discussions, code reviews and helping with experimental results on many projects. I would also like to thank Jun Shirako for helping me with the *phaser* discussions, and Yonghong Yan for setting up much of the runtime infrastructure. I am thankful to Sağnak Taşlılar and Milind Chabbi for painstakingly collecting results which have greatly helped this dissertation. I will always be grateful to Raghavan Raman for introducing me to my advisor and helping me with my application process. I would like to thank all the wonderful office administration staff in the Computer Science department for making sure my life went smoothly, and Ratna Sarkar for graciously hosting the Habanero group members on many occasions.

I would like to thank my friends who have helped me remain sane during my PhD. I want to particularly thank my friend Pratim Chowdhury for being an immense support during the last few months before graduation.

Finally, I am ever thankful to my wonderful and supportive family. I cannot imagine my PhD years without their help. My parents have always motivated me with their great enthusiasm and respect for higher education. To this day, their belief in me inspires me to overcome the greatest of challenges in my life. My wife, Sucharita, has been my best friend and greatest source of strength during my PhD years with her unfathomable love and immense sacrifice. The happiest moment of my life arrived when our daughter, Anousha, was born. I feel so proud to have shared my PhD journey with my family and so I end with the following dedication.

To my mother, Ranu

To my father, Sanjiban

To my sister, Srimoyee

To my daughter, Anousha

To my beloved wife and my greatest strength, Sucharita

Contents

Abstract	ii
List of Illustrations	x
List of Tables	xiii
1 Introduction	1
1.1 Thesis Statement	7
1.2 Organization of this Dissertation	8
2 Related Work	10
3 Background	23
3.1 Dynamic Task Parallelism	23
3.2 Habanero-C: Intra-node Task Parallelism	27
3.2.1 HC Task Model	27
3.2.2 HC Data Driven Task Model	30
3.2.3 HC Runtime	31
4 Habanero-C Runtime Communication System	35
4.1 HCMPI Programming Model	38
4.1.1 HCMPI Structured Communication Task Model	41
4.1.2 HCMPI Message Driven Task Model	42
4.1.3 HCMPI Implementation for MPI Blocking Semantics	43
4.1.4 HCMPI Collective Synchronization Model	45
4.2 HC-COMM Runtime Implementation	46

4.3	Results	51
4.3.1	Micro-benchmark Experiments	51
4.3.2	UTS Case Study:	55
4.4	Summary	68
5	Locality Control of Compute and Data	69
5.1	Research Contributions	70
5.2	The Habanero Asynchronous Partitioned Global Name Space Model .	71
5.2.1	HAPGNS Programming Model	72
5.2.2	Implementation	75
5.2.3	Results	77
5.3	Habanero-C Tuning Framework	79
5.3.1	Hierarchical Place Trees for Spatial Locality	80
5.3.2	Tuning Framework for Spatio-Temporal Task Locality	83
5.3.3	HPT Implementation	86
5.3.4	Tuning Tree Implementation	93
5.3.5	Results	95
5.4	Summary	107
6	Task Synchronization for Iterative Computation	108
6.1	Past Work on Phaser Synchronization Model	110
6.1.1	Phaser Programming Model in HJ	111
6.1.2	Hierarchical Phasers for Tree-based Barriers in HJ	116
6.1.3	Phaser Implementation in HJ	119
6.2	Research Contributions	121
6.3	Phasers for Multicore Synchronization	122
6.3.1	Programming Model for Habanero-C	122
6.3.2	Phaser Data Structure	124
6.3.3	A Generalized Tree-based Phaser Synchronization Algorithm .	128

6.3.4	Results	140
6.4	Phasers for Manycore Synchronization	144
6.4.1	Optimization Using Hardware Barriers	145
6.4.2	Optimization Using Thread Suspend and Awake	146
6.4.3	Adaptive Phasers	147
6.4.4	Memory Optimizations	148
6.4.5	Results	148
6.5	Phasers for Hybrid Synchronization	151
6.5.1	Implementation	153
6.5.2	Results	155
6.6	Summary	157
7	Conclusions	159
	Bibliography	163

Illustrations

3.1	An example code schema with <code>async</code> and <code>finish</code> constructs	28
3.2	Task parallel programming using <code>async</code> and <code>finish</code> ¹	29
3.3	Deque operations for a workstealing runtime	33
4.1	HCMPI Structured Communication Tasks: Starting asynchronous communication and waiting for its completion.	42
4.2	HCMPI Await Model	43
4.3	Using the <code>finish</code> construct in HCMPI. A <code>finish</code> around <code>HCMPI_Irecv</code> , a non-blocking call, implements <code>HCMPI_Recv</code> , a blocking call.	44
4.4	HCMPI Wait and Status Model	45
4.5	HCMPI Barrier Model	46
4.6	The HC-COMM Intra-node Runtime System	47
4.7	Lifecycle of a Communication Task	48
4.8	HC-COMM DDF Runtime	49
4.9	Thread Micro-benchmarks for MVAPICH2 on Rice DAVinCI cluster with Infiniband interconnect	53
4.10	Thread Micro-benchmarks for MPICH2 on Jaguar Cray XK6 with Gemini interconnect	54
4.11	Scaling of UTS on MPI.	59
4.12	Scaling of UTS on HCMPI.	60
4.13	HCMPI speedup compared to MPI	61

4.14	HCMPI speedup compared to MPI on UTS T3XXL with extra communication worker	62
4.15	HCMPI Speedup compared to MPI+OpenMP on UTS T1XXL	66
5.1	Simplified Smith-Waterman implementation	74
5.2	Smith-Waterman dependency graph, its hierarchical tiling and execution wavefronts	75
5.3	Scaling results for Smith-Waterman for 8 to 96 nodes with 2 to 12 cores	78
5.4	An example HPT structure	82
5.5	Tuning tree of queues matches the target platform structure	84
5.6	Tuning action to unpack a group and move down the steps	86
5.7	An example of a HPT XML description	87
5.8	Bucket deque expansion	90
5.9	Bucket deque reuse after contraction	91
5.10	Releasing steps from tuning tree to domain tree	93
5.11	Cholesky decomposition dependences	96
5.12	Cholesky decomposition execution times for various tile sizes	97
5.13	Tuning actions on GroupC, the outer level group in Cholesky	100
5.14	Set1 Cholesky Tuning experiments on 2000 x 2000 matrix	101
5.15	Set2 Cholesky Tuning experiments on 6000 x 6000 matrix	101
5.16	Rician denoising dependencies	103
5.17	Grouped rician denoising steps	103
5.18	Pyramid computation for tiles in successive iterations	104
5.19	Rician Denoising performance comparison of untuned vs tuned	104
6.1	Phaser Mode Lattice	111
6.2	Semantics of synchronization operation	111
6.3	Single-level phaser with single master	117

6.4	Hierarchical phaser with sub-masters	118
6.5	Data structures for flat phaser	119
6.6	Data structures for tree phaser	120
6.7	Barrier Example	124
6.8	Generalized Phaser Tree Data Structure (Degree = 2)	125
6.9	Barrier Synchronization on x86 node	141
6.10	Barrier Synchronization on Power7 node	142
6.11	Phaser barrier overhead on a dual-CPU Niagara T2 machine	143
6.12	Cyclops64 Architecture Details	144
6.13	SRAM optimization for phasers on Cyclops64	149
6.14	Barrier and Point-to-Point Microbenchmarks	150
6.15	HCMPI Phaser Barrier Model	152
6.16	HCMPI Phaser Accumulator Model	154
6.17	HCMPI Phaser Barrier	155

Tables

1.1	The exascale challenge	2
4.1	HCMPI Types	39
4.2	HCMPI API for point-to-point and collective communication	40
4.3	HCMPI Runtime API	41
4.4	Best UTS configurations on Jaguar for 64 compute nodes	57
4.5	UTS overhead analysis for T1XXL runs on Jaguar	63
6.1	Semantics of phaser operations as a function of registration mode on <i>ph</i>	114
6.2	Cyclops64 TNT APIs for Hardware Synchronization Primitives	145
6.3	HCMPI PHASER API	151
6.4	HCMPI Ops	153
6.5	EPCC Syncbench with MVAPICH2 on Infiniband	157

List of Algorithms

1	Push operation for resizable dequeues	92
2	PhaserRegistration	129
3	InsertSigIntoPhaserTree	131
4	FixSubPhaser	132
5	PhaserSignal	134
6	PhaserWait	135
7	doWaitTree	136
8	doWaitNode	136
9	doWaitPhaser	137
10	PhaserDropSig	139

Chapter 1

Introduction

As we head towards exascale computing, future software technology needs to embrace systems using homogeneous and heterogeneous many-core processors [1]. Based on the design targets from the exascale challenge program by DARPA [2] shown in Table 1.1, future extreme-scale systems are projected to use up to $O(10^3)$ processor cores per compute node and $O(10^6)$ nodes overall. The primary software challenges on such systems are to efficiently express and manage large scales of parallelism of variable granularity (to address platform heterogeneity) on constrained energy budgets and being resilient to faults and failures. The performance of these systems will heavily depend on the entire software stack, spanning programming models, languages, compilers, runtime systems and operating systems. It is critical to find software solutions that can effectively exploit the extreme-scale of combined inter-node and intra-node parallelism. Current state-of-the-art techniques that combine distributed- and shared-memory programming models, have demonstrated the potential benefits of combining both levels of parallelism, including increased communication-computation overlap, improved memory utilization, and effective use of accelerators. However, these *hybrid* programming approaches often require significant rewrites of application code and assume a high level of programmer expertise.

One popular direction is to integrate asynchronous task parallelism with a Partitioned Global Address Space (PGAS) [3] model as exemplified by the DARPA HPCS programming languages (Chapel [4] and X10 [5]), and by recent multithreading ex-

Systems	2015	2018
System Peak Flops	100-200 Peta	1 Exa
System Memory	5 PB	10 PB
Node Performance	400 GF	1-10 TF
Node Memory Bandwidth	100 GB/s	200-400 GB/s
Interconnect Bandwidth	25 GB/s	50 GB/s
Node Concurrency	O(100)	O(1000)
System Size (Nodes)	500000	O(Million)
Total Concurrency	50 Million	O(Billion)
Storage	150 PB	300 PB
I / O	10 TB/s	20 TB/s
Power	10 MW	20 MW

Table 1.1 : The exascale challenge

tensions to established PGAS languages (UPC [6] and CAF [7]). PGAS programming models offer HPC programmers a single-level partition of a global address space with control of data-to-thread affinity/locality. In contrast, the Message Passing Interface (MPI) [8] still provides an effective path for implementing the majority of applications on the largest supercomputers in the world. Although it has been shown that there are certain classes of applications for which the PGAS models are superior, many challenges still remain for the PGAS languages to catch up with MPI in supporting these applications due to the overheads associated with maintaining a global address space, as well as the software engineering challenges of migrating MPI-based codes to PGAS. On the other hand, harnessing $O(10^3)$ -way parallelism at the intra-node

level will be a major challenge for both MPI and PGAS programmers, for multiple reasons. The parallelism will have to exploit strong rather than weak scaling, since the memory per node is not increasing at the same rate as the number of cores per node. Finally, programs will have to be amenable to dynamic adaptive scheduling techniques to deal with heterogeneous processors, non-uniform clock speeds and other load imbalances across cores due to power management, fault tolerance, and other runtime services.

Dynamic task parallelism is one model that is well suited to addressing these imbalances at the intra-node level. It is now recognized as a programming model that combines the best of performance and programmability for shared-memory computations. Dynamic task parallel languages, such as Habanero-C [9], Cilk [10] and X10 [5], can express fine-grained parallelism with the help of lightweight tasks and are assisted by efficient load balancing runtime systems for achieving scalable performance. The runtimes typically depend on hardware support for fast atomic operations to implement high frequency task load-balancing operations on shared-memory multicore systems. While recent MPI [8] standards have made provisions for remote atomic communication calls, such as `MPI_COMPARE_AND_SWAP`, it is infeasible to replicate the current shared-memory runtime model at the inter-node level because the latency of load balancing operations will be prohibitively high at the inter-node level. Further, whereas in a shared-memory multithreaded work-stealing runtime, a thief does not interrupt the work of the victim during a steal operation, distributed work-stealing usually requires victim participation. Future runtimes will need specific hardware and software support to address these problems.

In our work, we focus on the critical role played by the runtime system in enabling programmability in upper layers of the software stack that interface with the

programmer, and in enabling performance in lower levels of the software stack that interface with the hardware. The scope of our research can be broadly classified into three specific areas where the runtime system will have a major impact on the performance.

- Designing scalable runtime communication systems
- Enabling locality control of compute and data at runtime
- Efficient synchronization for iterative computations in long running tasks

This work builds on the Habanero-C (HC) language [9, 11] which provides dynamic asynchronous task parallelism support with the `async` and `finish` constructs on a shared-memory platform. We have implemented the `phaser` task synchronization construct and the Hierarchical Place Tree (HPT) model in HC, based on past work [12, 13]. A `phaser` is a unification of point-to-point and collective task synchronization. It is an efficient synchronization model for applications with long running synchronized tasks. A HPT is a user defined runtime data structure that allows tasks to be scheduled with affinity towards a core or set of cores. The affinity is modeled as a tree of *places* which typically represent the memory hierarchy of the system and the runtime executes tasks which are closer in the hierarchy first before going further out. This allows the user to execute parallel tasks which share data access to benefit from spatial locality at some level of the memory hierarchy.

We have integrated the intra-node HC model with a communication layer (currently MPI), to create a runtime execution model for distributed systems, called HC-COMM. Our goal is to ensure scalable performance on extreme-scale systems along with easy portability of existing applications and enhanced programmability for future applications. The HCMPI (Habanero-C MPI) programming model, offers

a practical approach for programmers wanting to take incremental transitional steps starting from either a shared- or distributed-memory program. It is a unified programming model for shared and distributed memory systems with integrated support for asynchronous intra-node tasking and asynchronous inter-node communication using the MPI message passing interface. All MPI calls are treated as asynchronous tasks, thereby enabling unified handling of messages and tasking constructs. Point-to-point communication tasks can be offloaded from the computation task’s critical path. System-wide collective synchronization is achieved with integrated task- and process-level collective synchronization using **phaser** primitives. We achieve our portability goals by providing easy transitional steps for introducing shared-memory task parallelism to sequential MPI programs, or for introducing MPI calls to shared-memory task parallel programs.

We also introduce **HAPGNS** (Habanero Asynchronous Partitioned Global Name Space) as a distributed data-driven programming model that integrates intra-node and inter-node data-flow programming. This model does not require any knowledge of MPI. In this model, producer and consumer tasks, called data-driven tasks, communicate data using **put** and **get** operations. Consumer tasks specify the set of data dependences using distributed data driven future (DDDF) objects. A DDDF object carries a globally unique identifier which helps tasks to communicate data in a global name space.

The **HC-COMM** runtime design uses dedicated communication cores on the system. Our approach is motivated in part by the fact that future extreme scale systems, driven by a limited power budget, will have reduced shared-memory capacities, leading to an increased focus on efficient communication. For applications, this translates to exploiting overlaps between computation and communication for improved per-

formance. Our design is based on the premise that it will be feasible to dedicate one or more cores per node to serve as *communication workers* in future many-core architectures. Thus, a program’s workload can be divided into computation and communication tasks that run on computation and communication workers respectively. Our experimental results show that even for today’s multicore architectures, the benefits of a dedicated communication worker can outweigh the loss of a computation resource. Further, the foundational synchronization constructs in our programming model such as **finish**, **phaser** and **await** can be applied uniformly to computation tasks and communication tasks.

We propose data locality optimization techniques at both inter-node and intra-node level. Locality aware distribution functions in the **HAPGNS** model control inter-node data locality. Within a node, programs can benefit from spatial and temporal data reuse at cache hierarchies with the help of the **HPT** runtime data structure. We have designed a *tuning* framework which can enable performance experts, to contribute performance improvements via tuning operations on existing applications. Tuning experts with detailed knowledge of a machine’s characteristics can guide or tune an application’s schedule at runtime using a set of API functions. The tuning framework layer, which is an abstraction on top of the task execution runtime, is able to dynamically decide where to execute a task. This decision power enables the tuning expert to co-locate tasks that will benefit from spatial and/or temporal data reuse.

An **HCMP**I program follows a task parallel model within a node and a **SPMD** model across nodes. It supports many commonly-used synchronous, asynchronous and collective **MPI** operations. We present a synchronization scheme for combined inter-node and intra-node collective operations using the **phaser** model.

1.1 Thesis Statement

Programming extreme-scale platforms can be aided by a unified runtime system that combines inter-node communication with intra-node computation, extends work-stealing schedulers with hierarchies and affinities for locality, and supports scalable synchronization primitives for long running iterative tasks.

Runtime systems are expected to have a major impact on the performance of extreme-scale systems. They play a critical role in enabling high performance, programmability, and productivity for dynamic task parallel systems on shared-memory platforms. Runtime systems that support dynamic task parallelism have demonstrated scalable performance for shared-memory programs. However, using such runtimes for extreme-scale computing throw up few key challenges.

First, a scalable runtime communication system will be a key enabler for extreme-scale computing. The runtime should leverage benefits of asynchronous dynamic task parallel programming models, as well as the scalability of popular communication models. It has to overlap communication with computation as well as manage contention on the communication sub-system.

Second, locality of computation and data is critical for performance and lower energy resulting from data reuse on faster memories and redundant communication avoidance. The runtime has to leverage both spatial and temporal locality of compute and data. A programmer should be able to express affinities between task computations and associated data to help the runtime make locality guided scheduling decisions. Abstracting the hardware characteristics with an appropriate machine model will also help the runtime in making intelligent scheduling decisions.

Third, efficient synchronization models for iterative computations in long running

tasks will be an important scalability requirement for task parallelism. The model should support the expression of various synchronization patterns. The runtime system should enable collective synchronization across compute nodes with unified primitives at intra-node and inter-node levels, as well as leverage hardware support when available.

Runtime support for scalable locality aware task scheduling and synchronization at both intra-node and inter-node levels are key requirements for extreme-scale computing. Addressing these challenges will lead us to tackle further issues in future such as managing heterogeneity, energy efficiency and resiliency.

1.2 Organization of this Dissertation

The rest of this dissertation is organized as follows.

- Chapter 2 summarizes related work in this area, and compares the results and approaches in this dissertation with past work.
- Chapter 3 introduces the Habanero-C research language which forms the background to our work. In this chapter, we also explain the intra-node implementations of the Habanero-C dynamic task parallel runtime.
- Chapter 4 presents the HC-COMM runtime communication system and the HCMPI programming model. We present experimental results on current large scale systems that validate the design of our runtime system for extreme-scale computing.
- Chapter 5 describes the locality control framework for computation and data. We present the HAPGNS programming model that supports user directed data

distribution functions. We provide examples and results to demonstrate the efficacy of our approach. This chapter also describes the design and implementation of the Habanero-C locality tuning framework. Our experimental results show improvements on current optimized implementations of important applications.

- Chapter 6 describes the design and implementation of **phaser** synchronization for the Habanero-C language. We present a tree based intra-node synchronization algorithm with applicability to both barriers and point-to-point synchronization modes. We show extensions of the **phaser** barrier model for inter-node synchronization. We also present a **phaser** design that can adapt at runtime to leverage hardware support for synchronization.
- Chapter 7 presents our conclusions. We review the approaches and results of our research.

Chapter 2

Related Work

The computing landscape has undergone a shift from the sequential von Neumann execution model to a parallel computing model. Increasing single-thread performance as a direct outcome of higher clock frequencies is no longer feasible due to power and energy constraints. Subsequently, the focus has shifted to exploiting parallelism at the multiprocessor-level as a practical approach for improving performance. We have witnessed a surge of multicore processors across all computing platforms ranging from HPC systems to desktops, and in some cases to mobile and embedded systems as well. As a result, in a fundamental paradigm shift, software technology has now become the driver of system performance due to its role in exposing the parallelism inside application programs. There has been much research in the recent past related to programming systems for such platforms, and in this chapter, we shall review some of the important related work in this area.

Parallel computers of the past relied on an interconnection of high performance serial processors. With the advent of ubiquitous tightly coupled multicore processors with memory hierarchies consisting of shared levels of caches, it has become necessary to develop novel software strategies to take advantage of the benefits shared-memory intra-node parallelism. The evolution of programming systems has created a multi-dimensional view of the software technology necessary to program a combination of inter-node and intra-node parallelism. Choice of the programming model, the execution model, the view of memory, the communication model, the synchronization

model, and the locality/affinity control model for compute and data are some of the key design parameters for these programming systems. Designers of software technology for such systems are faced with distinct parallel programming questions.

- What is the parallel control model?
- What is the model for sharing and communication?
- What are the synchronization models and how to avoid their overheads?

The popular parallel control models of today can be classified into the data parallel model with a single thread of control, the dynamic thread model and the single program multiple data (SPMD) model. Data parallelism emphasizes the distributed nature of the data and has been shown to scale on large number of parallel processors when the application is regular. The dynamic thread model allows creation of parallel computation at runtime with relatively low overhead and is best geared towards handling imbalances in the system resulting from workloads, heterogeneity, non-uniform clock speeds and failures. The SPMD model emphasizes the distributed nature of both compute and data where the total amount of available parallelism is fixed and parallel tasks typically communicate using message passing techniques. SPMD models are the most popular models for current distributed systems, because it has the lowest overhead of the three (but not the most generality).

The sharing and communication models are primarily of two kinds, the load / store model for global shared address spaces and the message passing model for distributed address spaces. All global shared address spaces are implemented by a communication layer which abstracts the physical distributed memory from the user and presents a view of shared memory to the program. Although there is an additional overhead

associated with the extra communication layer, programmers have found this to be a more elegant and productive alternative to dealing with physical distributed memory.

Traditional synchronization models include collective operations (such as barriers and reductions) [14, 15, 16, 17, 18], and point-to-point operations (such as busy-waiting on flags, semaphores, data flow synchronization and directed communication messages) [19, 20, 21]. *Futures* [22, 23] are an embodiment of the data flow dependence model. A future is a data object passed from the producer to the consumer to serve as the value of computation performed in a future order of evaluation. These synchronization operations vary in the degree of asynchrony supported in the participating tasks. Task data flow is an example of a model that is inherently asynchronous. Asynchronous collectives such as barriers and reductions are now finding wide adoption through popular standards such as MPI [8]. Task termination constructs such as X10’s *finish* [24] and Chapel’s *sync* [25] are collective synchronization models that overlap computation and communication through the use of continuation tasks. (A continuation [26] refers to the computation context required for a task to start execution at a certain point in the program.)

One of the most popular programming models for distributed memory systems is the Message Passing Interface (MPI) [27]. MPI is a standard specification [8] for a library interface for which there exists multiple implementations. The computation in a MPI program is distributed among processes, known as ranks. Processes maintain their own local memory and communicate data as messages. MPI’s point-to-point (P2P) model of message passing is a two sided model, with a sender and receiver process. There is also support for collective synchronization primitives and more recently for distributed atomics [8]. MPI supports communication and computation overlap through asynchronous synchronization operations, both P2P and collective.

Although there is no support for remote compute placement, the user can specify affinity amongst processes using the communicator model. The communicator topology provides a way for mapping heavily communicating processes onto computation resources that are close to each other for improved locality [28, 29]. MPI has been widely used in scientific applications (having both C and Fortran bindings), and has been shown to scale on large systems with hundreds of thousands of processors under right conditions [30, 31, 32].

Cera et al. [33] evaluate MPI-2’s dynamic processes, and whether they might be an efficient way of supporting dynamic task parallelism in MPI. MPI-2’s dynamic processes allow the dynamic creation of new MPI processes in the MPI runtime using `MPI_Comm_spawn`. While this maintains a familiar API, all intra- and inter-node parallelism is done using MPI processes with inter-process communication, which can introduce significant overheads compared to communicating in a shared address space.

In high-performance communication systems such as Nemesis [34] and Portals [35], aggressive optimizations are applied to reduce intra-node message passing latency by bypassing queues. While most MPI implementations can differentiate whether a communication between two MPI processes is between nodes or across nodes, and optimize intra-node message passing using shared-memory, the node-level core and memory architectures are mostly ignored, limiting certain optimizations that use shared resources on a node, such as shared caches. The MPI model cannot take advantage of parallel algorithms for shared memory and its data structures. Due to this limitation many users have modified their programs from the ”MPI everywhere” approach to a MPI + threads model. Extending MPI with threads, known as hybrid MPI, enables programs to use intra-node parallelism as a shared memory approach.

One of the most popular shared-memory models used in the hybrid MPI approaches is OpenMP [36]. OpenMP is also a standard specification with multiple implementations. It is a collection of compiler directives, library routines, and environment variables that supports both SPMD and dynamic tasking programming models. Parallel regions of computation can be started in SPMD mode in which parallel loops are executed through worksharing constructs. The OpenMP synchronization model allows barrier and collective synchronization in parallel regions while the dynamic tasking model allows for specific task dependencies and taskwait synchronization. OpenMP 4.0 [37] allows compute affinity to be expressed with the `proc_bind` clause to specify the places to use for the threads in the team within the parallel region. The places for machine abstraction can be described through environment variables and accessed as ICV (internal control variables). The *master*, *close* and *spread* parameters can specify the distribution of new compute tasks, and the static schedule clause can be used to enforce affinity across multiple loop constructs.

In most hybrid MPI/OpenMP programming practices [38, 39, 40, 41, 42], computation is performed in OpenMP parallel regions, and MPI operations are performed in the sequential path of the execution, outside a parallel region. In this approach, OpenMP parallel threads do not participate in inter-node operations. This pattern limits the flexibility of using asynchronous MPI operations for latency hiding and computation/communication overlap. It is also difficult to fully utilize the bandwidth of multiple network interfaces that are commonly available in high-end large-scale systems. If all threads are allowed to issue MPI communication in hybrid MPI, the program has to run in multithreaded mode for the MPI runtime. Multithreaded communication increases the contention on the MPI subsystem and may degrade performance dramatically in some MPI implementations.

PGAS (Partitioned Global Address Space) languages depart from the message passing model by providing a global memory address space view to the programmer with a portion of the memory being local to each process or thread. PGAS attempts to combine the advantages of a SPMD programming style for distributed memory systems (as employed by MPI) with the data referencing semantics of shared memory systems. One of the well-known PGAS languages is UPC (Unified Parallel C) [6]. UPC uses SPMD parallelism, with collective communication for data-parallel style programming [43]. Task programming is also possible through libraries on top of UPC. It provides an explicitly parallel execution model with local and shared address spaces and a one-sided communication model. Variables with a *shared* qualifier are treated as part of the global shared memory (arrays can have layout specifiers). Popular UPC implementations, such as Berkeley UPC [44], use the GASNet [45] communication layer. GASNet provides support for remote data and compute placement through efficient one-sided communication and active messages. Computation and communication overlap is achieved through one-sided puts and gets, while completion is achieved through sync operations on handles. Studies on the PGAS model [46] have shown that threads, processes and combinations of both are needed for maximum performance, with some unavoidable overheads such as locking overhead in the thread version and network contention in the process version. The synchronizations model supports collectives (full barriers, split-phaser barriers), notify / wait pairs, locks and fences.

Coarray Fortran (CAF) [7] is a PGAS language based on extensions to Fortran 90. It has a SPMD model intended for running across compute nodes. CAF is a shared-memory programming model based on one-sided put/get communication. CAF 2.0 [47] can dynamically allocate globally shared data as coarrays and directly

reference remote data using simple language extensions. Communication is done with one-sided put and get operations. The synchronization model includes events, locks and locksets. Events provide a way to allow delayed execution of tasks based on the satisfaction of a condition. The user can express compute affinity by creating process subsets known as *teams*. Team synchronization includes barriers, finish, and collectives including broadcast, reduce, allreduce, gather, allgather, scatter, scan, shift, alltoall. Asynchronous collectives and copy operations achieve computation and communication overlap. One can use function shipping to create dynamic multi-threaded parallelism within and across nodes.

Titanium [48] is an explicitly parallel dialect of Java for SPMD parallelism. Titanium provides a global memory space abstraction whereby all data has a user-controllable processor affinity through a type system, but parallel processes may directly reference each other's memory to read and write values or arrange for bulk data transfers [49]. It has support for multi-dimensional arrays, points, rectangles and general domains and user-defined immutable classes (often called "lightweight" or "value" classes). The language has a notion of single values that are used to ensure coherence at synchronization points, as well as soundness guarantees in single statements. A set of expression rules enable coherence by inserting conservative checks statically. The Titanium compiler make aggressive optimizations for unordered loop iterations and analyzes both synchronization constructs and shared variable accesses to prevent deadlocks on barriers.

Chapel [4] is an emerging parallel programming language with support for a multithreaded execution model via high-level abstractions for data parallelism, task parallelism, concurrency, and nested parallelism. It supports a global-view data and control model with an implicit communication model. Synchronization constructs

include *sync*, *cobegin* and *coforall*. The *locale* construct allows remote placement of data and compute. For example, "*on locale {stmt};*" assigns *stmt* execution to a specific locale, while "*on var do {stmt};*" assigns *stmt* to the locale associated with *var*. Chapel supports many data aggregates such as records, classes, tuples, ranges, domains, arrays and maps. Chapel permits users to gradually optimize code from high-level abstract representations.

The X10 [5] language integrates asynchronous task parallelism with the PGAS model (APGAS) with support for programming within a node, across nodes, and across accelerators (GPUs, others). Tasks can be dynamically created using the *async* construct while the *finish* construct provides the mechanism for waiting for their completion. X10 allows locality control through the use of *places* and support for multi-dimensional arrays over a variety of regions and distributions. Stencil computations can be described compactly using regions and iterations. Synchronization in X10 is achieved through constructs such as *finish*, *atomics* and *clocks*. The X10 clock is generalization of barrier operation that supports dynamic task registration. There is also support for map-reduce parallelism using *collecting finish*, such that tasks spawned within the control of a *finish* can send results back to the *finish*, where the results are combined with a reducer. X10 supports arbitrary communication between tasks using RPC. The communication layer uses the X10RT network transport API. Global data on a distributed heap memory is referenced through *globalRef* handles. A place in X10 is a virtual shared-memory multi-processor: a data and computational container with a finite (though perhaps changing) number of hardware threads and a bounded amount of shared memory, uniformly accessible by all threads in the same place. It is used for both data distribution and computation distribution. Application data may be distributed among places using defined distribution policies. The

data processed by a task should be associated with the task’s target place for data affinity. The overhead of accessing remote data (data in other places) by an activity is higher than the overhead of accessing local data (data in current place). To read a remote location, a task should spawn another task asynchronously, with a future handle used to read the results. For the best affinity between data and computation, a task should be spawned in the place with the most data it is going to process.

The Sequoia programming language and runtime [50] were designed to facilitate the development of portable applications across machines of different memory hierarchies. In Sequoia, system memory hierarchy is abstracted using a generic model, the Parallel Memory Hierarchy (PMH) model [51]. Programmers view memory systems as a tree, each node representing a memory module of the system. A Sequoia program is organized in a recursive hierarchy. A program task, which operates entirely within its own private address space on a tree node, spawns child tasks onto the child nodes of the tree. Parent tasks may partition data into blocks that are to be processed by children tasks. Bikshandi et al [52] proposed Hierarchically Tiled Array (HTA) to facilitate the direct manipulation of tiles across processors. Their programming model distributes the array data but permit arbitrary element access. The HTA model focuses on tiling the array data and exports this explicit information to compiler to partition loop for locality or parallelism. Concurrent Object Oriented Language (Cool) [53] extends C++ to express a concurrent programming model and runtime assisted locality optimization. Cool provides abstractions for the programmer to supply hints about the data objects referenced by parallel tasks. These hints are used by the runtime system to appropriately schedule tasks and migrate data, and thereby exploit locality in the memory hierarchy.

Charm++ [54] is a C++-based parallel programming system based on the migrat-

able objects programming model. In this model, a program is decomposed into computation units called chares. Interactions between chares is achieved asynchronous messages that invoke an entry method on a remote object. The runtime manages a work-pool of chare seeds, that is, newly created chares that have not been scheduled for execution. The synchronization model in Charm++ allows structured parallelism completion scopes known as the structured dagger approach. There is also support for futures and sync constructs. Chare arrays can specify data aggregates for distributed computing while chare groups and nodegroups can be used to place compute at logical distributed places. Overall, chare collections help to express affinity among compute tasks while the machine topologies can be abstracted using the TopoManager.

The StarSs [55] programming framework consists a family of programming models based on data-flow execution of sequential programs using dynamic asynchronous tasks. The memory view of the programmer is a flat global address space where coherence and consistency is managed by the runtime. The OmpSs [56, 57] programming model extends StarSs with OpenMP syntax. The OmpSs execution model is a thread pool model where OpenMP parallel directives are ignored. All threads are created on startup and one of them executes main. Other threads pull work from the task pool and push newly created work into the task pool. This model also provides point-to-point inter-task synchronizations using task dependences (in, out, and inout) and has support for heterogeneity through the *target* clause. The communication model in this framework uses MPI where all MPI calls are taskified. An extra communication thread is created which blocks for blocking MPI (e.g MPI_Send). Its preemption is managed by the runtime.

The Legion [58] programming model and runtime uses dynamic tasks for computation. Legion is organized around logical regions, which express both locality and

independence of program data, and tasks, functions that perform computations on regions. The runtime system dynamically extracts parallelism from Legion programs, using a distributed, parallel scheduling algorithm that identifies both independent tasks and nested parallelism. Legion also enables explicit, programmer controlled movement of data through the memory hierarchy known as region passing. Legion’s data mapper and compute mapper enable remote placement of data and tasks based on locality information via a mapping interface.

The ParalleX [59] runtime system provides a unified programming model for parallel and distributed applications using *actions*. The memory view of the system is called active global address space where every object allocation is given a globally unique identifier (GUID). The communication model uses active messages called parcels which use GUIDs to communicate data. ParalleX process localities are used as a machine abstraction. Computation actions are both data-driven and message-driven and can be given a locality id parameter for specific placement.

TASCEL [60] (Task Scheduling Library) is a framework to address the challenges associated with programming abstractions supporting finer-grained concurrency. It supports various threading modes together with SPMD and non-SPMD execution. Dynamic tasks are supported only in non-SPMD mode. It uses an active message framework built on multithreaded mode MPI. The synchronization model supports finish while asynchrony is allowed through retentive work-stealing.

SWARM [61] (SWift Adaptive Runtime Machine) is runtime framework that supports dynamic task parallelism using the codelet execution model on distributed memory. The communication model uses the remote procedure calls (RPC) framework. The synchronization model for task dependences are supported only within a compute node. There is also support for collectives. Asynchronous execution for computation

and communication overlap is achieved through continuation codelets. SWARM uses a locale tree machine abstraction for expressing computation affinity in locale schedules.

The PaRSEC [62] runtime scheduler and execution controller is framework for scheduling computation tasks in a program that is represented as a directed acyclic graph (DAG) using a unique internal representation called JDF. PaRSEC assigns computation tasks to the worker threads and overlaps communications and computations. It uses workstealing for load balancing and improves locality guarantees by enqueueing newly created tasks in the local queue of the worker thread.

The distributed CnC [63] model creates dynamic tasks through a CnC graph specification of computation steps, data items and control tags. The view of the memory in this model is a globally shared one. The communication model uses both socket programming and MPI. The data driven execution model provides asynchronous execution of tasks. Remote data placement is possible by pushing data to consumer tasks while computation is distributed using predefined policies such as round-robin or custom policies created through the tuner framework. Synchronization is explicitly handled through item collection put / get operations and control tags. Data items in CnC are single-assignment objects, meaning there can only be one producer. This makes CnC a deterministic model. I-Structures [20] were also single-assignment constructs that support synchronization by allowing a single producer per memory location. In systems supporting I-Structures, readers are forced to wait (often using hardware support) for the producer to write during memory operations. M-Structures [21] allow multiple assignments, but each value has a single producer.

The framework proposed by Fu and Yang [64] executes general DAG (directed acyclic graph) computations with mixed granularities using a fast communication

mechanism. A dependence-complete task graph is built and a schedule is constructed based on it. When a processor executes a task it issues receive operations for each data it needs from its predecessors and send data to its successors. The communication module uses asynchronous RMA, buffered message-passing and communication aggregation. Each processor needs to know remote addresses it needs to pull from (or push to) and each data item at a processor is associated with a usage counter. Jégou [65] relies on a task migration model to execute chunks of the program. A task can fork independent subtasks but cannot communicate or synchronize with them. A task can only access data from local memory. If the task needs to read/write variables located in others' memory it must either spawn a remote task or migrate and bring all its private data there to resume execution. Ramaswamy et al. [66] introduce an annotated form of High Performance Fortran for extracting task and data parallelism from an application. It constructs a computation graph with a cost model for scheduling data-parallel tasks and data transfers between them in a distributed memory machine, attempting to do automatic scheduling for the programmer.

Chapter 3

Background

This work is motivated by the fact that future extreme scale systems will require novel programming and runtime execution models to meet the challenge of programming a system with up to $O(10^6)$ computational nodes and $O(10^3)$ cores per node on a limited power and memory budget. Scalable performance on such a system will require the programming model and underlying runtime to exploit intra node and inter node parallelism effectively by overlapping high latency memory and communication operations with parallel computation. A typical shared memory task parallel execution model with non blocking worker threads executing lightweight tasks serves as a good starting point for achieving our goals. As such, we use the intra node shared memory dynamic asynchronous task parallel execution model as the basis of this research work. In the rest of this chapter we look at approaches for dynamic task parallelism and provide a brief overview of the Habanero-C language.

3.1 Dynamic Task Parallelism

Dynamic asynchronous task parallelism has been an active research topic in the past, and has been gaining popularity as a shared memory parallel programming model for multi-core and many-core architectures. Modern languages and libraries provide lightweight dynamic task parallel execution models for improved programmer productivity. Task parallelism refers to expressing the parallel computation as concurrent

fine grained *tasks* that execute on top of a runtime scheduler which is responsible for scheduling and synchronizing the tasks across the processors. The two basic requirements of task parallelism is the ability to create asynchronous tasks and a way to enforce ordering or dependences in the program via synchronization constructs. Task parallelism subsumes data parallelism in that data parallelism may be expressed as task parallelism but the converse is not true. Many platforms also provide efficient constructs for embedding data parallelism within tasks. We can roughly classify task parallelism implementations in three categories:

1. New languages, such as X10 [24], Chapel [25], and Fortress [67].
2. Extensions to existing languages, such as the Cilk [10] and OpenMP [68, 69] extensions to C.
3. Libraries extensions that provides parallel APIs, such as Intel Threading Building Blocks [70].

There are many practical advantages and disadvantages to choosing a language or a library approach [71]. A key advantage of a library-based approach to task parallelism is that it can integrate with existing code easily without relying on new compiler support. However, the use of library APIs to express all aspects of task parallelism can lead to code that is hard to understand and modify, especially for beginning programmers. A key advantage of a language-based approach is that the intent of the programmer is easier to express and understand, both by other programmers and by program analysis tools. However, a language-based approach usually requires the standardization of new language constructs.

Cilk [10] is language for multithreaded parallel programming based on ANSI C. Its current version, called Intel Cilk Plus [72], extends both the C and C++ pro-

programming languages to support multithreading. Cilk adds dynamic asynchronous task parallelism with few keywords: `cilk`, `spawn` and `sync`. The `cilk` keyword identifies a function as a *Cilk procedure*, which is the parallel version of a C function. When the `spawn` keyword is used to invoke a Cilk procedure, then a parallel task is created. The `sync` statement in a Cilk procedure ensures that the task creates a join point for all immediate children. A Cilk procedure contains an implicit `sync` at the end of the function. This ensures that all transitively spawned tasks will be complete by the end of the `sync` statement. Cilk’s `spawn-sync` model is known as *fully strict*. Fully-strict computations can be scheduled with provably efficient time and space bounds using work-stealing with the work-first policy [73].

OpenMP version 3.0 [74] introduced the `task` constructs for explicitly creating tasks within a parallel region. The `taskwait` construct specifies a wait on the completion of child tasks generated since the beginning of the current task. OpenMP tasks by default are *tied* to the thread that starts executing the task. This means that the code after a `taskwait` suspension can only be executed by the thread that is holding the task’s context. Using this style of synchronization, the runtime efficiency depends heavily on the granularity of parallelism built into the program. The *untied* clause lifts the restriction on tying to the thread but causes a restricted form of programming. Untied tasks cannot depend on threadprivate variables and the user has to employ task barrier constructs to ensure the safety of stack local variables.

Intel Threading Building Blocks (TBB) [70] is a C++ template based library approach for task parallelism. Tasks provides an abstraction over thread programming with the library mapping the logical tasks onto physical threads. TBB provides algorithms that concurrently perform work on collections of data resembling the Standard Template Library (STL), such as a `parallel_for`. The major drawback of parallel

libraries is that programmers must take care of creating, scheduling and managing tasks and continuations. TBB allows creating a continuation task which would be passed to all parallel predecessor tasks. Every new task that gets created bumps up the reference count on the continuation task and then bumps down once the task execution completes. The TBB runtime schedules the continuation only when the reference count reaches 0.

Chapel [4] is a high-level parallel programming language that implements a PGAS (Partitioned Global Address Space) model. It is designed to be an imperative block structured language but includes object-oriented programming and type-generic programming. It can express different kinds of parallelism. Chapel provides constructs for dynamic task creation using the **begin** keyword, and for task synchronization using **sync** statements [25].

The X10 [24] language provides task parallelism using the **async** and **finish** constructs. Currently, X10 differentiates itself as a object-oriented programming language that supports the APGAS (Asynchronous Partitioned Global Address Space) programming model for distributed systems. X10 uses **places** for representing distinct computation resources which supports tasks being scheduled at remote places. The **finish** construct in X10 provide a single termination scope for all **async** tasks created (directly or transitively) to complete before execution can move past the **finish** scope. This implies that the parent task which created a child task with the **async** construct may finish execution before the child has finished. This model **async-finish** model is known to be *terminally strict*. In fact, the Habanero programming model is born out of X10's [5] early versions.

3.2 Habanero-C: Intra-node Task Parallelism

The work in this dissertation builds on the Habanero-C (HC) research language being developed at Rice University. HC extends the C programming language with shared-memory dynamic asynchronous task parallelism. It support two forms of task parallel programming models: structured and data-flow. Structured task parallelism uses the `async` and `finish` constructs for exploiting intra-node parallelism. This is based on the Habanero-Java [75] and X10 [5] task programming models, The language uses the `async` construct to dynamically create new asynchronous tasks. The `finish` scope construct creates a synchronization point for all asynchronous tasks created within the scope to complete execution. A program written with `finish` and `async` is guaranteed to never deadlock. The data flow model uses *data-driven tasks* (DDT) to express a task parallel program typically visualized a task graph. A dependence between two DDTs is expressed as a *data driven future* (DDF) object.

3.2.1 HC Task Model

The Habanero-C language supports structured task parallel programming in a *terminally strict* model. In this model, every task has a defined termination scope. When a parent task creates a child task for asynchronous execution, the child task will inherit the enclosing termination scope of the parent. Subsequently, the parent is allowed to finish execution before a child completes. Lightweight dynamic task creation and termination is supported by the `async` and `finish` constructs. The statement `async<stmt>` causes the parent task to create a new child task to execute `<stmt>` asynchronously (i.e. before, after, or in parallel) with the remainder of the parent task. The `finish` statement, `finish<stmt>`, performs a join operation that causes the parent task to execute `<stmt>` and then wait until all the tasks created within `<stmt>`

have terminated (including transitively spawned tasks). While Cilk `spawn` and `sync`, or the OpenMP `task` and `taskwait` constructs have similar syntax and effects, the `async-finish` constructs supports more general dynamic execution scenarios that are difficult to express in Cilk or OpenMP [76]. Figure 3.1 illustrates this concept by showing a code schema in which the parent task, T_0 , uses an `async` construct to create a child task T_1 . Thus, `STMT1` in task T_1 can potentially execute in parallel with `STMT2` in task T_0 .

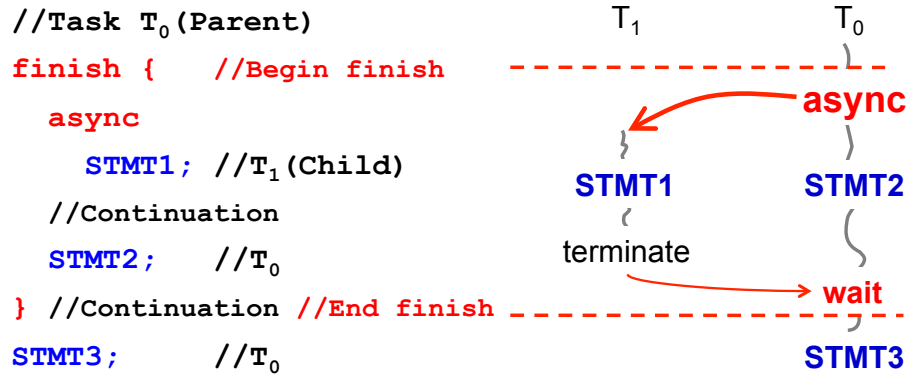


Figure 3.1 : An example code schema with `async` and `finish` constructs

Any statement can be executed as a parallel task, including for-loop iterations and method calls. The `finish` statement, `finish<stmt>`, performs a join operation that causes the parent task to execute `<stmt>` and then wait until all the tasks created within `<stmt>` have terminated (including transitively spawned tasks).

Figure 3.2, shows a vector addition example of using `async` and `finish`. We use loop chunking and each `async` task performs the addition on a chunk of data. The `IN` keyword ensures that the task will have its own copy of the `i` variable, initialized to the value of `i` when the task is created. This semantics is similar to the OpenMP

```

int PART_SIZE=16;

/* vector addition: A + B = C, size is modular of 16 */
void vectorAdd(float * A, float * B, float * C, int size) {
    int i, parts = size/PART_SIZE;
    finish for (i=0; i < parts; i++) {
        async IN(i) {
            int j, start = i*PART_SIZE;
            int end = start + PART_SIZE;
            for (j=start; j < end; j++)
                C[j] = A[j] + B[j];
        }
    }
}

```

Figure 3.2 : Task parallel programming using `async` and `finish`¹

`firstprivate` keyword.

While Cilk `spawn` and `sync`, or the OpenMP `task` and `taskwait` constructs have similar syntax and effects, the `async-finish` constructs are more flexible and support execution scenarios that are difficult to express in Cilk or OpenMP.

- `finish` defines a synchronization scope for transitively spawned `async` tasks; Cilk and OpenMP dedicate an implicit `sync` upon return of a function, thus a task created within a function cannot outlive the function. The Habanero-C model

¹Illustrative Purposes Only

does not have this restriction.

- Cilk `spawn` requires a Cilk function as the body of the new task. `async`, also OpenMP `task`, allow for arbitrary statements in the task body.
- In the `async` body, it is illegal to reference variables that are defined outside of the `async` scope. Instead, we add `IN`, `OUT` and `INOUT` keywords for specifying how the data is passed to and from a task. Habanero-C enforces a copy-in/copy-out semantics for variables passed to the child tasks. For a variable modified with `IN` (similar to the OpenMP `firstprivate` keyword) and `INOUT`, the variable will be initialized with the value from the parent scope when the task is created. For a variable reference modified with the `OUT` and `INOUT` modifiers, the value that the variable contains will be copied to the corresponding variable in the parent scope when the task is completed.

3.2.2 HC Data Driven Task Model

HC also supports a data-flow programming model through creation of tasks with data dependences. These tasks, called data-driven tasks, (DDT) [77], synchronize with other tasks through full-empty containers named data-driven futures (DDF). A DDT specifies the set of data dependences using DDF objects in a `await` clause. This ensures that the DDT will wait for all its dependences to be met before starting execution. Producer and consumer DDTs, communicate data using `put` and `get` operations on DDF objects. A DDF obeys the dynamic single assignment rule, thereby guaranteeing that all its data accesses are race-free and deterministic. The Habanero-C language interface for DDFs includes:

- *Read*: `DDF_GET()` is a non-blocking interface for reading the value of a DDF. If the DDF has already been provided a value via a `DDF_PUT()` function, a `DDF_GET()` delivers that value. However, if the producer task has not yet performed its `DDF_PUT()` at the time of the `DDF_GET()` invocation, a program error occurs.
- *Write*: `DDF_PUT()` is the function for writing the value of a DDF. Since DDFs have single-assignment values, only one producer may set its value and any successive attempt at setting the value results in a program error.
- *Creation*: `DDF_CREATE()` is a function for creating a DDF object. The producer and consumer tasks use a pointer to DDF to perform `DDF_PUT()` and `DDF_GET()` operations.
- *Registration*: the `await` clause associates a DDT with a set of input DDFs: `async await (ddf_a, ddf_b, ...) <stmt>`. The task cannot start executing until all the DDFs in its `await` clause have been `put`.

Futures have been proposed by Baker and Hewitt in [22]. Implementations of the concept can be seen in MultiLISP by Halstead [23], and in many other languages since. It is possible to create arbitrary task graphs with futures, but each `get` operation on a future may be a blocking operation unlike the `await` clause in DDTs. Additionally, futures effectively requires that the DDF and `async` creation be fused, whereas DDTs allow a separation between DDFs and `asyncs`.

3.2.3 HC Runtime

The Habanero-C task parallel runtime uses a limited set of worker threads to execute unlimited number of lightweight tasks. When asynchronous tasks are dynamically created, they are pushed onto the worker thread's deque for execution in the future.

A deque, which is an abbreviation for double ended queue, holds scheduled tasks that are ready for execution. The HC runtime uses a work-stealing algorithm to deal with load-balancing issues on the deques. It supports two execution modes: *work-first* and *help-first*. Before we delve into the details of these execution modes, let us look at some terminology. In HC, a new asynchronous task can be dynamically created when an `async` statement is executed by the program as mentioned earlier. The task which creates the `async` is the parent task while the `async` itself is the child. The code in the parent task after the `async` statement can now potentially execute in parallel with the `async`. This code is called the *async continuation* and holds the current context of the parent task.

In the work-first execution mode [73], the worker thread that excutes the `async` statement will switch to the new `async` child task and temporarily suspends the parent. The parent task will resume at the `async` continuation point. The worker pushes this parent task continuation on to it's deque before it executes the child `async` task. This ensures that if there exists an idle worker looking for new work, then this continuation can now be *stolen* by that worker to be executed in parallel with the `async`. If the continuation is not stolen, then the worker which pushed it would pop it back to execute it after it completes execution of the `async`. HC also supports the help-first execution model [76]. In the help-first mode, the worker that executes an `async` statement pushes the `async` child task onto the deque and continues execution of the parent task's `async` continuation. When the parent task suspends at the end of a finish scope or simply completes execution, the worker can pop back the `async` if it had not been stolen by other workers yet.

Figure 3.3 shows the deque operations in the HC runtime derived from past work by Chase and Lev [78]. The contents of a deque are scheduled tasks that are ready

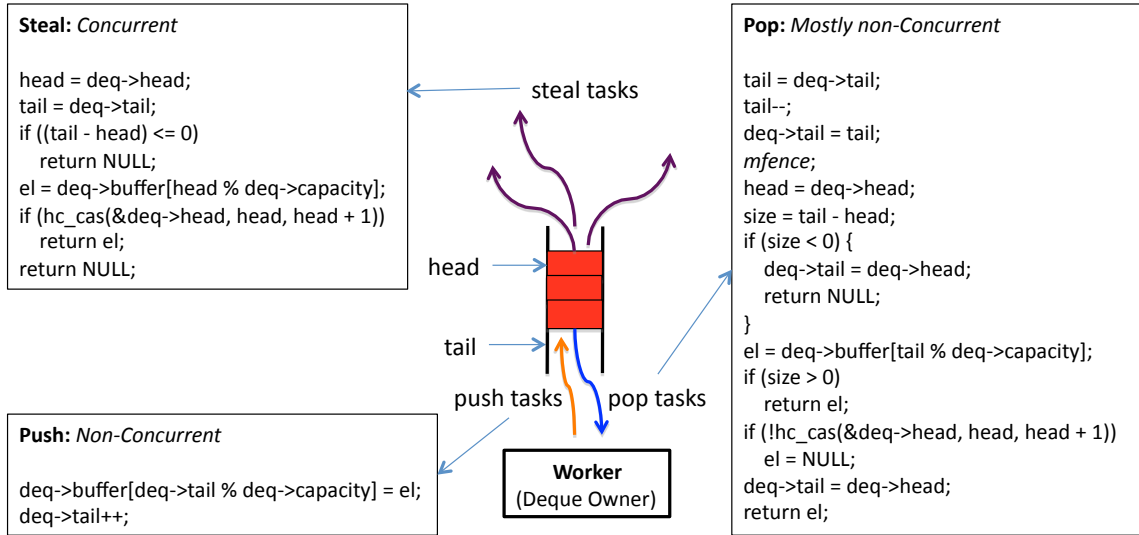


Figure 3.3 : Deque operations for a workstealing runtime

to run. In a work-stealing runtime, the deque supports *push* and *pop* operations on one end and a *steal* operation on the other end. Every deque in the HC runtime has one associated worker which is the deque's owner. Only the owner is responsible for the push and pop operations on that deque. Non-owners perform steals on the deque. When an asynchronous task is dynamically created, the worker pushes the task onto it's own deque. When a worker is done executing a task, it pops a new one from it's own deque and starts to execute that. If the worker's deque is empty, it tries to steal tasks from other deques that it does not own. A deque maintains a *head* and a *tail* variable, one for each end as shown in Figure 3.3. The push operation places the task on the deque and increments the tail. Since, the owner is the only one pushing a task to the deque, this operation is non-synchronized. The pop operation is non-synchronized except when there is only one task left in the deque. In that case, the owner has to compete with other workers trying to steal that last task,

effectively turning into a pop into a steal. The steal operation has to be synchronized since multiple workers may try to concurrently steal from one deque. A successful *compare-and-swap* atomic operation of the deque head ensures a successful steal.

Chapter 4

Habanero-C Runtime Communication System

Effective combination of inter-node and intra-node parallelism is recognized to be a major challenge for extreme-scale systems. One way to approach this challenge is the “MPI everywhere” model. This approach applies distributed-memory programming with MPI ranks uniformly across all processors on the system and does not distinguish between intra-node and inter-node parallelism. MPI remains a popular choice among many programmers writing distributed-memory applications. This model benefits from simplicity, portability and backward compatibility but lacks key requirements for scalability on extreme-scale systems. First, a MPI program designed for SPMD style execution needs to statically decide on the parallelism which could be a scalability bottleneck for applications that benefit from dynamic parallelism. Second, the MPI model cannot leverage optimized algorithms and data structures designed specifically for shared-memory programming. Third, the MPI specification needs to address many scalability issues [79]. Growth of memory requirement of some functions linearly with the number of ranks, a non-scalable graph topology, inadequate support for fault tolerance and inefficient one-sided communication are some of the major issues. Finally, although optimized intra-node communication may be available depending on the implementation of MPI, it is not a guarantee. Hence communication latency can become another bottleneck for this model.

State-of-the-art techniques that combine distributed- and shared-memory programming models [80], as well as many PGAS approaches [6, 24, 47, 48], have demon-

strated the potential benefits of combining both levels of parallelism [81, 82, 39, 83], including increased communication-computation overlap [84, 85], improved memory utilization [86, 87], power optimization [88] and effective use of accelerators [89, 90, 91, 92]. The hybrid MPI and thread model, such as MPI and OpenMP, can take advantage of those optimized shared-memory algorithms and data structures. On the downside, such programs have to deal with either multithreaded contention on the MPI subsystem or segmented MPI and OpenMP regions in the code which may suffer from lack of asynchrony. Even the synchronization model can be difficult to orchestrate due to a lack of unified synchronization primitives for threads and processes. PGAS models on the other hand are simpler and provide a global shared-memory view to the programmer. There are also many PGAS languages that include support for multithreading. However, all these hybrid programming approaches often require significant rewrites of application code and assume a high level of programmer expertise.

The Integrated Native Communication Runtime (INCR) [93] is an effort to unify UPC [6] and MPI [8] codes. This work extended and optimized the MVAPICH-Aptus [94] MPI runtime on Infiniband to support the GASNet API [45]. INCR included native support for active messages to avoid the limitations of mapping the GASNet API to use a MPI stack. In this framework, UPC codes get compiled to GASNet API's as in normal UPC toolchains. From then, GASNet API's use the INCR interfaces. They have shown that this framework can deliver equal or better performance than current GASNet performance on Infiniband, and at the same time have the flexibility to allow MPI and UPC codes to run together in a program and use the same communication layer. However, its scalability is yet unproven when MPI is used in a multi-threaded mode and integrated with a dynamic threading model.

Our approach to address the programming challenge of extreme-scale systems is based on dynamic task parallelism. Dynamic task parallelism has been widely regarded as a programming model that combines the best of performance and programmability for shared-memory programs. These programming systems are typically assisted by efficient runtimes for task management on a limited number of worker threads. Users can express fine-grained parallelism using lightweight tasks and the runtime guarantees fully asynchronous execution without having to block worker threads at any time. Task management responsibilities of the runtime involve dynamic task creation, scheduling, synchronization and load balancing. Although they are well suited for shared-memory systems, it is infeasible to replicate this runtime model at the inter-node level. These runtimes typically depend on hardware support for fast atomics (low-latency operations) to support load-balancing operations on shared-memory multicore systems. On distributed-memory systems, these operations have to be performed by relatively high latency communication operations. Clearly, this runtime model needs some adjustments with respect to communication systems before we can scale dynamic task parallelism on distributed systems.

In this chapter, we present the **HC-COMM** framework [11], a scalable runtime communication system that integrates Habanero-C with a communication system. The **HC-COMM** runtime communication system addresses the challenges faced by a dynamic task parallel runtime to scale on distributed-memory systems. The scope of this work is to focus on how a dynamic task parallel runtime should interface with a communication system. The focus is not to design the best communication system today but to leverage one that is already available. This runtime can integrate any popular communication system, such as MPI, which is the communication system of choice used in this work. The **HC-COMM** runtime is designed using dedicated compu-

tation and communication cores to provide scalable and sustainable performance. The goal of the HC-COMM system is to leverage benefits of asynchronous dynamic task parallel programming models and the scalability of popular communication models. We aim to hide communication latency with non-blocking execution and also avoid contention on the communication sub-system as well.

We present HCMPI, a programming model that integrates asynchronous task parallelism with MPI. HCMPI offers a rich new platform with novel programming constructs, while also offering a practical approach for programmers wanting to take incremental transitional steps starting from either a shared- or distributed-memory program. In this model, a programmer can take an existing MPI application and gradually add task parallelism to it. On the other hand, one can also take a shared-memory program with dynamic task parallelism and create a distributed version of the application by adding MPI calls. In either case, the HC-COMM runtime system guarantees highly scalable non-blocking execution for computation worker threads. All MPI calls are treated as asynchronous tasks in this model, thereby enabling unified handling of messages and tasking constructs.

4.1 HCMPI Programming Model

HCMPI unifies the Habanero-C intra-node task parallelism with MPI inter-node parallelism. A HCMPI program follows the task parallel model within a node and MPI’s SPMD model across nodes. The tasking model introduces communication tasks in addition to regular shared-memory computation tasks. Communication tasks deal with MPI calls. Computation tasks have the ability to dynamically create asynchronous communication tasks, and also wait for their completion. HCMPI seamlessly integrates computation and communication task wait using Habanero-C’s `finish` and `await` con-

HCMP_BYTE	HCMP_CHAR	HCMP_SHORT
HCMP_INT	HCMP_LONG	HCMP_UCHAR
HCMP_USHORT	HCMP_UINT	HCMP_ULONG
HCMP_FLOAT	HCMP_DOUBLE	HCMP_LONG_DOUBLE

Table 4.1 : HCMPI Types

structs. These constructs are also used to capture MPI’s blocking semantics. The HC-COMM runtime guarantees non-blocking execution of the computation workers. HCMPI will not introduce any deadlocks when extending from deadlock-free MPI code.

The HCMPI types and APIs, shown in Table 4.1 and Table 4.2 are very similar to MPI, making the initial effort of porting existing MPI applications to HCMPI extremely simple. Most MPI applications can be converted into valid HCMPI programs simply by replacing APIs and types that start with `MPI_` by `HCMPI_`¹. The arguments to these functions follow the structure of their MPI counterparts using appropriate HCMPI types. Table 4.3 shows the runtime extensions specific to HCMPI. We use all upper case to distinguish these functions from the regular MPI specific interface.

HCMPI treats all communication calls as asynchronous tasks, thereby enabling unified handling of messages and tasking constructs. It supports blocking or waiting for communication through HC’s task blocking feature. HCMPI is uniquely positioned as a programming model that can help shared-memory task parallel applications transition to distributed-memory versions, while distributed-memory applications can integrate shared-memory task parallelism. The HC-COMM runtime ensures that com-

¹While this replacement can be easily automated by a preprocessor or by API wrappers, we use the `HCMPI_` prefix in this work to avoid confusion with standard MPI.

Point-to-Point API
Blocking send: HCMPISend(void *b, int c, HCMPI_Type t, int dest, int tag, HCMPI_Comm cm)
Non-blocking send: HCMPI_Isend(void *b, int c, HCMPI_Type t, int dest, int tag, HCMPI_Comm cm, HCMPI_Request **r)
Blocking recv: HCMPI_Recv(void *b, int c, HCMPI_Type t, int dest, int tag, HCMPI_Comm cm)
Non-blocking recv: HCMPI_Irecv(void *b, int c, HCMPI_Type t, int dest, int tag, HCMPI_Comm cm, HCMPI_Request **r)
Test for completion: HCMPI_Test(HCMPI_Request *request, int *flag, HCMPI_Status **status)
Test all for completion: HCMPI_Testall(int count, HCMPI_Request **requests, int *flag, HCMPI_Status **statuses)
Test any for completion: HCMPI_Testany(int count, HCMPI_Request **requests, int *index, int *flag, HCMPI_Status **status)
Wait for completion: HCMPI_Wait(HCMPI_Request *request, HCMPI_Status **status)
Wait for all to complete: HCMPI_Waitall(int count, HCMPI_Request **requests, HCMPI_Status **statuses)
Wait for any to complete: HCMPI_Waitany(int count, HCMPI_Request **requests, int *index, HCMPI_Status **status)
Cancel outstanding communication: HCMPI_Cancel(HCMPI_Request *request)
Get count of received data: HCMPI_Get_count(HCMPI_Status *status, HCMPI_Type t, int *count)
Collectives API
Barrier synchronization: HCMPI_Barrier()
Broadcast: HCMPI_Bcast(void *b, int c, HCMPI_Type t, int root, HCMPI_Comm cm)
Scan: HCMPI_Scan(void *sb, void *rb, int c, HCMPI_Type t, HCMPI_Op op, HCMPI_Comm cm)
Reduce: HCMPI_Reduce(void *sb, void *rb, int c, HCMPI_Type t, HCMPI_Op op, int root, HCMPI_Comm cm)
Scatter: HCMPI_Scatter(void *sb, int sc, HCMPI_Type st, void *rb, int rc, HCMPI_Type rt, int root, HCMPI_Comm cm)
Gather: HCMPI_Gather(void *sb, int sc, HCMPI_Type st, void *rb, int rc, HCMPI_Type rt, int root, HCMPI_Comm cm)

Table 4.2 : HCMPI API for point-to-point and collective communication

Runtime API
Create request handle : HCMPI_REQUEST_CREATE()
Status query: HCMPI_GET_STATUS(HCMPI_Request *request, HCMPI_Status **status)

Table 4.3 : HCMPI Runtime API

putation and communication can seamlessly integrate onto one unified platform. The HCMPI programming model integrates computation tasks with communication in two ways, the structured communication task model and the message driven task model.

4.1.1 HCMPI Structured Communication Task Model

This model integrates MPI communication with the structured task model described in section 3.2.1. We have seen earlier that a parent task can initiate an asynchronous computation child task using the `async` construct. Similarly, computation tasks can also initiate asynchronous non-blocking point-to-point communication via runtime calls to `HCMPI_Isend` and `HCMPI_Irecv`. These calls are converted to asynchronous communication tasks by the runtime. Control returns immediately to the parent task which can proceed to execute the next statement. The only difference between the computation tasks and communication tasks is that the communication task's functionality is driven by a specific API as shown in Table 4.2, unlike a computation task which can accept any user statement code. The structured task model uses the `finish` construct as a synchronization point for all asynchronous tasks that were created transitively within its scope. The same model applies in HCMPI to both computation and communication tasks. Using the `finish` construct one can not only wait for computation tasks to complete but will also block for all communication

tasks that were issued within its scope. In other words, all communication tasks will have the same immediately enclosing finish scope as the parent computation task. Figure 4.1 shows that the execution of *foo* is asynchronous to the send and receive communication calls, while the *finish* ensures that the communication is complete when *baz* runs.

```

finish {
    async foo();

    HCMPI_Isend(send_buf, ...);

    HCMPI_Irecv(recv_buf, ...);

    ... //do asynchronous work
}

baz(); // Isend and Irecv are complete after finish scope

```

Figure 4.1 : HCMPI Structured Communication Tasks: Starting asynchronous communication and waiting for its completion.

4.1.2 HCMPI Message Driven Task Model

This model integrates MPI communication with the HC data-driven producer-consumer task model shown in section 3.2.2. A data-driven consumer task uses the **await** construct to wait for the satisfaction of dependences by the producer before it can execute. In this model, the producer may be a communication message, such that the consumer will not execute until that message has completed. The data-driven task model uses DDF objects for both synchronizing as well as passing data between the producer and consumer. The HCMPI model uses a similar object called a *request* handle. Table 4.2

```

HCMPI_Request * r;

HCMPI_Irecv(recv_buf, ..., &r);

async AWAIT(r) IN(recv_buf, r) {
    HCMPI_Status * s;

    HCMPI_GET_STATUS(r, &s);

    ... //read status and recv_buf
}

... //do asynchronous work

```

Figure 4.2 : HCMPI Await Model

shows that `HCMPI_Isend` and `HCMPI_Irecv` calls return a request handle object called `HCMPI_Request`, similar to `MPI_Request`. This request handle can be used exactly the same way as a DDF object inside the `await` clause of the consumer task. As with the DDF model, the HCMPI request object is used to pass data from the communication to the consumer task. Specifically, a request handle can be queried by the consumer task for the status of the communication using `HCMPI_GET_STATUS` call as shown in Table 4.3. The status object is implicitly allocated by the runtime and its type is `HCMPI_Status`, similar to `MPI_Status`. Figure 4.2 shows the message driven computation model where the asynchronous computation task get created but does not get scheduled for execution until the receive communication completes. In this model, waiting for completion becomes fully asynchronous with the rest of the tasks.

4.1.3 HCMPI Implementation for MPI Blocking Semantics

In the HCMPI programming model, MPI calls are implemented on a task parallel runtime using HC task parallel constructs. This enables a HCMPI to operate on

a fully asynchronous runtime with unified computation and communication tasks. All blocking communication is handled by the `finish` construct. For example, figure 4.3 shows how a blocking receive operation is implemented in `HCMPI`. As can be noted, the actual communication call still remains an asynchronous call (`HCMPI_Irecv`). However, the blocking semantics is ensured by the `finish` that is wrapped around the asynchronous communication call. The `HC-COMM` runtime ensures that a blocking call using the `finish` construct will only block the current task but will not block the worker thread.

```
finish {
    HCMPI_Irecv(recv_buf, ...);
} // Irecv must be completed after finish
...
```

Figure 4.3 : Using the `finish` construct in `HCMPI`. A `finish` around `HCMPI_Irecv`, a non-blocking call, implements `HCMPI_Recv`, a blocking call.

Another way to wait for the completion of a communication task is through `HCMPI_Wait` and its variants `HCMPI_Waitall` and `HCMPI_Waitany`. In the MPI model, if a `MPI_Wait` call blocks, then the whole worker thread block unlike in this model. In the `HCMPI` model, `HCMPI_Wait` is implemented simply as `finish async await(req)`, where *req* is the request handle as shown in Table 4.2. The computation task logically blocks at the `HCMPI_Wait` for the asynchronous communication task to complete. The synchronization event is provided by a `HCMPI_Request` handle and returns a `HCMPI_Status` object. Figure 4.4 shows an example of using `HCMPI_Status` to get the count of the elements received in a buffer after the completion of a `HCMPI_Irecv` operation.

```

HCMPI_Request * r;

HCMPI_Irecv(recv_buf, ..., &r);

... //do asynchronous work

HCMPI_Status * s;

HCMPI_Wait(r, &s);

int count;

HCMPI_Get_count(s, HCMPI_INT, &count);

if (count > 0) { //read recv_buf }

```

Figure 4.4 : HCMPI Wait and Status Model

4.1.4 HCMPI Collective Synchronization Model

Inter-node-only collective operations in HCMPI are similar to MPI collectives. Table 4.2 includes a partial list of supported HCMPI collectives. All HCMPI collective operations follow the blocking semantics discussed earlier. When the blocking HCMPI_Barrier call is executed, the computation task blocks but the computation worker thread does not. We will add support for non-blocking collectives to HCMPI once they become part of the MPI standard. Figure 4.5 shows how to perform an inter-node-only barrier. In this example, asynchronous task A() is created before the barrier and can logically run in parallel with the barrier operation. However, function call B() must be completed before the barrier, and function call C() can only start after the barrier.

```

async A();
B();
HCMPI_Barrier();
C();

```

Figure 4.5 : HCMPI Barrier Model

4.2 HC-COMM Runtime Implementation

The HC-COMM runtime is a novel design based on dedicated computation and communication workers in a work-stealing scheduler, shown in Fig. 4.6. The HC-COMM runtime has to create one communication worker per MPI-rank. The number of computation workers can be set at runtime by the `-nproc` command line option. Experimental results reported in this work were obtained by designating one core in a node to be the communication worker, and using the remaining cores in the node as computation workers. Support for multiple communication workers per node is possible through more MPI ranks on the node. Our experiments show that the benefits of a dedicated communication worker can outweigh the loss of parallelism from the inability to use it for computation. We believe that this trade-off will be even more important in future extreme scale systems, with large numbers of cores per node, and an even greater emphasis on the need for asynchrony between communication and computation.

The HC-COMM runtime is an extension of the Habanero-C work-stealing runtime. Computation workers are implemented as pthreads (typically one per hardware core/thread). Each worker maintains a double-ended queue (deque) of lightweight computation tasks. A worker enqueues and dequeues tasks from the tail end of its

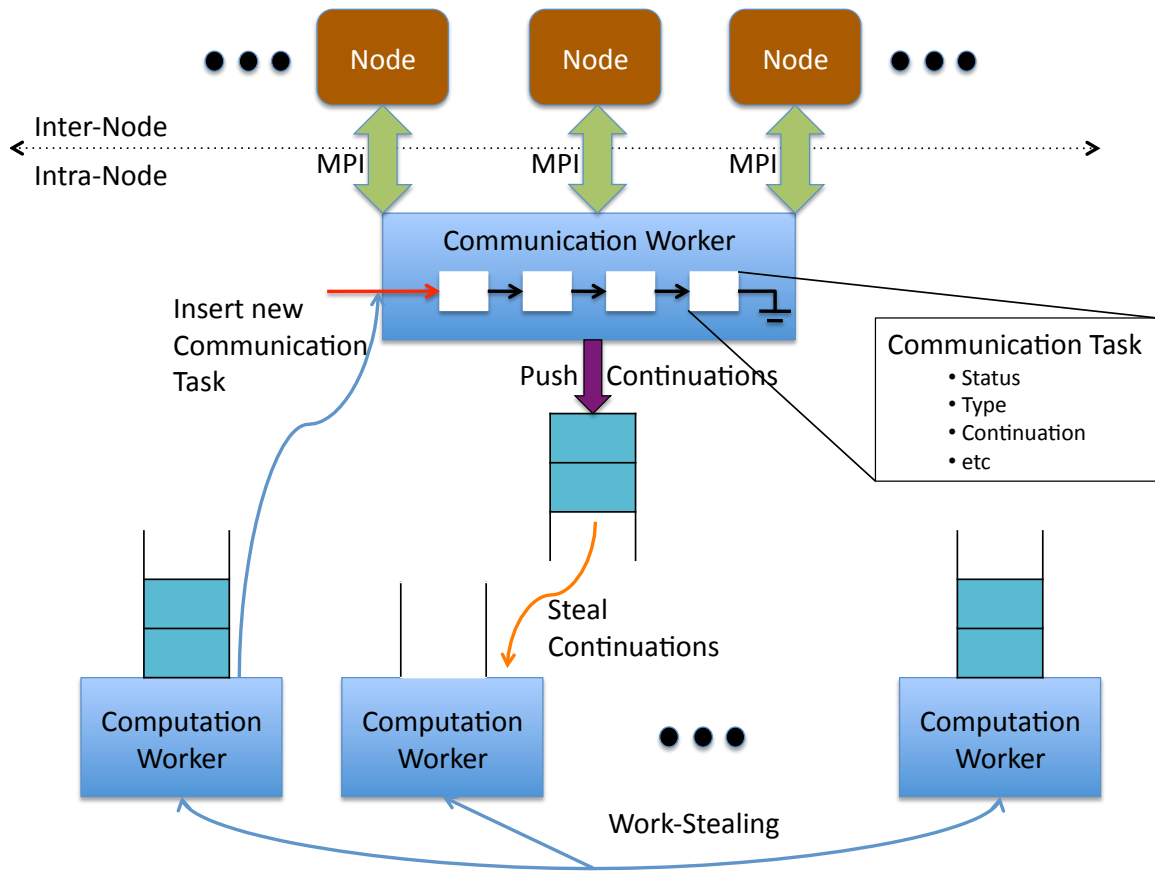


Figure 4.6 : The HC-COMM Intra-node Runtime System

deque. Idle workers steal tasks from the head end of the deques of other workers. A communication optimization scheme, such as the one implemented in [95], will be a natural extension to our implementation of HC-COMM workers.

The HC-COMM communication worker is dedicated to execute MPI calls, using a worklist of communication tasks implemented as a lock-free queue. Figure 4.7 shows the lifecycle of a communication task. When a computation worker makes an HC MPI call, it creates a communication task in the **ALLOCATED** state. The task is either recycled from the set of **AVAILABLE** tasks, or it is newly allocated and enqueued into the worklist. The task structure is initialized with required information, such



Figure 4.7 : Lifecycle of a Communication Task

as buffer, type, etc. and then set as **PRESCRIBED**. When the communication worker finds a **PRESCRIBED** task, it either issues an asynchronous MPI call for point-to-point communication or blocks for a collective MPI call. For asynchronous calls, the worker sets the task state as **ACTIVE** and moves on to the next task in the worklist. The worker tests **ACTIVE** tasks for completion using `MPI_Test`. Once an MPI operation has completed, the task state is set to **COMPLETED**. If the task is the last one to complete in the enclosing `finish` scope, the communication worker pushes the continuation of the `finish` onto its deque to be stolen by computation workers. The **HC-COMM** compiler parses `async` and `finish` statements, recognize the `HC_MPI_` calls in the code, and replace them with appropriate library and runtime calls to create task data structures, enable task creation and execution, and to ensure proper task termination within each finish scope. We have implemented our compiler on top of the ROSE source-to-source compiler framework [96].

HC-COMM implements event-driven task execution using Habanero-C’s Data-Driven Tasks (DDTs) and Data-Driven Futures (DDFs), introduced in Section 3.2.2. DDFs allow the programmer to specify task dependences in the `await` clause of a DDT. When a DDT’s task dependences are satisfied, it is scheduled by the runtime for execution. Currently, there is no support for a priority scheduling. A DDT can *await* on one or more DDFs, while a DDF can have one or more DDTs *awaiting* its satisfaction. DDFs follow *put-get* semantics. An *await* on a DDF by a consumer DDT is to wait for the *put* on that DDF by a producer DDT. A DDF is a single-

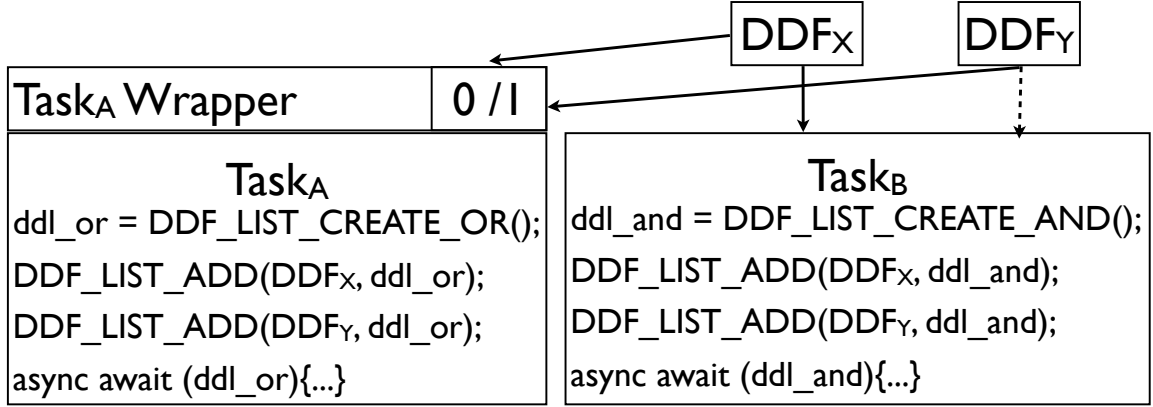


Figure 4.8 : HC-COMM DDF Runtime

assignment object, meaning there can be only one producer for that DDF. A `HC_MPI_Request` handle is implemented as a DDF. Computational tasks created using `async await(req)`, where `req` is the `HC_MPI_Request` handle, will start executing once the communication task represented by the handle has been completed. We have seen that `HC_MPI_Wait` is implemented as `finish async await(req)`; an elegant solution using Habanero-C constructs. `HC_MPI_Waitall` and `HC_MPI_Waitany` are implemented as extensions to `HC_MPI_Wait` where a task waits on a list of DDFs, as shown in Fig. 4.8. The key difference is that the *waitall* list is an AND expression while the *waitany* list is an OR expression. A novel contribution of this work is the extension of the implementation of DDF lists to support the OR semantics, in addition to the AND semantics that were proposed in [77]. The DDF AND and OR lists are created by apis `DDF_LIST_CREATE_AND()` and `DDF_LIST_CREATE_OR()` respectively. A DDF is added to the list by the `DDF_LIST_ADD(ddf, ddl_list)` api. The handling of an AND list is similar to the one described in [77]. In case of the OR list, the runtime iterates over the list of DDFs found in the `await` clause. If a DDF is found to have been satisfied by a `put`, the task becomes ready for execution immediately. If no satisfied DDF is

found, the task gets registered onto all DDF's on the list. When a `put` finally arrives on any of the DDF's the task get released and is pushed into the current worker's deque. To prevent concurrent `puts` from releasing the same task with an OR DDF list, each task contains a wrapper with a token bit to indicate if the task has already been released for execution, as shown in Fig. 4.8. This token is checked and set atomically to ensure the task is released only once. After a DDT starts executing following a `put` on a DDF in a OR list, the programmer has the option to find out which DDF in the list satisfied the dependence through a runtime API called `DDF_LIST_INDEX`. Given a DDF OR list, `DDF_LIST_INDEX` will return a integer index of the DDF on the list (a runtime error is thrown for AND lists). It is the user's responsibility to pass an array of DDFs into the task to retrieve the DDF object corresponding to the index. The HC-COMM communication runtime is itself a client of the DDF runtime. It uses DDFs to communicate `MPI_Status` information to the computation tasks via a `DDF_PUT` of the `HCMPI_Status` object on to the `HCMPI_Request` DDF. `HCMPI_GET_STATUS` internally implements a `DDF_GET`.

Charm++ AMPI [97] is an implementation of MPI that supports dynamic load balancing and multithreading for MPI applications. It enables adaptive overlap of communication and computation through the virtualization of processors, automatic load balancing and easy portability from MPI. These features are similar to `HCMPI` with a few key differences. While the AMPI runtime uses the Charm++ communication runtime, `HCMPI` is built on existing MPI runtimes. The AMPI runtime achieves loadbalancing through predictive models based on runtime workload information, whereas `HCMPI` relies on workstealing. Our choice of dedicating a core for communication is based on supporting fine-grained task parallelism at intra-node level and avoiding scalability issues of multithreaded MPI.

4.3 Results

In this section we present results measuring HCMPI performance on some standard benchmark programs. From our experiments, we aim to explain the performance ramifications of our design choices in the HCMPI programming model and the HCCOMM runtime. We test the HCMPI implementation for micro-benchmark performance and strong scalability. For micro-benchmark performance, we use a test suite of multi-threaded MPI programs. We conduct our strong scaling experiment on UTS, a standard benchmark application that does tree-based search. We compare our performance against existing reference codes.

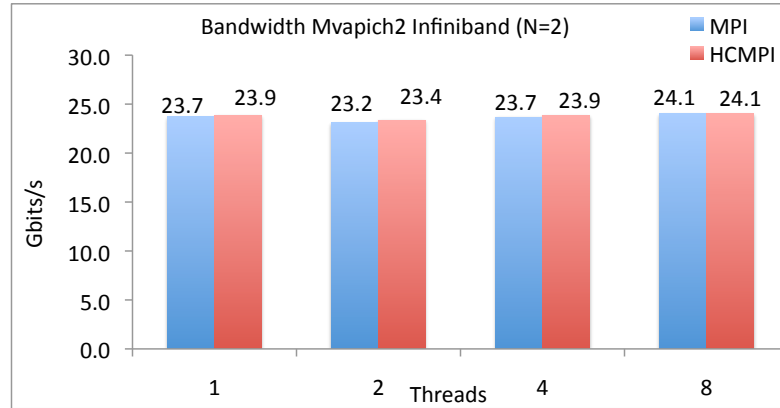
Our experimental framework used the Jaguar supercomputer at Oak Ridge National Labs and the DAVinCI cluster at Rice University. The Jaguar supercomputer was a Cray XK6 system with 18,688 nodes with Gemini interconnect. Each node was equipped with a single 16-core AMD Opteron 6200 series processor and 32 GB of memory. For our experiments, we scaled up to 1024 nodes (16384 cores) and used the default MPICH2 installation. The DAVinCI system is an IBM iDataPlex consisting of 2304 processor cores in 192 Westmere nodes (12 processor cores per node) at 2.83 GHz with 48 GB of RAM per node. All nodes are connected via QDR InfiniBand (40 Gb/s). Our experiments on DAVinCI used up to 96 nodes (1152 cores) and MVAPICH2 1.8.1.

4.3.1 Micro-benchmark Experiments

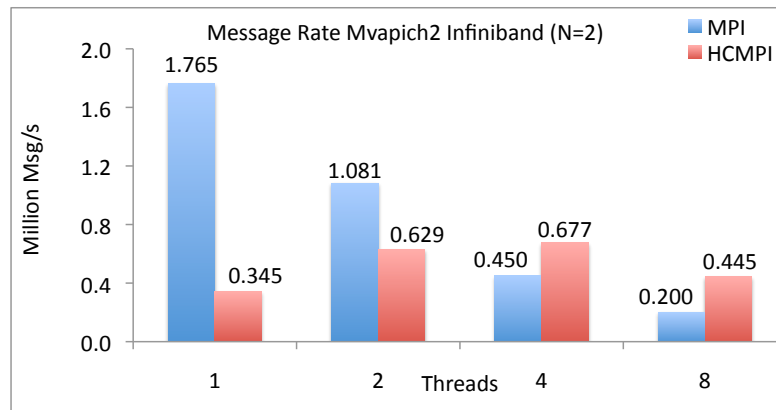
HCMPI proposes an integrated shared- and distributed-memory parallel programming model. Many current hybrid models use MPI with Pthreads or OpenMP to expose a combination of threads and processes to the user. Such a model would have to deal with concurrent MPI calls from multiple threads. This implies that MPI has

to operate either on one of its multi-threaded modes, or there has to be additional synchronization effort from the programmer. As a result our comparison baseline would be against hybrid models using MPI in a multi-threaded mode of operation. For our first set of micro-benchmark experiments, we used the test suite [98] developed at ANL to evaluate multi-threaded MPI. The shared-memory multithreading is achieved using `pthread`s. A *bandwidth* test is performed by measuring delays caused by sending large (8Mbyte) messages with low frequency. A *message rate* test transmits empty messages with high frequency. In the *latency* test 1000 sends and 1000 receives are performed for different message sizes ranging from 0 to 1024. The average time delay for each size is reported. The reference benchmark programs initialize MPI using `MPI_THREAD_MULTIPLE` and issue MPI calls from multiple threads. The HCMPI equivalent is to create as many computation workers as there are `pthread`s in the MPI version. HCMPI also adds a dedicated communication worker thread to the process. The motivation of this benchmark is to evaluate the feasibility of using MPI in multithreaded mode compared to HCMPI (which has to deal with the overhead of a dedicated communication worker). Parallel tasks on multiple computation workers can communicate concurrently through the communication worker. HCMPI inherently uses `MPI_THREAD_SINGLE` due to the dedicated communication worker. This avoids using multi-threaded MPI, which typically (on most MPI runtimes currently available) performs worse than single-threaded MPI due to added synchronization costs. This rationale currently precludes HCMPI from using multiple communication workers per process.

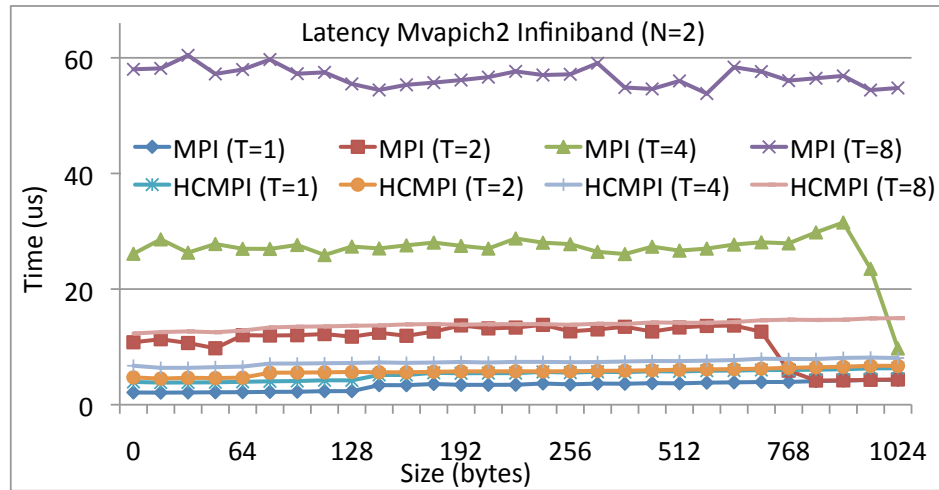
These micro-benchmark tests always use two processes communicating with each other. In our experiments, they are placed on two different nodes. The results in Fig. 4.9 are for MVAPICH2 with Infiniband on DAVinCI, and the results in Fig. 4.10



(a) Bandwidth

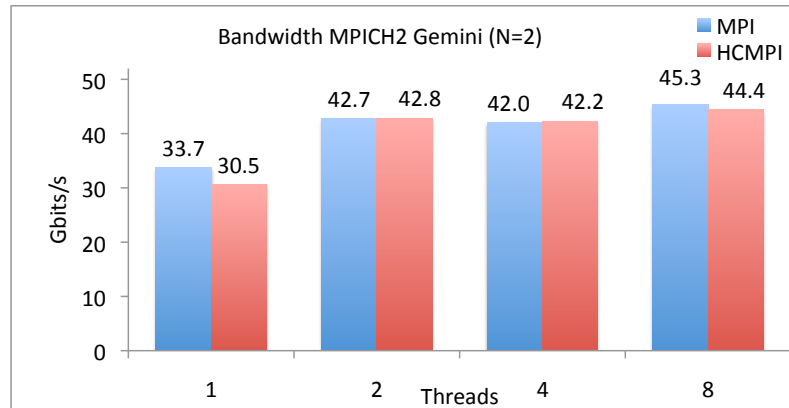


(b) Message Rate

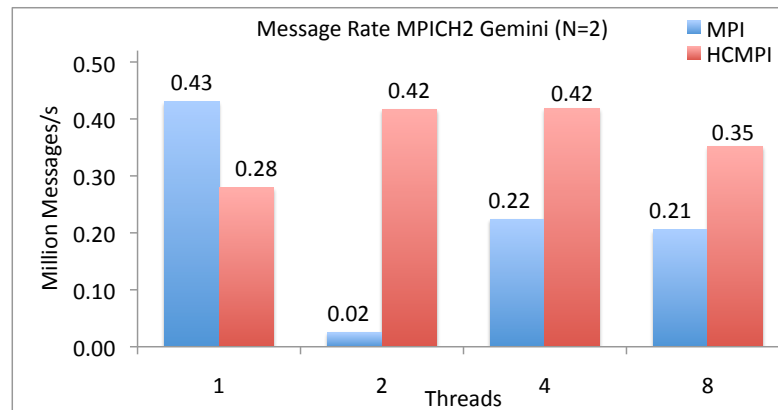


(c) Latency

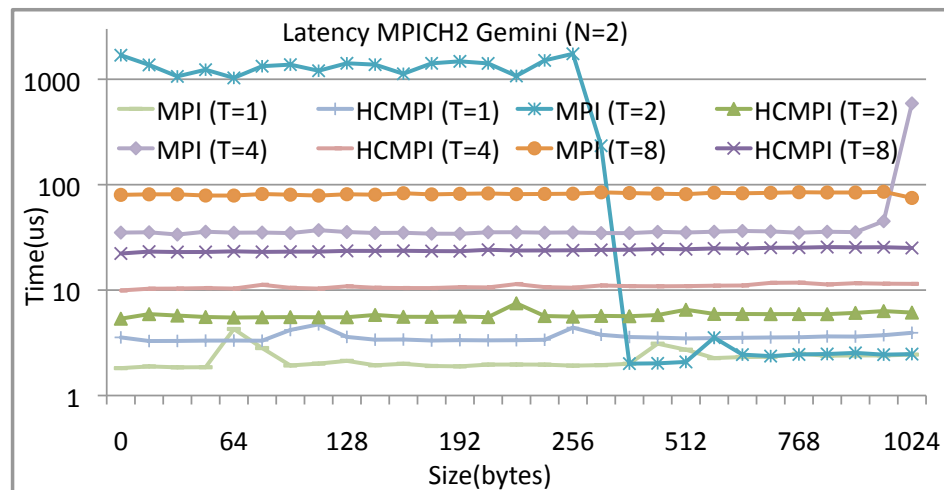
Figure 4.9 : Thread Micro-benchmarks for MVAPICH2 on Rice DAVinCI cluster with Infiniband interconnect



(a) Bandwidth



(b) Message Rate



(c) Latency

Figure 4.10 : Thread Micro-benchmarks for MPICH2 on Jaguar Cray XK6 with Gemini interconnect

are for MPICH2 with Gemini on Jaguar. The bandwidth experiments in both cases show MPI and HCMPI performing close to each other. This is because the bandwidth test communicates a high volume of data per message which easily overwhelms the network. Adding more threads does little to ease the situation. The message rate tests sends a large number of low data volume messages. In this case, HCMPI starts performing better than multi-threaded MPI when we scale up the number of threads inside the process. We conclude that it reflects higher synchronization overheads for using the MPI subsystem concurrently from different threads. The latency tests confirm our conclusion by showing HCMPI latencies scale more gracefully than MPI when increasing the number of threads. For extreme-scale systems with $O(10^3)$ cores per node, there is a possibility of requiring more than one dedicated communication thread to avoid overloading. HCMPI can handle this scenario by employing more than one HCMPI process on a node (instead of the one process used in our experiments), which will create the desired number of communication threads (one per process). The Jaguar message rate test shows a dip in performance when using two threads. This phenomenon was consistently repeatable over multiple runs of the benchmark. This fact is also reflected on the latency chart where we see that latency in MPI with two threads is an order magnitude higher than MPI with eight threads.

4.3.2 UTS Case Study:

For our scaling experiment we chose the Unbalanced Tree Search (UTS) application [99, 100]. The benchmark contains a reference implementation using MPI in the publicly available version [101]. The UTS tree search algorithm is parallelized by computing the search frontier tree nodes in parallel. The search typically leads to unbalanced amount of work on parallel resources, which can then benefit from load

balancing techniques. The reference MPI implementation of the benchmark, used as the baseline for creating the HCMPI version, performed parallel search using multiple MPI processes, and load balancing using inter-process work-sharing or work-stealing algorithms. In our experiments we have focused on the work-stealing version due to better scalability [100]. We scale our experiment up to 16,384 cores on the Jaguar supercomputer.

The HCMPI implementation of UTS adds intra-process parallelization to the reference MPI implementation. It does not modify the inter-process peer-to-peer work-stealing load balancing algorithm. HCMPI’s goal is to benefit from shared-memory task parallelism on a compute node and uses only one process per node. In this context, compute node and compute process can be used interchangeably. In the HCMPI implementation a task has access to a small stack of unexplored tree nodes local to the worker thread it is executing on. When the stack fills up, tree nodes from the stack are offloaded to a deque for intra-process work-stealing. This strategy generates work for intra-process peers before it sends work to global peers. The use of non-synchronized thread-local stacks is for superior performance over deques. Global communication is handled by the communication worker. The HCMPI runtime uses a *listener* task for external steal requests while the computation workers are busy. When another process requests a steal, the listener task looks for internal work, trying to steal from the local work-stealing deques. If the local steal was successful, it responds with that work item, if not, with an *empty* message. Inside a compute node, when a computation worker runs out of work and is unable to steal work from local workers, it requests the communication worker to start a global steal. A global steal uses the reference MPI inter-process steal algorithm. During a global steal, if an active local computation worker has been able to create internal work, then some

	T1XXL		T3XXL	
	chunk size	polling	chunk size	polling
MPI	8	4	15	8
HCMPI	8	4	4	16

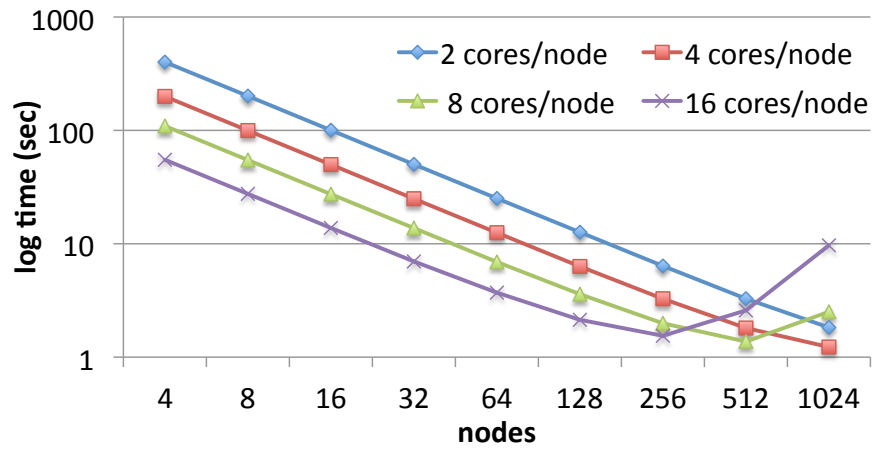
Table 4.4 : Best UTS configurations on Jaguar for 64 compute nodes

idle computation workers may get back to work. Once the communication worker receives a globally stolen work item, it pushes that item onto its own deque to be stolen by idle computation workers. Finally, the communication worker participates in a token passing based termination algorithm, also used in the reference MPI code.

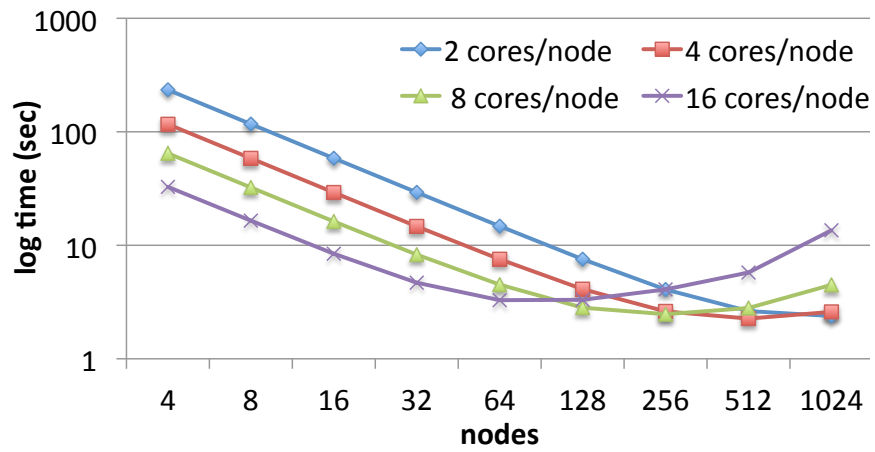
In our experiments, we use two UTS tree configurations, T1XXL and T3XXL. T1XXL uses a geometric distribution and generates about 4 billion tree nodes. T3XXL uses a binomial distribution and generates about 3 billion tree nodes. We varied the number of compute nodes from 4 to 1024 and cores per node from 1 to 16 in our experiments. To identify the best performing UTS configurations on Jaguar, we explored various chunk sizes, $-c$, and polling intervals, $-i$, on 64 compute nodes with 16 cores on both MPI and HC MPI for T1XXL as well as T3XXL. The chunk size parameter refers to the number of nodes that are offloaded to a thief during work-stealing. The polling interval parameter refers to the number of tree nodes that a worker explores before releasing a chunk of nodes from the stack to the work-stealing deque, provided the stack contains sufficient number of tree nodes. Adjusting the chunk size and polling interval are important as they help in mitigating the overheads of steals and stack-to-deque release operations while maintaining a balanced load across workers. Table 4.4 provides the best chunk size and polling intervals we

found. The best configuration of MPI for T1XXL was $-c = 4, -i = 16$, while for T3XXL was $-c = 15, -i = 8$. These configurations performed better on Jaguar than the published configurations in [100]. The best HCMPI configuration for T1XXL was $-c = 8, -i = 4$, while for T3XXL was again $-c = 8, -i = 4$. Finding the best UTS chunk size and polling intervals for each node and cores per node combination is outside the scope of this work. Only fixed size chunks and fixed polling intervals considered. Using adaptive algorithms can be considered in future work. Hence we use the values presented in Table 4.4 for all possible node-core combinations. In our experiments, we allocate the same number of resources for both MPI and HCMPI. This means HCMPI runs one fewer computation worker per node than MPI because it dedicates one thread as communication worker. E.g. When using 4 nodes with 16 cores per node, MPI runs $4 \times 16 = 64$ processes, whereas HCMPI runs $4 \times 15 = 60$ computation workers and 4 communication workers, one per node. The MPI implementation uses `MPI_THREAD_SINGLE`. Our results show that despite this disparity, HCMPI performs exceedingly well compared to MPI. This underlines our premise that dedicating cores for communication by using one or more MPI processes per node will be inexpensive for compute nodes with hundred of cores in the near future.

Figures 4.11a and 4.11b show the running times of MPI for T1XXL and T3XXL workloads respectively. Similarly, Fig. 4.12a and 4.12b show the running times of HCMPI for T1XXL and T3XXL workloads. Individual lines show the performance for different number of cores per node. For MPI, each extra core amounts to an extra MPI process per node, where as for HCMPI it amounts to an extra thread in the process on that node. For T1XXL, MPI stops scaling after approximately 4096 cores, and then starts degrading rapidly. In contrast, HCMPI scales perfectly to about 8192 cores without further degradation. Results for T3XXL also show similar trends.

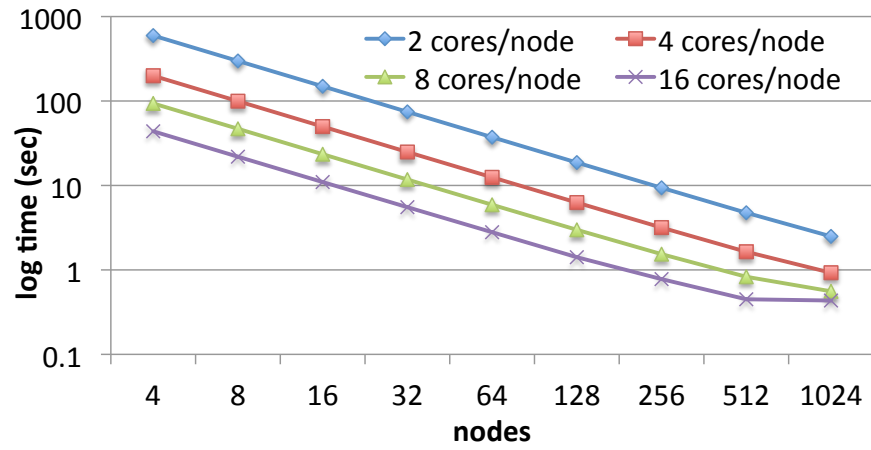


(a) T1XXL

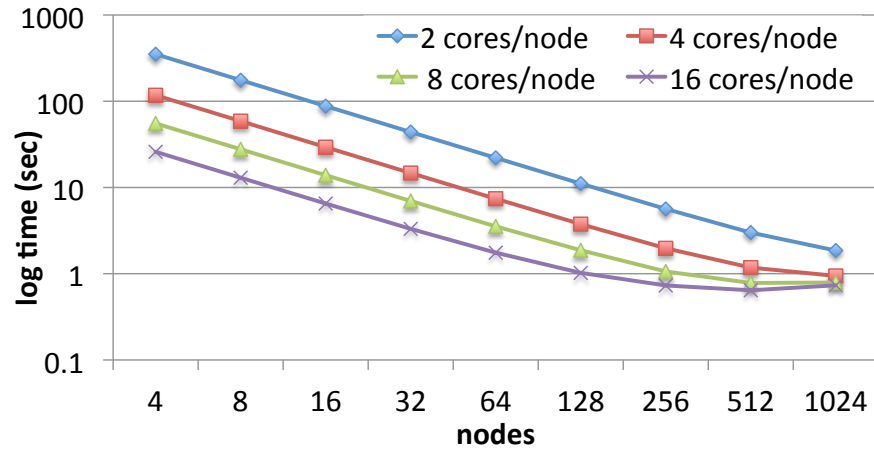


(b) T3XXL

Figure 4.11 : Scaling of UTS on MPI.

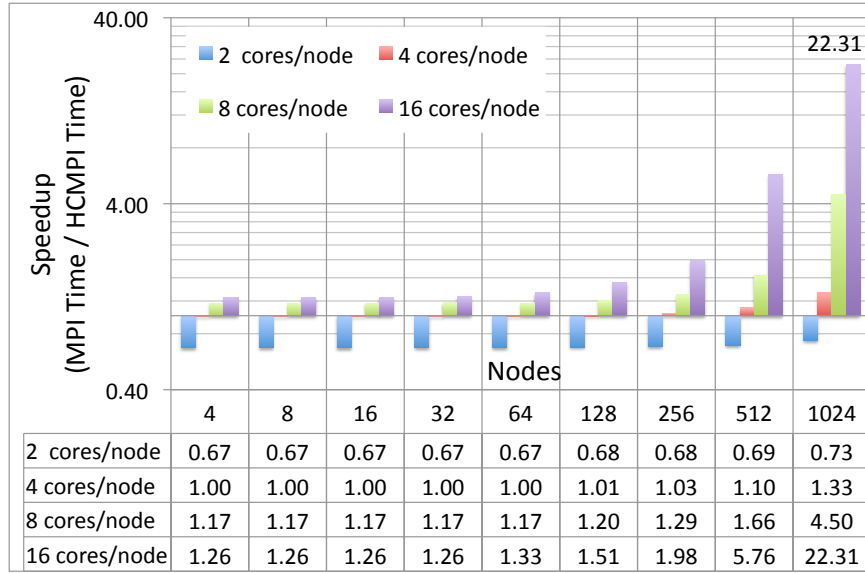


(a) T1XXL

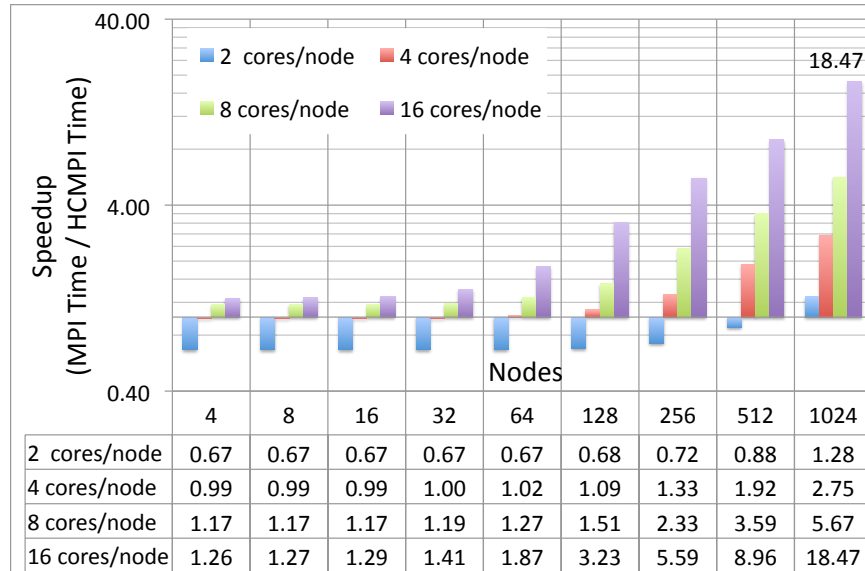


(b) T3XXL

Figure 4.12 : Scaling of UTS on HCMPI.



(a) T1XXL



(b) T3XXL

Figure 4.13 : HCMPI speedup compared to MPI

Figures 4.13a and 4.13b compare performance of HCMPI with MPI on T1XXL and T3XXL respectively. The peak performance improvement is about 96% for 1024 nodes with 16 cores per node. In regions where MPI scales very strongly, HCMPI achieves almost 50% improvement. A distinct crossover point in performance can be noticed in favor of HCMPI when the number of cores per node scales up. At 2 or 4 cores per node, HCMPI suffers from lack of parallel workers compared to MPI. But, as we scale up to 8 and 16 cores on the node, HCMPI outperforms MPI.

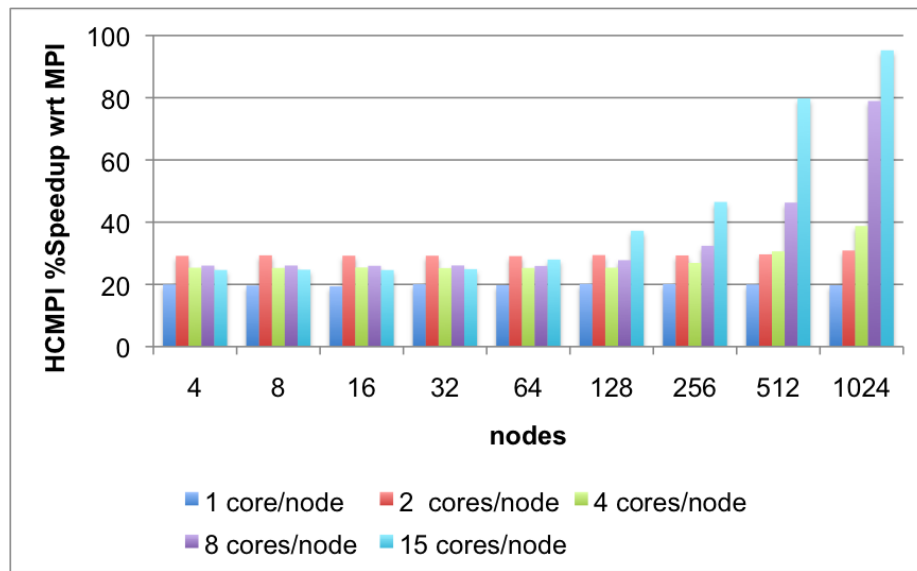


Figure 4.14 : HCMPI speedup compared to MPI on UTS T3XXL with extra communication worker

We also compared MPI with HCMPI by allocating HCMPI one more core than MPI to compensate for the communication worker which does no actual computation. In such configuration, shown for T1XXL in Fig. 4.14, the HCMPI performance is always better than MPIs performance, with a minimum speedup of 19% for 16 nodes in 1 core per node case.

1024 Nodes	MPI					HCMPI				
Cores	Time(s)	Work(s)	Overhead(s)	Search(s)	Fails	Time(s)	Work(s)	Overhead(s)	Search(s)	Fails
2	1.696	1.416	0.047	0.225	2703979	2.663	2.377	0.014	0.260	9861326
4	1.245	0.702	0.026	0.440	7869775	0.963	0.786	0.005	0.162	6279535
8	2.376	0.392	0.019	1.715	47102587	0.728	0.368	0.003	0.331	9212784
16	10.770	0.195	0.011	9.295	94754150	0.443	0.171	0.002	0.261	8835986
256 Nodes	MPI					HCMPI				
Cores	Time(s)	Work(s)	Overhead(s)	Search(s)	Fails	Time(s)	Work(s)	Overhead(s)	Search(s)	Fails
2	5.941	5.698	0.169	0.073	601384	9.641	9.511	0.053	0.076	584293
4	3.052	2.818	0.090	0.142	1603756	3.240	3.148	0.021	0.071	640242
8	1.829	1.532	0.054	0.233	2027647	1.561	1.479	0.011	0.069	562496
16	1.457	0.775	0.034	0.510	2353054	0.793	0.691	0.005	0.095	824427
64 Nodes	MPI					HCMPI				
Cores	Time(s)	Work(s)	Overhead(s)	Search(s)	Fails	Time(s)	Work(s)	Overhead(s)	Search(s)	Fails
2	23.231	22.534	0.643	0.054	33814	38.216	37.947	0.215	0.054	54509
4	11.708	11.323	0.339	0.046	127823	12.736	12.608	0.078	0.049	74264
8	6.518	6.237	0.207	0.073	456853	6.017	5.919	0.041	0.057	104471
16	3.431	3.075	0.127	0.189	203836	2.842	2.765	0.019	0.057	80501

Table 4.5 : UTS overhead analysis for T1XXL runs on Jaguar

To analyze this result further, we profiled both MPI and HCMPI codes using the built-in performance counters in the UTS application. First, the overall execution time is split into the following components: *work*, *overhead*, *search* and *idle*. *Work* represents the actual time spent on computation, that is, exploring nodes in the search tree. *Overhead* represents the time spent on making progress for others with global communication. MPI computation workers interrupt *work* every polling interval for this. In HCMPI, the communication worker handles all external requests for work, which implies that the computation workers are never interrupted. The *overhead* component for computation workers comes from releasing chunks of work from the local stack to the work-stealing dequeues. *Search* represents the time spent trying to globally locate work. MPI workers enter this mode once they completely run out of work. When an HCMPI worker runs out of local work and cannot steal work from the other intra-process workers as well, it starts the *search* phase by requesting the communication worker to globally locate work. There can be only one active *search* phase per process. Searching for intra-process work is not counted. When a *search* phase is active, the idle worker keeps looking for intra-process work and may start computation if it can find work. *Idle* time is the time spent in startup and termination. This is irrelevant for our comparison as we use the same startup and termination algorithms in both MPI and HCMPI. Next, we also profiled the total number of failed steal requests during program execution. These numbers do not include intra-process failed steals in HCMPI. Inter-process failed steals represents the total amount of redundant communication in the system.

Table 4.5 provides statistical data for three node configurations: 64, 256 and 1024. We chose these three nodes as being representative of three regions of MPI’s scaling results: strongly scaling, partly scaling, reverse scaling. We show these results

for only T1XXL for brevity. We have verified that results on T3XXL have similar characteristics. As before, we provide exactly the same number of resources for MPI and HCMPI for fair comparison.

It is evident that for both MPI and HCMPI, *work* overshadows the *overhead* time, although HCMPI consistently shows $5\times$ smaller overhead. This is because the computation worker only ever interrupts itself to inject more work into the work-stealing deque. It never has to deal with responding to communication, something which is handled by the communication worker. For lower number of cores per node (e.g., 2 cores per node), the *work* component is higher for HCMPI compared to MPI which directly influences the overall running time, since HCMPI has few workers compared to MPI. For low core counts, this leads to up to 50% more work per computation worker thread. Most importantly, it is evident that for higher cores per node, the *search* component becomes the biggest bottleneck for MPI performance. For example, on 1024 nodes, when going from 8 cores to 16 cores, MPI spends $5.4\times$ more time in the *search*. In comparison, HCMPI’s *search* component remains fairly stable. Consequently, HCMPI’s improvement over MPI when scaling from 8 cores to 16 cores in that configuration is $22.3/4.5 \approx 5\times$. Similarly, when going from 4 to 8 cores, MPI spends $3.9\times$ more time in *search*, which is reflected in HCMPI’s $4.5/1.33 \approx 3.4\times$ speedup during the same scaling when compared to MPI.

To understand why MPI spends more time in the *search* phase, we profiled the number of failed steal requests (see Fails column in Table 4.5). We observed that MPI has $10.7\times$ and $5.1\times$ more failed steal requests for 1024 nodes with 16 and 8 cores per node cases respectively, which can be accounted for the bulk of extra *search* time presented before. MPI steal requests are two-sided. The thief has to send a steal request to the victim and wait for a response. Failed two-sided steals imply redundant

communication, an inherent drawback of the MPI work-stealing model. On the other hand, majority of HCMPI steals are intra-node shared-memory steals where a worker thread can directly steal from another worker's deque without disturbing the victim. From these results, we conclude that HCMPI's faster stealing policy coupled with a highly responsive communication worker per node results in better computation and communication overlap and scalable performance.

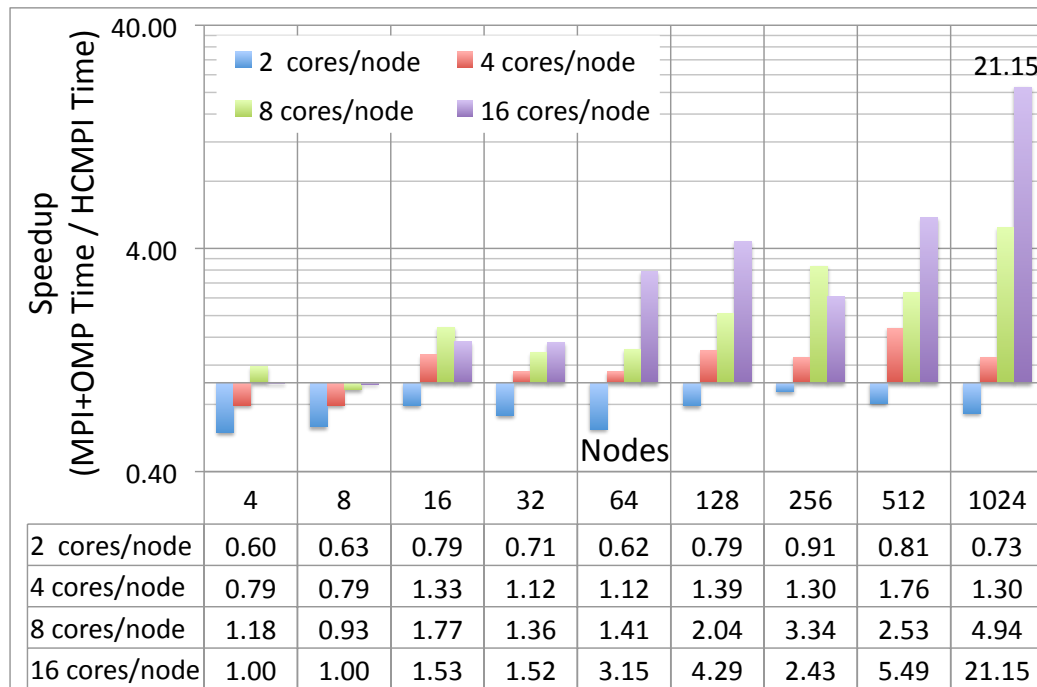


Figure 4.15 : HCMPI Speedup compared to MPI+OpenMP on UTS T1XXL

Comparison with MPI + OpenMP:

Although there is no publicly available reference implementation of UTS using MPI and OpenMP in a hybrid model, we have created one ourselves by integrating the reference MPI and OpenMP codes. Similar to HCMPI, the OpenMP threads participate in intra-process work-stealing. The key difference is that the hybrid model

does not dedicate a thread to be a communication worker. In the initial implementation plan, the MPI process first ensures locally available work before starting an OpenMP parallel region to execute that work. After the threads complete execution locally, the parallel region ends and the program goes back to MPI mode to search for more global work. This naive staged approach however suffered terribly from thread idleness problems resulting in worse performance than MPI. As an improvement we increased the computation and communication overlap. In the OpenMP parallel region when threads run out of work and cannot find anything to steal, they wait at a cancelable barrier. In case more local work becomes available, the barrier gets canceled and waiting threads re-enter the execution region. In our hybrid implementation, when a thread gets to the cancelable barrier, it requests for global work. So, a global steal request goes out even when some threads are busy computing. If global work arrives when the parallel region is active, the work gets folded into local work by the thread that receives it. This approach drastically improved performance over the naive implementation. This hybrid model has to deal with two issues. First, an OpenMP thread has to interrupt its work every polling interval to service external steal requests if no other thread is already acting as the communication worker. Second, MPI has to be used in one of the multithreaded modes, such as `MPI_THREAD_SERIALIZED` or `MPI_THREAD_MULTIPLE`. We compare its performance against HCMPI on T1XXL in Fig. 4.15. In this experiment the hybrid code used one MPI process on every node. The number of OpenMP threads were the same as the total number of worker threads (computation + communication) used by HCMPI, for a fair comparison. The results show similar speedups for HCMPI over the hybrid version.

4.4 Summary

In this chapter we presented the HC-COMM runtime and the HCMPI programming model targeted towards a software solution for extreme-scale systems. We demonstrated scalable performance with the help of a novel runtime design that dedicates one core for communication and the others for computation in every compute node. We evaluated our approach on a set of micro-benchmarks as well as larger applications and demonstrate better scalability compared to the most efficient MPI implementations. We presented a unified programming model to integrate asynchronous task parallelism with distributed-memory parallelism. For the UTS benchmark on the ORNL Jaguar machine with 1024 nodes and 16 cores/node, HCMPI performed $22.3\times$ faster than MPI for input size T1XXL and $18.5\times$ faster than MPI for input size T3XXL (using the best chunking and polling parameters for both HCMPI and MPI).

Chapter 5

Locality Control of Compute and Data

Future extreme-scale systems will be severely constrained by energy and power budgets. Innovative memory designs are expected to be critical for meeting those challenges. Current memory architecture designs in multicore systems typically involve an off-chip large capacity low bandwidth DRAM module, and assisted by faster on-chip low capacity high bandwidth coherent cache modules. There are two basic problems in such designs. First, scaling the large DRAM for tightly coupled node architectures to service thousands of cores on a node is not feasible because of energy and bandwidth limitations. Second, scaling the current cache coherency designs is also not feasible due to energy constraints and memory controller bottlenecks. Extreme-scale designs will need to sacrifice both coherent memory as well as shared memory per core. As a result, future memory designs for such architectures will target high bandwidth fast local software controlled memory units that are physically close to each processor.

A direct outcome of future memory architecture changes make software technology a key factor in achieving high performance. Without a coherent cache architecture and with fast local memories, software needs to explicitly control both data movement and the consistency of shared data on the system. Intra-node data locality optimization will have one of the biggest influences on performances and there two ways to approach the challenge. One way is for compilers to optimize data layout and data access patterns in order to get maximum reuse of the data inside a task's computation.

There has been much past work related to the role of compiler in maximizing data reuse. Another approach is to influence the spatial and temporal locality of task computations that use similar data blocks in memory in order to get maximum reuse of data across tasks. This is an area that has not been explored very well yet and forms a part of our research focus. Both approaches can coexist. Finally, it is also necessary to optimize inter-node data distribution for applications such that we can reduce the amount of inter-node communication. Such an optimization would also directly translate into energy savings.

In this chapter, we focus on two areas for locality control. First, we present a programming model for inter-node data distribution called **HAPGNS** (Habanero Asynchronous Partitioned Global Name Space). **HAPGNS** is a distributed data-driven programming model that integrates intra-node and inter-node macro data-flow programming. We build this model on top of the **HC-COMM** runtime that was described in chapter 4. Unlike the **HCMPI** programming model, **HAPGNS** does not require any knowledge of MPI. In the second focus area for locality control, we describe a locality tuning framework for controlling locality of tasks sharing the same data in a dynamic task parallel environment. This framework is geared towards its use by experts with detailed system knowledge. These optimizations aim to benefit from spatial and temporal task locality using runtime co-scheduling of tasks for **HPT**, a hierarchical place tree construct used to model the memory hierarchy of a system.

5.1 Research Contributions

The contributions of this research work can be summarized as follows.

- A novel macro data flow programming model for distributed systems, called **HAPGNS**, is presented. The design and implementation uses the **HC-COMM**

runtime but the programmer is abstracted from the use of MPI. The HAPGNS model allows users to control data locality with custom data distribution functions.

- The design and implementation of the HPT model for the Habanero-C language and runtime. The HPT model is drawn from past work in Habanero-Java [13] with a few differences. First, the HPT implementation in HC maintains a deque per worker on each place. This makes the process of pushing work on a place to be non-synchronized with other workers. Second, the HPT model is completely integrated with the Habanero-C runtime scheduler for both regular tasks and data-driven tasks.
- The design and implementation of a novel deque resizing algorithm that enables lock free expansion and contraction along with greatly reduced memory copy operations.
- The design and implementation of a novel tuning framework that allows spatio-temporal locality control of compute and data. We describe the tuning execution model which integrates a tuning scheduler and the HC runtime scheduler. We integrate the tuning tree data structure with the HPT model for a unified tuning framework.

5.2 The Habanero Asynchronous Partitioned Global Name Space Model

Habanero APGNS (Asynchronous Partitioned Global Name Space), is a distributed data-driven programming model that integrates intra-node and inter-node macro

data-flow programming. It does not require any knowledge of MPI. The model assumes a global *name* space, instead of an *address* space as in PGAS languages. The programmer perspective is to partition the problem size into data blocks referred with globally unique identifiers. Data movement is abstracted with simple **put** and **get** operations. The goal of this distinction is to simplify both programmability and implementation of the model.

5.2.1 HAPGNS Programming Model

In the Habanero APGNS model, we introduce *distributed* data-driven futures (DDDF) as an extension to the intra-node DDFs introduced in Section 3.2.2. DDDFs enable unconstrained task parallelism at the inter-node level, without concerning the user about details of inter-node communication and synchronization. Thus, DDDFs can even be used by programmers who are non-experts in standard MPI. DDDFs carry the dynamic single assignment property of a DDF object. They also include a node affinity known as a *home* location. The API `DDF_HANDLE(guid)` creates a handle on a DDDF identified by `guid`, a user managed globally unique id for the DDDF. The user provides two callback functions for the HCMPI runtime called `DDF_HOME(guid)` and `DDF_SIZE(guid)`. These functions should respectively provide a mapping from a `guid` to a DDDF home rank and the **put** data size.

DDDFs can be used just the same way as DDFs are used in the intra-node HC model. DDDFs can be used for specifying task dependences in an **await** clause of an **async** statement. Producer and consumer tasks coordinate data movement through **put** and **get** operations. To understand the programming model better, let us consider a simplified version of the Smith-Waterman local sequence alignment benchmark in Fig. 5.1 as a DDDF example. A 2D matrix of DDDFs is allocated in which each DDDF

element corresponds to a 2D computation block on the SmithWaterman matrix. A task is created for computation of each block and has 3 data dependencies: the left tile on the same row, the upper tile on the same column and the diagonal tile on the previous row and column. This is shown by the `async await` statement on line 25 which the three dependences being *above*, *left* and *uLeft*. Once a task is ready for execution, the 3 data inputs are fetched using the `DDF_GET` API. The `await` clause ensures that the `DDF_GET` is a non-blocking call. Once the inputs are ready, the tile computation is done inside the *compute* function. Finally, after the computation ends the `DDF_PUT` on the current tile `DDDF` is done to satisfy the dependence on other tasks waiting on this tile. The code in Fig. 5.1 implements a distributed memory data-driven version of the benchmark. The only change from a shared memory version is the use of `DDF_HANDLE` instead of `DDF_CREATE`, and the creation of user-provided `DDF_HOME` and `DDF_SIZE` function definitions. The `DDDFs` are of size `Elem`, which is the data type used for `DDF` data fields in this benchmark. The `DDF_HOME` macro in this example performs a cyclic distribution on the global id, which enforces a row-major linearization of the distributed 2D matrix.

The actual implementation of the SmithWaterman algorithm employs a 4D tiling to exploit both inter- and intra-node parallelism. The 4D tiling is a hierarchical decomposition such that outer level tiles are distributed among the nodes and each outer level tile is further decomposed into inner level tiles to execute on the cores. Its parallelism structure is shown in Fig. 5.2. `DDDFs` are a natural fit for describing such data dependence patterns and can seamlessly integrate the inter- and intra-node level parallelism. OpenMP tasks or Cilk, on the other hand, require additional coding efforts to describe these task dependencies, while OpenMP threads requires barrier synchronization after every wavefront.

```

#define DDF_HOME(guid) (guid % NPROC)
#define DDF_SIZE(guid) (sizeof(Elem))

DDF_t** allocMatrix(int H, int W) {
    DDF_t** matrix=hc_malloc(H*sizeof(DDF_t*));
    for (i=0;i<H;++i) {
        matrix[i]=hc_malloc(W*sizeof(DDF_t));
        for (j=0;j<W;++j) {
            matrix[i][j] = DDF_HANDLE(i*H+j);
        }/*for*/ }/*for*/
    return matrix;
}

DDF_t** matrix2D=allocMatrix(height,width,0);
doInitialPuts(matrix2D);
finish {
    for (i=0,i<height;++i) {
        for (j=0,j<width;++j) {
            DDF_t* curr = matrix2D[i][j];
            DDF_t* above = matrix2D[i-1][j];
            DDF_t* left = matrix2D[i][j-1];
            DDF_t* uLeft = matrix2D[i-1][j-1];
            if ( isHome(i,j) ) {
                async await (above, left, uLeft) {
                    Elem* currElem = init(DDF_GET(above),
                                           DDF_GET(left),DDF_GET(uLeft));
                    compute(currElem);
                    DDF_PUT(curr, currElem);
                }/*async*/ }/*if*/ }/*for*/ }/*for*/
        }/*finish*/

```

Figure 5.1 : Simplified Smith-Waterman implementation

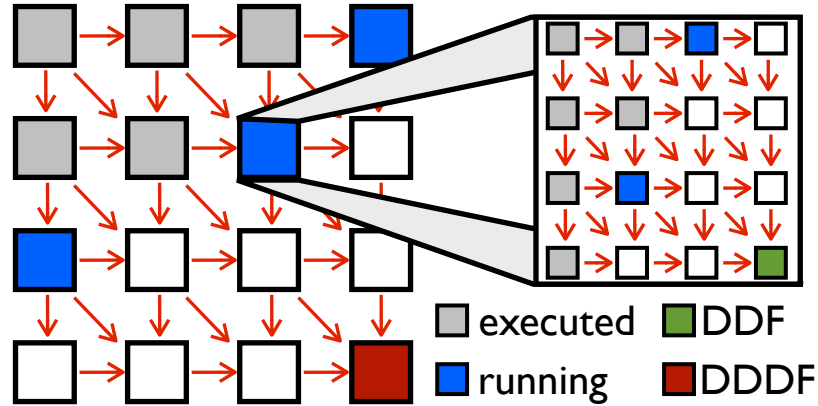


Figure 5.2 : Smith-Waterman dependency graph, its hierarchical tiling and execution wavefronts

5.2.2 Implementation

The Habanero APGNS model is implemented as an extension of the runtime infrastructure described in Section 4.2. This runtime design extends the data-driven scheduler to support *distributed* data-driven scheduling, and introduces *listener* tasks on the communication worker. Distributed data-driven futures, introduced in Section 5.2.1, are created using the `DDF_HANDLE` interface. The call always returns a locally allocated handle. The user-provided `DDF_HOME` function is used by the creation routine to identify if the DDDF is owned locally or remotely, and the local handle is marked accordingly. The DDDF *home* provides a fixed location for remote tasks to either transfer data in case of a remote `put` or to fetch data in case of a remote `get`.

In a typical Habanero APGNS program, after a producer task completes computation on a data block, it performs a `put` operation on the associated DDDF object. If the `put` happened on a remote node, then the data is transferred to its *home* location through a listener task. Listener tasks are persistent tasks that the DDDF runtime

uses on a communication worker’s worklist to listen to asynchronous messages with predefined tags. The runtime executes a global termination algorithm to take down all the *listener* tasks at the end of the program. These tasks support a handler routine which is called by the communication worker whenever a message arrives for the listener. In the case of a remote **put** received by the listener, the handler routine would make sure that the data is first buffered locally. The follow-on operations at the home location are common for both the local and remote **put**. The runtime checks if there are any outstanding fetch requests of the DDDF data, and if so, then the data is transmitted to all of them. Then the communication worker starts another *listener* task for this particular DDDF object to respond to future fetch requests.

On the consumer side, a data-driven task performing an **async await** on a remote DDDF would register on the local copy of the DDDF handle. After the first DDT registers, the runtime sends the DDDF home location a message to register its intent on receiving the **put** data. The runtime also allocates a local buffer to receive the data, and waits for the response from the home node. Once the data arrives, the runtime does a **put** on the local DDDF handle. This releases all DDTs registered on the local handle. A consumer node always keeps a locally cached copy after the data arrives so that every subsequent **await** can immediately succeed. The dynamic single assignment property of DDDFs ensures the validity of this local copy. Hence, the data transfer from home to remote happens at most once.

The basic idea behind distributed DDFs is similar to the Linda [102] coordination language. The Linda model works with a *tuplespace*, akin to a globally shared memory, and supports operations such as *in*, *out*, *rd* and *eval*. The *out* and *rd* operations write and read from the tuplespace, similar to the **put** and **get** operations supported by the DDDF model, while the *in* operation destructively reads from the tuplespace. While

the DDDF model is based on the single assignment property of data objects, Linda allows multiple assignments. This causes a complication for the Linda runtime as data needs to be coordinated by a runtime manager process. For example, an *out* operation broadcasts that write to all the processors. Also, without the support for data distribution function like the DDDF model, Linda's performance comes at the cost of communication bandwidth and local memory.

5.2.3 Results

Habanero APGNS provide high programmability where simple extensions to existing shared memory programs can create a scalable distributed memory application. We introduced a simple Smith-Waterman benchmark in section 5.2.1 and here we show a hierarchically tiled implementation of the benchmark. This implementation performs hierarchical tiling as in Figure 5.2. This allows us to tune granularity to minimize communication for the outer-most tiling and to minimize intra-node task creation overhead for the inner most tiling, while retaining sufficient parallelism at both levels.

An outer tile consists of a matrix of inner tiles, and three DDDFs. On Figure 5.2, we show an enlarged outer tile consisting of a matrix of inner tiles. To minimize communication, the DDDFs for the outer tile are the right-most column, the bottom-most row and the bottom-right element, since these are the edges of a tile visible to neighboring tiles. Similarly, an inner tile encapsulates a matrix of elements and three shared memory DDDFs to represent the intra-node visible edges of an inner tile. Given this representation of the dynamic programming matrix, we have exposed both the inter-node and intra-node wavefront parallelism through registering neighboring tiles' distributed and shared memory DDDFs respectively.

On Figure 5.3, we present a scaling study of the implementation mentioned above.

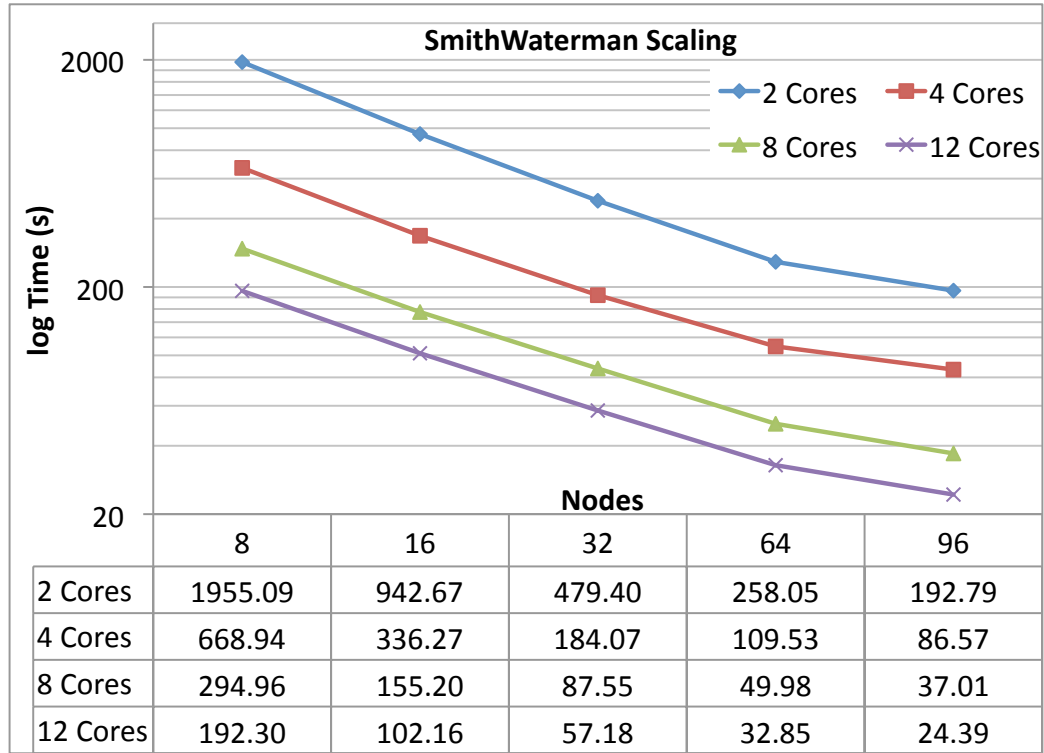


Figure 5.3 : Scaling results for Smith-Waterman for 8 to 96 nodes with 2 to 12 cores

Our sequences are of length 1.856M and 1.92M, giving us the dimensions for our matrix. We chose tile sizes 9280 by 9600 for outer tile sizes for a matrix of 200 by 200 tiles.

We chose this tile size to ensure the number of wavefronts provides sufficient slackness with respect to the number of nodes. The top left and the bottom right sections of the matrix do not provide sufficient parallelism and as their size passes beyond a minute fraction, it constrains parallelism due to Amdahl's law. Since the number of parallel tasks at any given time is the size of an unstructured diagonal (as in figure 5.2), to provide enough parallelism, we need to have at least a factor of the number of nodes on most diagonals. The same logic applies to the inner tiles too, and we have chosen 290 by 300 tile sizes to have 32 by 32 tiles.

Using a distribution function, `DDF_HOME`, for DDDFs, we implemented a tiling strategy as follows. Every proper diagonal is measured in size and every contiguous chunk of that diagonal is assigned to nodes iteratively. This provides a mapping to nodes which for each node creates bands perpendicular to the wavefront and leads to less communication.

Given a fixed number of cores we observe speedups in the range $1.7 - 2$ when doubling the number of nodes until 64 nodes. This trend is hampered on the 64 node to 96 node jump because, because the first and last 96 diagonals do not have enough parallelism for 96 nodes, where the total number of diagonals is 399.

Given a fixed number of nodes, we observe speedups in the range 2.2-2.9 for 2 to 4 core case, since one of the workers is designated as a communication worker. The range is between 5.2-6.6 for 2 to 8 cores (for 1 to 7 computation workers), and 7.9-10.2 for 2 to 12 cores (for 1 to 11 computation workers).

5.3 Habanero-C Tuning Framework

The software challenges in future extreme-scale systems are compounded by the need to support new workloads and application domains that have traditionally not had to worry about large scales of parallelism in the past. Adapting these applications to run optimally on extreme-scale systems would be beyond the expertise of programmers with only domain knowledge. As a result, a *tuning* expert with detailed system knowledge will extract superior performance from the application. However, without a detailed knowledge about the application domain, the tuning expert will find it difficult to be highly productive. We aim to bridge this gap between the tuning and domain experts by forming a tuning framework which makes it possible for the tuning expert to make performance optimizations without much domain knowledge.

The considerations of parallelism, load balancing and locality, are separate from considerations of the application domain and algorithms. When creating or modifying the application algorithms, there are no explicit parallel constructs to worry about. When thinking about mapping to the platform, there is no need to wade through the application semantics. The tuning framework targets performance benefits from spatial and temporal locality of tasks in a dynamic task parallel environment. With the cost of moving data projected to become increasingly prohibitive in future, the performance of a system will be increasingly sensitive to the the spatio-temporal locality of tasks which access common data blocks. Spatial locality of tasks mean execution of parallel tasks on parallel processors with a shared memory structure. Spatial locality should also be in combination with task temporal locality for tangible performance benefits due to the limited size of memory units in future memory designs.

5.3.1 Hierarchical Place Trees for Spatial Locality

Future extreme scale systems are expected to have computing nodes containing thousands of processor cores and designing a memory subsystem for such an architecture is great challenge. It will not be feasible to build a large DRAM-like memory structure shared among all processor cores mainly due to bandwidth and power limitations. Current indications point towards an architecture with deep memory hierarchies with computing cores provided with fast local limited memories. Data accesses latencies are expected to dramatically increase as memories further up the hierarchy are used. Exploiting data locality in parallel programming on those complex is a challenge for users. Prior compiler and runtime research has proved that, in sequential code, lots of data locality optimization can be achieved by advanced data flow analysis and sophisticated code transformation techniques, such as polyhedral model. Efforts

to bring those techniques into parallel programming needs supports from both the system modeling and the runtime. We present our approach of modeling complex memory hierarchy of various computing systems as a hierarchical place tree (HPT). HPTs provide an abstraction powerful enough to exploit locality at each level in the memory hierarchy, without compromising performance. Finally, it is a step towards performance tuning optimizations with explicit data locality control on exascale systems.

HPTs in Habanero-C abstract the underlying hardware using trees, which closely model the memory hierarchy of the node. It allows the program to spawn tasks at *places*, which for example could be cores, groups of cores sharing cache, nodes, groups of nodes, or other devices such as GPUs or FPGAs. Figure 5.4 shows an example HPT implementation structure of a Intel Xeon Dual Quad Core machine. A single node of this machine has a shared DRAM for all 8 processor cores. The chip has 2 sockets with 4 processors in each socket. The processors in each socket share a single L3 cache. Within each socket two groupings of 2 processors share a L2 cache. Each processor core comes with it own local L1 cache. The HPT structure shown in Figure 5.4 implements this memory hierarchy as a 3 level binary tree. Every node in the tree refers to a particular instance of the memory hierarchy. The leaf level nodes refer to the L1 cache of each processor core. The levels above the leaf refer to the L2 and L3 caches in the machine with the root of the tree referring to the shared DRAM. In the HPT each node of the tree is an unique **place**. Places are usually numbered starting at the root and proceed in a breadth first manner.

The Habanero-C language uses the **AT** clause with the **async** statement to spawn a task at a **place**. The **AT** clause takes a **place** argument. A typical usage is:

```
async AT(p) <stmt>
```

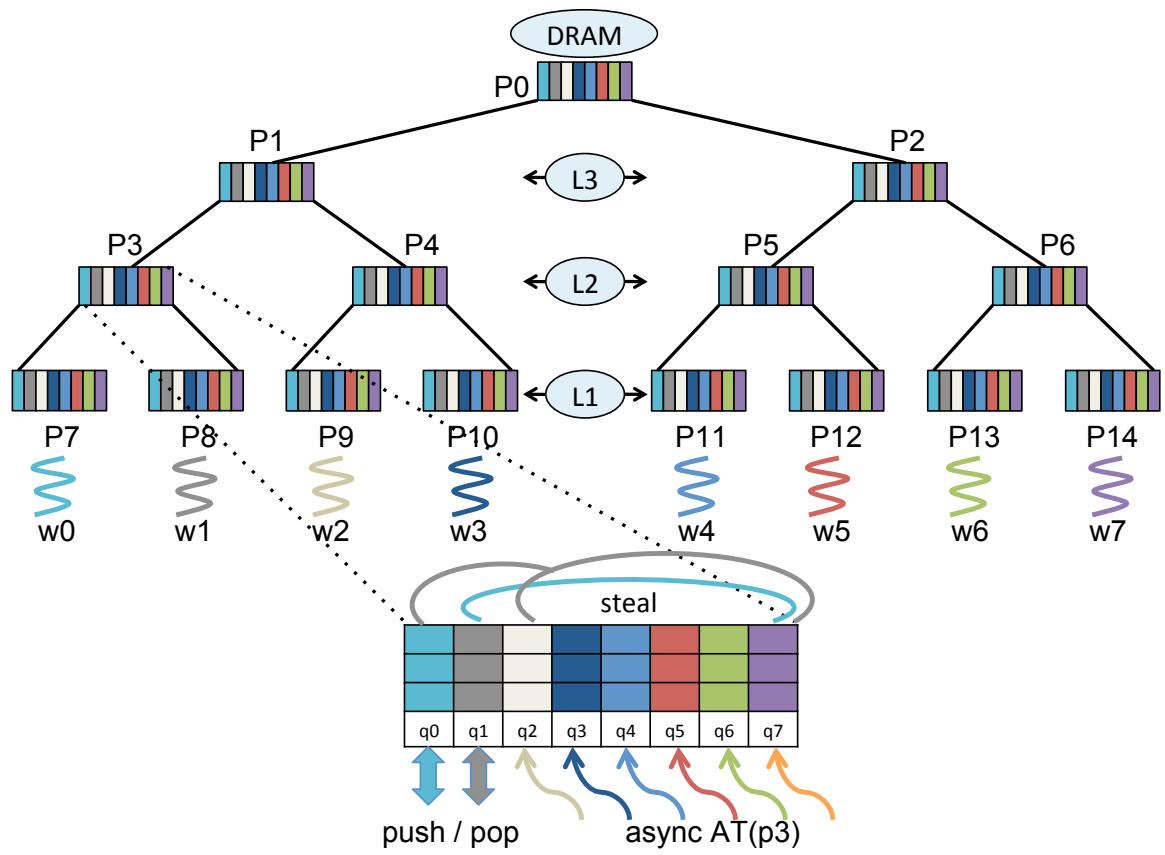


Figure 5.4 : An example HPT structure

This spawns the new task with body $\langle \text{stmt} \rangle$ at the place p . This way HPTs allow for explicit control of task locality on the system with the intention of shared data reuse. Worker threads, which are proxy for processor cores, are associated with leaf nodes of the HPT. A leaf **place** can have one or more worker threads attached. When a leaf **place** has only one worker thread attached, the node is usually the local exclusive memory of that processor, such as the L1 cache. However, if a **place** node in the HPT has multiple children, such as an internal node, or multiple workers on the leaf node, then, that **place** usually refers to a shared memory level. A task spawned at such a **place** will be executed by the worker thread associated with the subtree under that node. For example, a task that is put in place $p3$ can be executed by either worker thread $w0$ or $w1$. The main idea of the HPT is to limit access, as much as possible, to tasks to the set of worker threads in the subtree that share some memory hierarchy. However, a task placed in place $p7$ can only be executed by worker $w0$. The HC runtime provides APIs that help navigate the HPT structure and get a handle on a **place**.

5.3.2 Tuning Framework for Spatio-Temporal Task Locality

The Habanero tuning framework is a set of API's that can guide the execution of a task parallel program written in Habanero-C. The goal of the tuning framework is to support a tuning language or specification that can target these API's at the assembly-language level. This framework will use a separate tuning specification with distinct capabilities but used to complement the domain specification. Multiple tuning specifications can be associated with the same domain specification to target different in optimization goals on a target platform architecture. The foundation of the tuning specification is to identify computations that should be close in both time

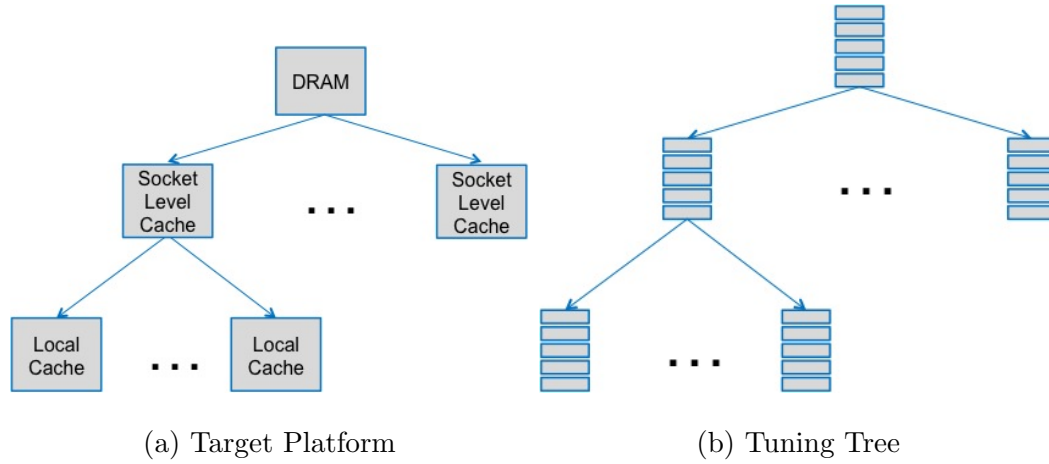


Figure 5.5 : Tuning tree of queues matches the target platform structure

and space. Closeness is identified by hierarchical affinities among computations and data. This allows the indication of relative degrees of locality. The basic concept of the tuning specification is the affinity collection, a group of steps, implemented as tasks, that the tuner suggests should be executed close in space and time. Hierarchical affinity groups allow the specification of relative levels of affinity, with tighter affinity at lower levels. Computations that touch the same data will not benefit from locality if they are too far apart in space or time. Hierarchical affinity groups are the tuning mechanism for indicating computations that must be proximate in both time and space. The tuning API provides the tuner with a mechanism to influence the scheduling of parallel tasks to take advantage of the space and time locality benefits.

The tuning execution model is based on a representation of the target platform, as shown in Fig. 5.5a. We currently assume that the platform is hierarchical, although the model can be adapted to other structures as well. The platform description names each level, for example, Level1, Level2, etc. or it might be address space, socket, core, etc. We distinguish between two components of the runtime: the tuning runtime and

the domain runtime. The tuning runtime serves as a staging area for the execution of steps in the domain component. A tuning action is defined for each affinity group. Tuning actions specify the low-level processing for that group in the tuning tree. The tuning actions control the flow of work to the domain runtime. The tuning tree has the same shape as the platform tree. There is a work queue associated with each node in the tuning tree, shown in Fig. 5.5b. The items in the queue are either static affinity groups/steps or dynamic instances of affinity groups/steps. Each queue contains work that is ready for an action to be performed (such as moving down the tree) and work that is not ready. The tuning runtime system selects from a queue the ready work item(s) that are nearest the head of the queue. Large static outer affinity groups start at the top of the tuning tree. As an affinity group is moved down a level in the tree, it will be decomposed into its components. Since components of a group at some node only move to children of that node (there is no work stealing), they have a tendency to remain close in the platform, in that nodes in the tuning tree correspond to nodes in the platform tree. Figure 5.6 shows an example tuning action for unpacking a group and moving it down the tuning tree. to execute a step, it has to get released from the tuning runtime onto the domain runtime. The set of tuning APIs that are currently supported are:

TUNING_PUT_AT_ROOT (group, args)

places a group or step at the root of the tuning tree

TUNING_MOVE_DOWN (group, args)

moves a group or step down unmodified one level in the tuning tree

TUNING_DISTRIBUTE_AMONG_CHILDREN (nargs, group, args)

unpacks a group and distributes the components among the children of the node

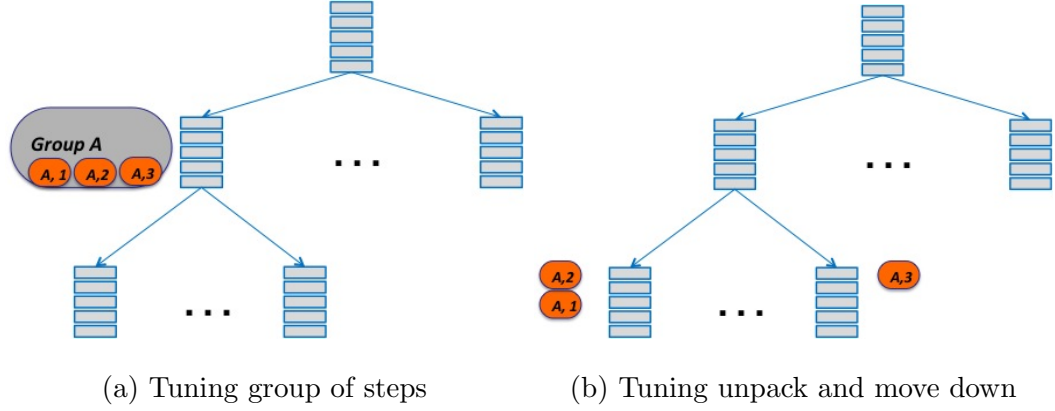


Figure 5.6 : Tuning action to unpack a group and move down the steps

TUNING_RELEASE_STEP (step, args)

places the step onto the domain runtime for execution

5.3.3 HPT Implementation

The HPT structure for a Habanero-C program is specified as an XML input document. If the HPT input is not specified, the HC runtime assumes a single place consisting of all the workers. Figure 5.7 shows the XML file structure for the Intel Xeon Dual Quad Core machine HPT shown in Fig. 5.4. The nested structure of the *place* attributes show the tree hierarchy and the *num* values replicate the subtree on each child of a node.

The Habanero-C work-stealing runtime, described in Section 3.2, takes advantage of the HPT hierarchy to preserve locality when executing tasks. In our design, any worker can push a task at any place in the HPT. Each place in the HPT contains one deque per worker. For example, Figure 5.4 shows each place having 8 dequeues, q_0 to q_7 , for the 8 workers, w_0 to w_7 . This gives each worker the ability to perform non-synchronized *push* and *pop* operations on their own dequeues at each place. The *steal*

```

<?xml version="1.0"?>
<!DOCTYPE HPT SYSTEM "hpt.dtd">
<HPT version="0.1" info="Dual quad-core Intel Xeon">
  <place num="1" type="mem">
    <place num="2" type="cache"> <! sockets >
      <place num="2" type="cache"> <! L2 cache >
        <place num="2" type="cache"> <! L1 cache >
          <worker num="1"/>
        </place>
      </place>
    </place>
  </place>
</HPT>

```

Figure 5.7 : An example of a HPT XML description

operations, however, have to be synchronized. The HC runtime limits pop or steal operations at a place to only the workers in the subtree of that node. For example, workers $w0$ and $w1$ only are permitted to perform pop and steal at place $p3$. Any of workers $w0$ to $w7$ are permitted to push at $p3$.

In the current scheduling heuristic employed by the HC runtime a worker starts the search for an executable task at the leaf place it is attached to. It first tries to pop tasks on its own deque in the place. If it fails to pop a task, it tries to steal from the other deques in the same place. When a worker runs out of work at a place, it tries to look for work at the parent place. The worker traverses the path from leaf to the root in search of work. After any successful pop or steal, the work executes the task and then resumes the search from its own deque on the leaf place, where it started from initially. The HC runtime makes sure that the worker threads are bound to the appropriate cores to resemble the correct sharing of the memory hierarchy.

One drawback of this design is the $O(n^2)$ number of deques on the system, where n refers to the number of workers. Although, this design provides non-synchronized push operation of a worker at any place, the overhead of searching for work increases. Each of n workers will search for work on $O(n \log n)$ deques. We are currently working on more efficient designs that will minimize this overhead without making all workstealing operations synchronous. One of design choices being considered is to maintain a deque per place for only those workers that are in the subtree and keep a separate deque for all other workers. So, if a worker is trying to push at a place while being outside the subtree of that place, that push would be a synchronous one. This rationale is based on application experiences where it was observed that the frequency of pushes to a place from a worker external to its subtree is relatively lower than pushes from within the subtree.

Scalable Deque Implementation

The current HC implementation requires all deques be initialized at the start of the program to a fixed size. The size of the deques may be set by the user (with the `-deqsize` runtime option) to be the maximum value that will fit all tasks than can potentially exist on one deque at any given instant. This is a problem because it may not always be possible to know this number before running the program. As a result, the user may try to over-provision the deque with a unnaturally large size to prevent deque overflow. This problem is exacerbated by the use of HPTs. We have seen from our design of the HPT that every place contains one deque per worker, meaning $O(n^2)$ deques for n workers. If large fixed sized deques are used, this would prove to be a severe scalability bottleneck for future extreme scale systems which are expected to have $O(10^3)$ processor cores per node.

This problem can be solved if the HPT is initialized with small *resizable* deques which can grow and shrink during program execution. It would avoid having the user to guess the largest deque size to avoid deque overflow. Further, one large fixed size need not be applied uniformly on all deques. On extreme scale systems, although there would be a high number of deques, the space complexity would be greatly improved. An efficient resizable deque solution will have two key requirements:

- Wait-free deque resize - We want to avoid freezing the deque when resizing so that concurrent steals are possible.
- Zero data copy - We want to avoid copying the whole deque for faster and reliable resizing.

The HC deque described in Section 3.2 supports push, pop and steal operations. The deques contain a head and tail to index both ends. Our solution for the resizable

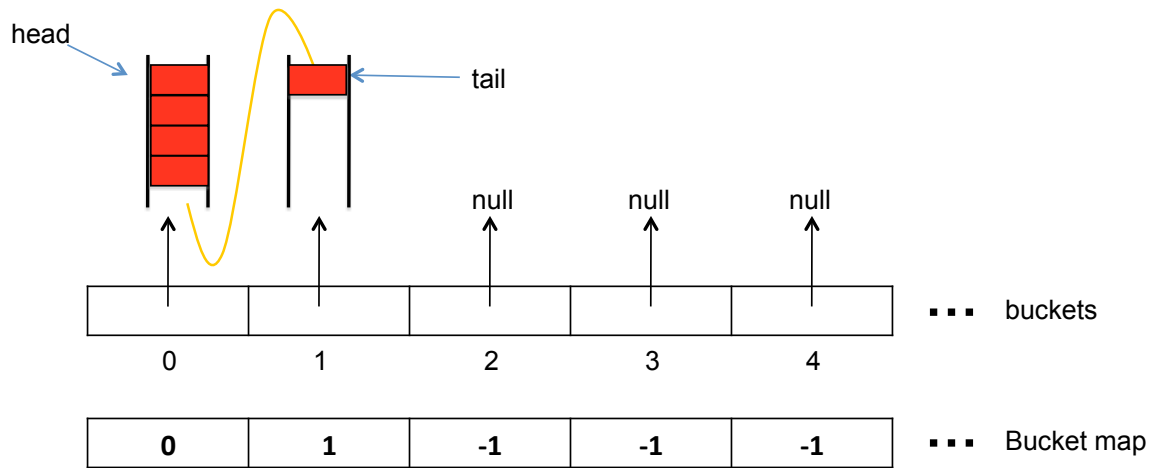


Figure 5.8 : Bucket deque expansion

deque is called the *bucket map* approach as shown in Figure 5.8. Deques are allocated in small chunks, called buckets, which are created and destroyed during the lifetime of a program. A new bucket is created when a deque needs to be expanded, while a bucket is destroyed when the deque shrinks. Each bucket is physically indexed through a bucket array. However, to map a head or tail position to a physical bucket, we use a bucket map. The bucket array and map are of the same size. In our design, the head and tail will keep increasing with the head following the tail in case of steals. The deque structure is initialized with the bucket array containing one deque bucket in the first location, or `bucket[0]`. When this deque fills up and needs to be expanded, a new bucket is allocated. The deque expansion scheme is shown in Figure 5.8, expanding the deque to two buckets. The new bucket is placed at the first available or *null* position in the bucket array. In this case, the first available position was the second location, or `bucket[1]`. The bucket map keeps track of this position by recording this bucket array index in the map. So, for example, when the tail has to be mapped to a bucket, we first need to find out the virtual bucket that contains the tail. The virtual

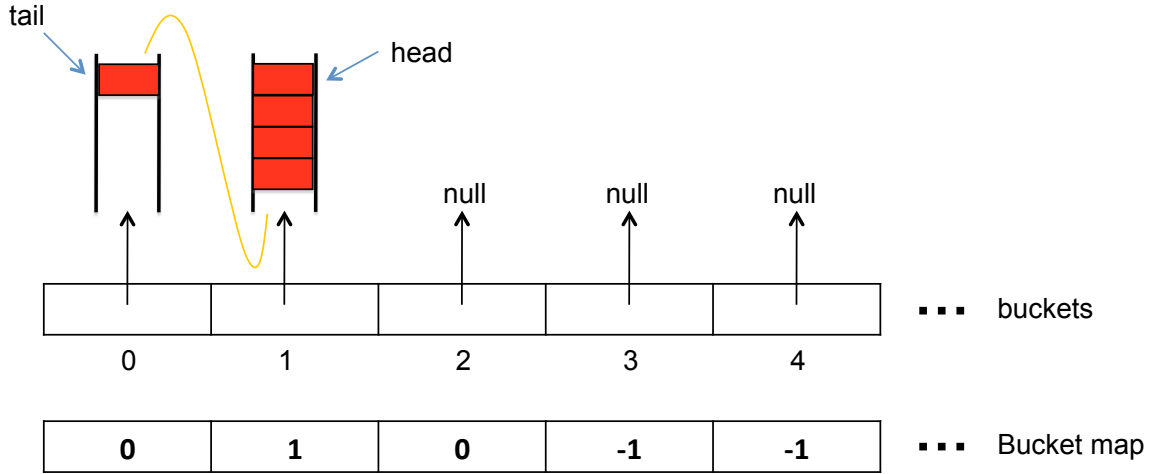


Figure 5.9 : Bucket deque reuse after contraction

bucket index on the bucket map provides the physical index into the bucket array for the actual physical bucket.

Now, say the steals on deque has reduced the deque size down to one bucket after it had expanded to two buckets. So, the bucket in position 0 of the bucket array is no longer used and it is freed. However, when the deque needs to be expanded once more, the new bucket can now be placed in bucket array position 0. This bucket reuse scheme is shown in Figure 5.9. The tail now has to map to the new location of the physical bucket via the bucket map. Hence, we can see that the virtual bucket index of the tail in the bucket map, which is 2, now contains the index 0, the actual physical location of the bucket.

Algorithms 1 shows the implementation of the deque push operation. Here, we can see how we use the deque tail ($deg.tail$) to identify the physical location of the deque where the task will be pushed. Since, the tail increases infinitely, we divide that number by the size of each deque bucket to get the virtual bucket number (vb) of the

Algorithm 1: Push operation for resizable dequeues

```

if deque is full then
  |   expand(deq);
end

vb ← deq.tail / deq.bucketSize ;           // virtual bucket
mapIdx ← vb % deq.mapSize ;               // bucket map index
b ← deq.bucketMap[mapIdx] ;               // physical bucket
deq.buffer[b][deq.tail % deq.bucketSize] ← entry ;   // setup task
deq.tail++ ;                             // push task

```

tail. This virtual bucket number should have an entry on the bucket map. Since, the map is limited in size, the virtual bucket number should wrap onto the bucket map. The deque buckets cannot be larger than what the bucket map supports. Hence, the virtual bucket remainder from the map wrap give us the bucket map index (*mapIdx*). We get the physical bucket (*b*) from the bucket map. Now, we are able to index onto the physical bucket where we place the task (*entry*). We complete the push operation by incrementing deque tail. For better efficiency divides and remainder operations can be replaced by shifts and & operations if bucket and map sizes are maintained at powers of two. The pop and steal operations, described in Section 3.2.3 have been similarly modified to use the bucket map approach. When the number of slots on the bucket array are completely full, the bucket array and bucket map will doubled and the data copied from the old arrays. Doubling the size keeps the modulo indexing same on the bucket array and map which keeps the concurrent steals going [78]. We currently do not free the old bucket array and map because it provides a way for threads to recover after being suspended while stealing. Chase and Lev [78] use a similar scheme

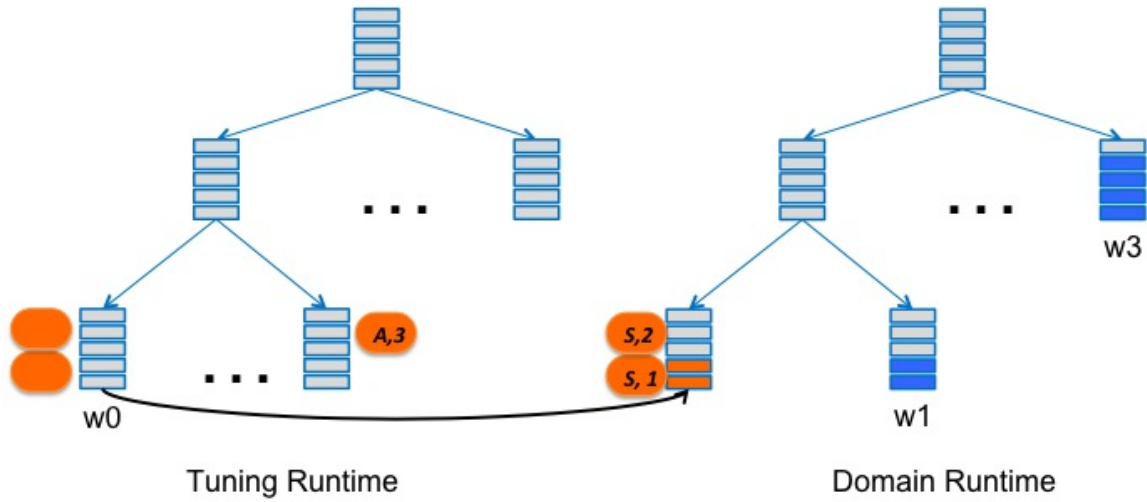


Figure 5.10 : Releasing steps from tuning tree to domain tree

but the amount of memory that is not freed in our algorithm is drastically less than theirs. Consequently, in our algorithm the amount of data copied will be an order of magnitude less while maintaining wait-free deque expansion and contraction.

5.3.4 Tuning Tree Implementation

The tuning runtime implementation is based on the DDF model, introduced in section 3.2.2. In this model, a consumer task can be created with an `await` clause to specify the incoming dependence. A producer task can satisfy an outgoing dependence by performing a `put` on that dependence variable. A tuning specification is currently translated manually to Habanero-C data-driven tasks (DDTs) for execution. We use DDTs to specify the tuning actions, and DDFs to specify the tuning dependences for groups and steps in the program.

We implemented the platform tree described earlier using Habanero-C's Hierarchical Place Trees. In our preliminary implementation, we use the HPT configuration as the tuning tree. An HPT configuration is specified by an XML file. This file can

specify a node (or place) in the HPT to be a `tuning` place. These tuning places contain a special kind of task queue used exclusively for tuning. When a group or step is pushed down a path in the tree, as specified in a tuning API, it gets enqueued into the tuning queue at that child place. When a step get released from the tuning tree, it gets immediately executed. HPT places also contain double-ended queues (dequeues). Any task that is not created by the tuning runtime gets scheduled at the dequeues in the HPT places. We have modified the Habanero-C runtime scheduler to perform both tuning actions and domain (user code) scheduling. We handle all tuning tasks, both groups and steps, in the tuning runtime scheduler. All other tasks in the application are executed in the domain runtime scheduler. A worker thread first searches for domain work. It executes all tasks in its own deque before searching for more domain tasks to steal from other workers. If the worker fails to find any domain work, it switches to the tuning scheduler. The tuning scheduler starts searching for work at the leaf node and moves up to the root. When it finds a tuning task at any node in the path from leaf to root, the worker locks the queue, executes the tuning task, unlocks the queue and finally switches over to the domain runtime. The locking of the queue ensures that the tuning actions in a tuning queue is completed in the order that they were enqueued in. Maintaining the order is critical for maintaining temporal locality. Figure 5.10 shows the action of releasing steps from the tuning runtime to the domain runtime. The tuning tasks are based on a set of tuning APIs. As mentioned before, the tuning APIs can push a group or step down the tuning tree. This operation involves pulling the tuning task from a nodes tuning queue and pushing it onto a child nodes tuning queue. These operations are synchronized with locks to handle concurrent enqueues and dequeues.

5.3.5 Results

In this section we look at some preliminary results of our experiments using the HPT. We use the Cholesky decomposition benchmark for our experiments. Cholesky decomposition is a dense linear algebra application that exploits loop, data, task and pipeline parallelism. The base version of this benchmark used in our experiments is implemented using data driven tasks [77]. This implementation of the benchmark runs a tiled version with each tile on every iteration being executed by a unique task. This data driven implementation enables an unconstrained execution of tasks that is not restricted by a structured task parallel model. Tasks get scheduled once their dependencies are satisfied. Figure 5.11 shows the dependence structure in a tiled Cholesky execution of one particular iteration instance. The iterations proceed with a pivot tile computation on the diagonal. The pivot tile in one iteration plane computes the serial *Cholesky* step. Once that is done, the *trisolve* steps are able to run on the pivot column. The trisolve computation enables the rest of the *update* computations tiles in the iteration. Each tile also had a dependence on itself in the subsequent iteration. We have not shown that dependence in the figure.

We run our experiments on a single node of the DaVinCi cluster at Rice University. Each computing node consists of an Intel Westmere processor with 12 cores running at 2.83 GHz. The 12 cores are divided into two sockets with 6 cores in each. Each socket consists of a shared L3 data cache of 6MB. Every cores has it's own local L1 and L2 data caches of size 32KB and 256KB respectively. The only data reuse within an iteration is from the reuse of the trisolve tile by the update tiles. However as shown in Figure 5.11 that all the update computations in one row uses all the trisolves until that row. As a result, trying to localize the computations to some part of the memory hierarchy would be difficult for the trisolve steps. So, our strategy for

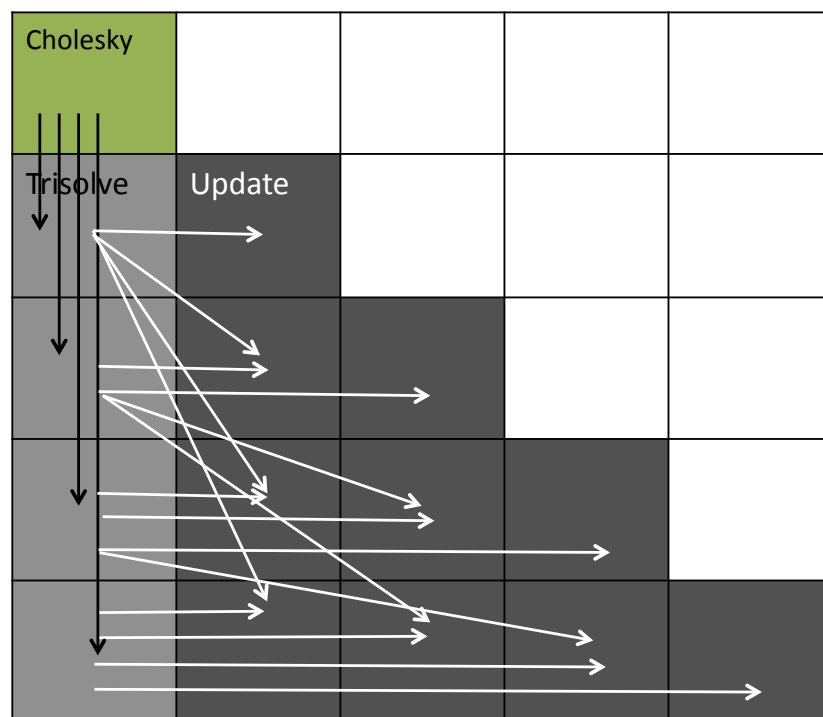


Figure 5.11 : Cholesky decomposition dependences

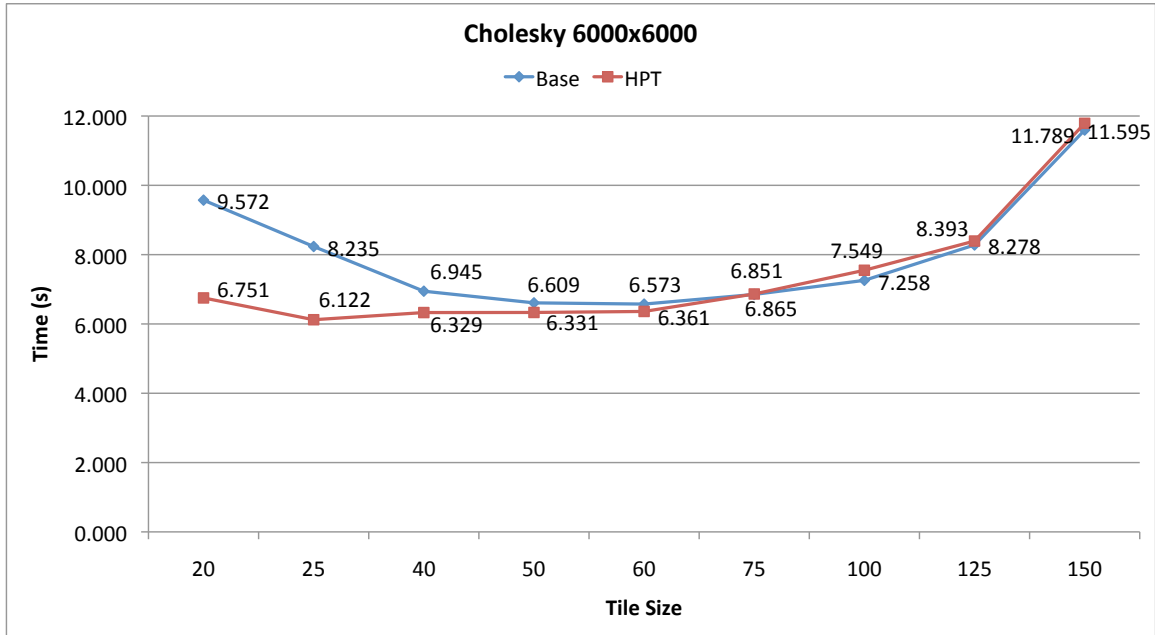


Figure 5.12 : Cholesky decomposition execution times for various tile sizes

exploiting data reuse is across iterations. We ensure that tiles in successive iterations are able to execute on the same socket so that they can benefit from L3 cache reuse. Also, since our experimental platform has two sockets, we divide the tiles on each iteration evenly between the sockets so that we don't lose much parallelism. Let us recall that our current HPT scheduling heuristic does not allow a worker to explore a new subtree while for searching stealable tasks. So, we lose some bit of parallelism due to the slight imbalance between sockets when the division is not perfect.

Figure 5.12 compares performance of the base version against the HPT version. We show execution times for varying tile sizes. In general, the HPT version performs better than the base version. The slight crossover in performance noticed past tile size of 75 is attributed to the loss of parallelism resulting from a higher tile size. This is due to our scheduling heuristic which does not allow a worker to search for work in

a different subtree. It can be seen that the execution times point out an best tile size for each version of the benchmark. However, the best tile sizes are different the base and **HPT** versions. The best time achieved by the base version is on a tile size of 60 and a time of 6.57 seconds. The **HPT** version on the other hand achieves it's best time of 6.12 seconds on a tile size of 25. This shows approximately 7% speedup achieved by the **HPT** version. Investigating this result further we were able to identify that the benchmark was compute bound. We found only 15% of execution time was actually being spent on memory accesses. In light of our finding, we believe that 7% speedup is about the maximum that can be achieved by any **HPT** version that optimizes on cache reuse.

Past work by Husbands and Yelick [103] proposed that for the LU factorization benchmark a prioritization of the tasks on the row and column of a pivot, called *panel* factorization, leads to better performance as it exposes more concurrency in the application. A similar approach will help Cholesky factorization as well but the current **HPT** model does not (yet) have a notion of priority for tasks. However, the tuning framework (with a modification of the scheduling heuristic) can enforce priorities on tasks execution. As an example, if high priority tasks arrive in the tuning tree when the domain runtime is already working on a set of tasks on the **HPT**, the scheduler should be able to pick up those tasks before completing all pending tasks. The tuning tree can keep a queue of high priority tasks for each worker. This requires a modification in the scheduler to check the tuning tree before it tries to pop a task from a deque in the **HPT**. In this way, both priority and locality can be controlled by the tuning expert. This approach will be considered in future work.

In this section we will also present results of our experiences with the tuning framework. We have experimented with two applications, namely, Cholesky factorization

and Rician denoising. We will present results of the Cholesky tuning experiment followed by the Rician denoising results. Our experimental platform is a 12-core Intel Westmere processor that contains two sockets with 6 cores each and a shared L3 cache in each socket. The tuning tree consists of 3 levels, with the root node as the DRAM memory. The second level contains 2 nodes to represent the 2 sockets. Each node in the second level had 6 children to represent the individual cores in the socket.

Tuning Cholesky Factorization

We have implemented multiple tuning specifications for the Cholesky Factorization program written in HC. While our current transformations from tuning specifications to DDTs are performed by hand, an implementation of a translator that will automatically generate DDTs from the tuning specification is a straightforward candidate for future work. We created an outer level group called GroupC, as shown in Figure 5.13. GroupC contains the Cholesky step and another group called GroupTU, which contains the trisolve and update steps. For example, a tuning function for the Cholesky group described above that releases the Cholesky step to the Habanero-C runtime for execution, while distributing the GroupTU among children can be written simply as:

We present two sets of experiments, namely Set1 and Set2. In the first tuning specification (Tuning1) of Set1, we placed the GroupC instances on the root node queue of the tuning tree. When a worker pulled a GroupC instance out of the root, it placed the Cholesky step for execution on either child. It then distributed the GroupTU instances among the two sockets. A worker that picked up a GroupTU would then unpack and execute the trisolve and update steps within the socket. The second tuning specification (Tuning2) of Set1 moved a GroupC instance down a child before unpacking GroupC. Subsequently the Cholesky step is placed in the socket

```

void groupC(void * args) {
    int k = ((cholesky_args*)args)->k;
    int numTU = numTiles - (k + 1);
    TUNING_RELEASE_STEP(cholesky_step, args);
    TUNING_DISTRIBUTE_AMONG_CHILDREN(numTU,
                                     groupTU, args_set[k]);
}

```

Figure 5.13 : Tuning actions on GroupC, the outer level group in Cholesky

level node while the GroupTU instances are distributed among the 6 children. This tuning restricts the execution of each instance of GroupC, that is, the Cholesky step and all the GroupTU instances, containing the Trisolve and Update steps to execute inside one socket. Further, each GroupTU instance executes only on one core. The Set1 experiments were performed on a 2000×2000 matrix and the results are shown in Figure 5.14. The results indicate that Tuning2 slowed down by almost a factor of 2 with respect to Tuning1, while the idleness of Tuning2 was $14.7 \times$ that of Tuning1. The reason for the slowdown in Tuning2 was that the schedule was constrained in parallelism when the groups were pushed down to one more level in the tuning tree. Tuning1 runs faster but Tuning2 would consume less power. This result implies that a tuning specification can affect performance and power at the same time.

In our second set (Set2) of experiments, we keep Tuning1 from Set1 which performs the row grouping of trisolve and updates as the first tuning specification. The second and third tuning specification would group some TU rows while others were grouped in columns. This division among the row and column grouping could ei-

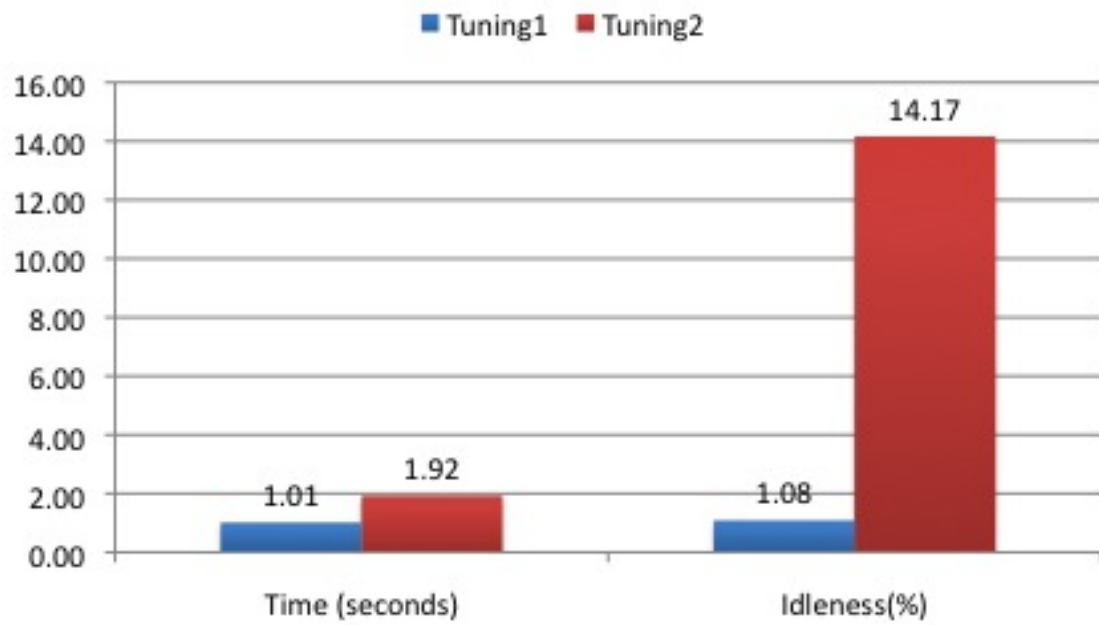


Figure 5.14 : Set1 Cholesky Tuning experiments on 2000 x 2000 matrix

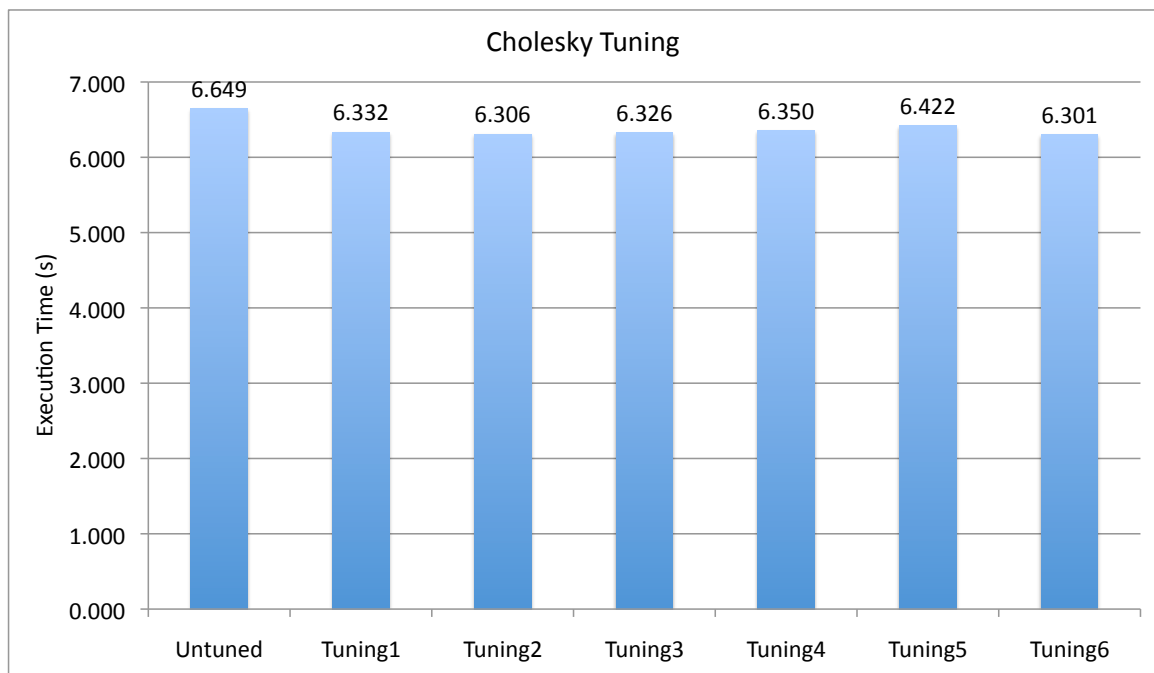


Figure 5.15 : Set2 Cholesky Tuning experiments on 6000 x 6000 matrix

ther dynamically adjusted with increasing number of iterations or statically assigned. Tuning2 does the dynamic adjustment while Tuning3 does the static assignment. Tuning4 tries to improve Tuning2 by coarsening the groups towards the tail end of the iterations in order to benefit from granularity of the steps. Tuning5 and Tuning6 simply puts all tasks at the socket level, the difference being that Tuning6 does a chunked distribution of the tiles. Results of the experiments are shown in Figure 5.15. Our untuned baseline version is an optimally tiled version. Tuning tries to achieve a better schedule for the execution of the tiles. We see that our maximum speedup of 5.16% is obtained from Tuning2. As mentioned earlier, speedups over an already tiled compute bound application will be limited. Comparing to the speedups obtained in the HPT experiment, the tuning shows a slightly lesser speedup. We attribute this to the overhead of maintaining the tuning scheduler. The tuning however is able to perform these optimizations without modifying the original application which was not the case with the HPT experiment.

Tuning Rician Denoising

In this section, we present the tuning experiments for the Rician Denoising application, which is used as part of the medical imaging pipeline in the CDSC project. This application performs a five-point stencil computation on every tile in parallel. This computation is done iteratively until a convergence value is reached. Figure 5.16 shows the dependencies between the various steps both within and across iterations. For example, `uDiffCompute` reads `uData` stencil elements from the previous iteration while `gCompute`, `ugCompute` and `rCompute` read data only on the current iteration. `uCompute` reads data both from the previous and current iteration. This complicated dependence pattern can be simplified by grouping the steps as shown in Figure 5.17.

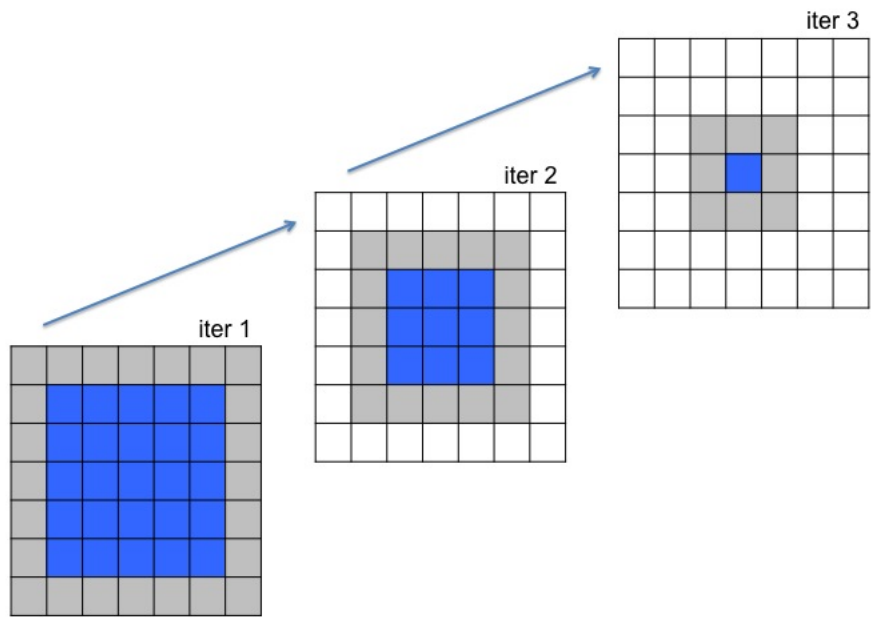


Figure 5.18 : Pyramid computation for tiles in successive iterations

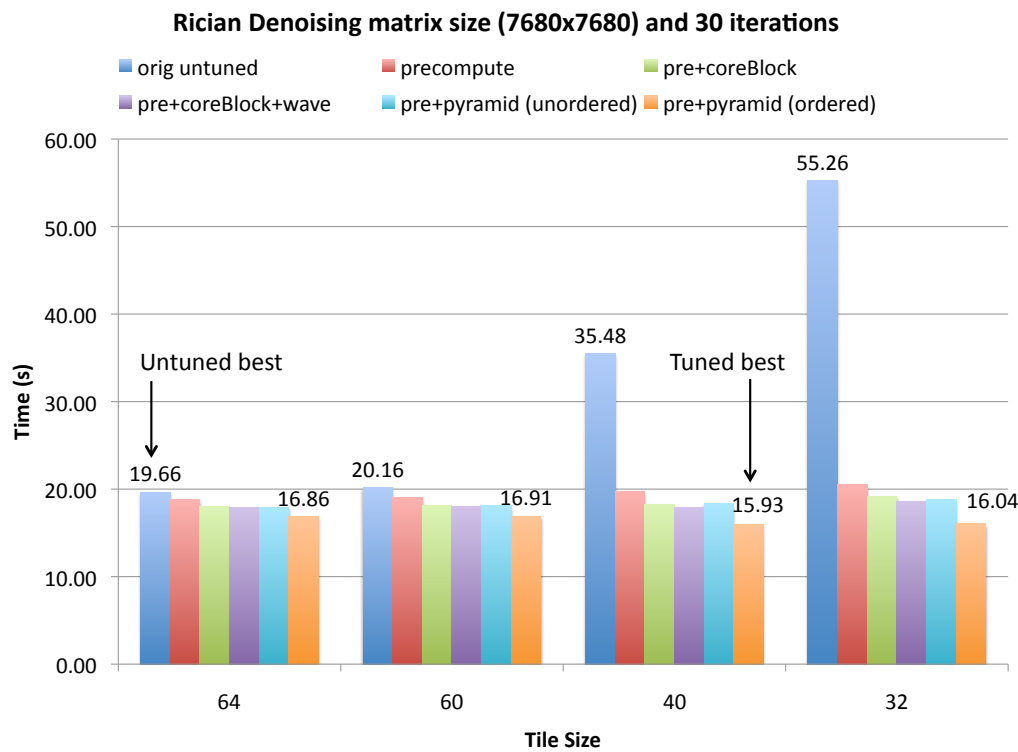


Figure 5.19 : Rician Denoising performance comparison of untuned vs tuned

In our tuning specification we call this the precompute group. Starting with this precompute specification, we formulated two tuning strategies. In the first strategy, we make simple iteration-wise tile executions. The "pre+coreBlock" tuning uses the precompute step and schedules a block of tiles in each iteration on each core. The matrix rows are first divided into sockets, followed by division into cores. The "pre+coreBlock+wave" tuning has each core trying to execute the scheduled set of tiles in a wavefront pattern. The second tuning strategy uses a pyramid computation, in which the motivation is to reuse tiles computed at current iteration in the next iteration, as shown in Figure 5.18. Since the stencil computation reads data from neighboring tiles, the plane of computation in successive iterations that use the same tiles will be decreasing. Layering these successive diminishing planes on top of each other, we get a visualization of a pyramid. In order to benefit from the tile reuse, the whole pyramid must fit in the socket level shared L3 cache. The "pre+pyramid (unordered)" tuning schedules the pyramids onto the sockets in unordered fashion. In the worst case, every worker may pull a different pyramid onto the socket. The "pre+pyramid (ordered)" tuning orders the pyramids such that a new pyramid is brought in only when the current pyramid is close to being done. Figure 5.19 shows the results of the tuning experiments and compares against the untuned version. Overall, the best tuned time we got was 15.93 seconds. Compared to the best untuned time of 19.65 seconds, the best tuned version shows an improvement of 20%. It is interesting to note that the ordered computation on the pyramid tuning produced the best result. In that tuning we hold back execution of steps to execute them together and that proves to be the better strategy than the unordered one. Hence, this is a proof of concept that temporal locality of tasks will make a positive impact on performance.

Past work for optimizing stencil computation include cache-oblivious algorithms, auto-tuners and domain specific stencil compilers [104, 105, 106]. They target data reuse from trapezoidal computations, similar to the pyramid structure in our work. The key difference is that the data reuse they target is specific to the cache hierarchy of each processor, while our work aims to benefit from data reuse of the shared caches through runtime co-scheduling of computations. For example, in our experimental platform, the Pochoir stencil compiler [106], would optimize data reuse for L1 and L2 caches, where as our tuning framework gets reuse from the L3 cache that is shared among the cores in a socket. For current stencil compilers, all shared cache reuse is fortuitous. In our experiment, we used flat tile computations. Using trapezoidal tiles instead, as generated by stencil compilers, would further improve our performance. Hence, integrating stencil compilers and our runtime tuning framework will be an important area of future work. Cache-oblivious algorithms target data reuse through recursive decomposition of a regular computation space. In contrast, the tuning framework is able to handle different types of computations at different levels of the hierarchy. Cache-oblivious algorithms also are based on many assumptions that may not hold for extreme-scale systems. For example, assumptions of an ideal hardware cache model with inclusion property across hierarchies and an optimal replacement property will likely be replaced by software managed memory hierarchies on extreme-scale systems. Cache-oblivious algorithms also assume computations on homogenous CPU architectures and an empty cache before and after task execution. Cache complexity of tasks are analyzed independently of other tasks without any co-location analysis with the assumption that randomized workstealing does not change asymptotic cache complexity. As discussed earlier, future extreme-scale systems will be qualitatively different from these assumptions.

5.4 Summary

In this chapter, we have presented methods for controlling locality of compute and data on shared and distributed memory systems. The **HAPGNS** model enables user directed data distribution functions to optimize data layout on distributed systems. Users can also use the **HAPGNS** model to take advantage of a distributed dataflow programming model using distributed DDFs as a simple extension to the shared-memory DDF model. Scalability results for the Smith-Waterman benchmark show the practicality of this approach, which offers high programmability. We implemented the **HPT** model for Habanero-C to affect spatial locality of computation tasks. We designed a novel deque resizing algorithm to work with the **HPT** model. We also presented a tuning framework for controlling spatial and temporal locality of computations at the intra-node level. The tuning framework is integrated with the Habanero-C runtime. Our experimental results with the tuning framework use the Rician denoising application. We show a performance improvement of 19%-20% over an already parallel, tiled (for local caches) and load balanced execution on a fairly small system (12 cores) and a fairly shallow hierarchy (3 level caches - local L1 and L2, socket shared L3) with today's data movement costs. We anticipate even better improvements on tomorrow's systems with more cores, deeper hierarchies and higher ratios in the costs of data movement vs computation.

Chapter 6

Task Synchronization for Iterative Computation

The Habanero-C dynamic task parallel language has the ability to express fine-grained parallelism with the help of lightweight tasks. Tasks get executed by worker threads that are governed by a runtime scheduling algorithm. The runtime scheduler ensures load-balanced execution by using a work-stealing algorithm. Although the runtime helps with efficient execution of parallel tasks, every runtime operation is considered overhead for the application's real work. This sounds counter-intuitive because users usually do not notice these overheads relative to the actual amount of work when the number of runtime operations are far less than the number of operations inside the tasks. However, when the ratio of runtime operations to actual work operations is no longer negligible, it could adversely affect the performance of the application. In other words, application performance can be viewed as being sensitive to task granularity. If the granularity is too small, it can cause time and space overheads due to the large number of tasks in the system. In such a scenario, the runtime has to spend more time scheduling these tasks and require more space storing them. Applications written with deeply nested parallelism in the structured task parallel model, a smaller granularity of computation may cause frequent task blocking leading to large runtime overheads. In the data-flow task model, unbounded queue sizes may cause second order effects such as non-uniform queue access latencies. If the granularity is too large, it may cause loss of parallelism and lesser overlaps between computation and data movement.

For iterative computations, tuning for task granularity will be a key process for scalable performance on extreme-scale systems. Iteration spaces for computations can very large for scientific applications. While it is possible to express every iteration as a distinct task, the total number of tasks can very easily reach $O(10^6)$ and higher for a typical loop based computation. The runtime overheads for such a scenario would be prohibitively high. One of the strategies to solve this problem is for the user to first decompose an application into the finest grain possible, and then gradually start coarsening until the best granularity is found. This strategy can be likened to a compiler employing maximal loop distribution followed by a heuristic loop fusion phase. Without adequate synchronization support, there is a limit to the maximum granularity that can be achieved through task coarsening. Such a limit would imply that a task can start execution and proceed to completion with having to synchronize with others. This limit may prove to be restrictive and so there will be a need to support inter-task synchronization for increasing task granularity. Based on this premise, we believe that a critical requirement for scalable dynamic task parallelism is an efficient synchronization mechanism to support task coordination at different levels of granularity.

The Habanero-C base language contains the `finish` construct for structured task parallel synchronization and the DDF model for representing data-flow task graph patterns. The `finish` construct is a *collecting* synchronization operation for tasks to signal their completion, while the DDF model supports single-assignment producer-consumer dependence relation. Neither model supports active task synchronization. With active synchronization, a task can synchronize with others multiple times at various points during computation while maintaining the context of execution. The `phaser` synchronization model [12], is an efficient technique for representing complex

active synchronization patterns among dynamically created tasks. It can support iterative synchronization in a scalable way. We use the **phaser** synchronization approach as the model of choice to targetting synchronization operations when tuning of task granularity in iterative computations.

In this chapter, we first provide an overview of past work on the Habanero-Java **phaser** synchronization model in Section 6.1. We summarize the contributions of this work in Section 6.2. In Section 6.3, we present the phaser design for shared-memory programming on multicore tightly coupled compute nodes. We present a programming models for the Habanero-C dynamic task parallel language. We also describe a generalized tree-based hierarchical synchronization algorithm for **phaser**. We present our experimental results on multicore compute nodes. In Section 6.4, we describe the **phaser** design, implementation and hardware optimizations for the Cyclops64 manycore architecture. We present our experimental results on this manycore architecture. In Section 6.5, we present a programming model and implementation for unified shared and distributed memory collective synchronization. We present our experimental results using current multicore cluster platforms. We summarize our work in Section 6.6.

6.1 Past Work on Phaser Synchronization Model

Phasers [12], first introduced in the Habanero-Java multicore programming system, are synchronization constructs for task parallel programs. The **phaser** construct unifies collective and point-to-point synchronization between tasks in a single interface, and are designed for ease of use and safety to help to improve programmer productivity in task parallel programming and debugging. The **phaser** synchronization model supports dynamic task parallelism by allowing tasks to dynamically regis-

ter and deregister with a phaser object. The use of **phaser** guarantees two safety properties: deadlock-freedom and phase-ordering. These properties, along with the generality of its use for dynamic parallelism, distinguish **phasers** from other synchronization constructs such as barriers [15, 17, 36], counting semaphores [107] and X10 clocks [5, 108]. A subset of phaser capability has been added to Java 7 libraries [109], and also can be added to other programming models such as OpenMP [37] and Intel’s Thread Building Blocks [70].

6.1.1 Phaser Programming Model in HJ

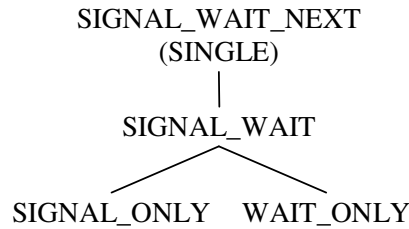


Figure 6.1 : Phaser Mode Lattice

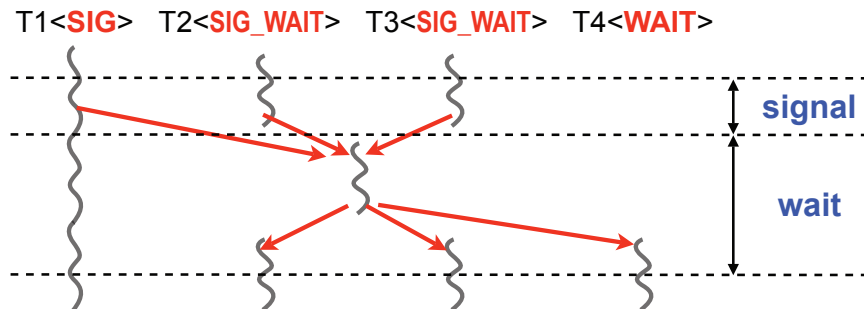


Figure 6.2 : Semantics of synchronization operation

The **phaser** synchronization model provides each task the option of registering with a **phaser** in one of four modes: **signal-wait-single**, **signal-wait**, **signal-only**, or

wait-only. For producer-consumer synchronization, the producer should register in **signal-only** mode and the consumer should register in **wait-only** mode. For barrier synchronization all tasks should register in **signal-wait** mode. In addition, a **next** statement for phasers can optionally include a **single** statement which is guaranteed to be executed exactly once during a phase transition. The registration mode defines the capabilities of the task with respect to the phaser, and the semantics of synchronization operation on phaser depends on the mode. There is a natural lattice ordering of the capabilities as shown in Figure 6.1. Figure 6.2 shows a synchronization operation on a phaser by four tasks, T_1 with **signal-only**, T_2 and T_3 with **signal-wait**, and T_4 with **wait-only** mode. The phaser operations that can be performed by a task, T_i , are defined as follows.

- **new:** When T_i performs “ $ph = \text{new phaser}(mode)$ ” statement, it results in the creation of a new phaser, ph , such that T_i is registered with ph according to $mode$. If $mode$ is omitted, the default mode assumed is **signal-wait-single**. At this point, T_i is the only task registered on ph .

There is another phaser constructor “ $\text{phaser}(mode, numTiers, numDegree)$ ” to create a hierarchical phaser, which support tree-based barrier synchronization with better scalability than normal phasers. In addition to $mode$, the constructor takes two tunable parameters, $numTiers$ is the number of tiers of the tree and $numDegree$ represents the number of children per tree node. In HJ, tasks can register on a hierarchical phaser with the **signal-only** mode. The following operations for registration, de-registration and synchronization are available on both normal flat-level phaser and hierarchical phaser in the same manner.

- **phased async:** When T_i performs

“**async phased** ($ph_1\langle mode_1 \rangle, ph_2\langle mode_2 \rangle, \dots$) T_j ” statement, it creates a child task T_j registered with a list of phasers with specified modes. If $\langle mode_k \rangle$ is omitted, the same mode as T_i is assumed by default. The following constraints are imposed on the transmission of phasers:

1. **Capability rule:** T_i can register T_j on phaser ph iff T_i is also registered on ph , and the capability possessed by T_i on ph must be same or higher than the transmitted capability to T_j in the lattice ordering. The capability rule is imposed to avoid race conditions on phaser operations.
2. **IEF scope rule:** T_i can register T_j on ph iff the phaser creation instruction (**new**) for ph has the same Immediately Enclosing Finish as the task creation instruction (**async**) of T_j . The IEF rule is imposed to avoid a potential deadlock between the **end-finish** synchronization and phaser synchronizations.

An attempt to transmit a phaser that does not obey the above two rules will result in a `PhaserException` being thrown at runtime. We also support the “**async phased** T_j ” syntax to indicate by default that T_i is transmitting all its capabilities on all phasers that satisfy the IEF scope rule to T_j .

- **drop:** There are three ways to de-register from phasers.

1. **Task termination.** When T_i terminates execution, it de-registers from all phasers.
2. **End-finish.** When T_i is the parent task of **finish** statement F and executes the **end-finish** instruction, it completely de-registers from each phaser ph

Operation	Registration Mode	Action
next	signal-wait-single / signal-wait	signal + wait
	signal-only	signal
	wait-only	wait
next $\langle stmt \rangle$ (next w/ single stmt)	signal-wait-single	signal + wait + single
	signal-wait	<i>error</i>
	signal-only	<i>error</i>
	wait-only	<i>error</i>
signal	signal-wait-single / signal-wait	signal <i>ph</i>
	signal-only	signal <i>ph</i>
	wait-only	<i>no-op</i>
wait	signal-wait-single / signal-wait	wait <i>ph</i>
	signal-only	<i>no-op</i>
	wait-only	wait <i>ph</i>

Table 6.1 : Semantics of phaser operations as a function of registration mode on *ph*

if the IEF for *ph*'s creation is *F*.

3. **Phaser-specific drop.** T_i can perform “**ph.drop()**” to de-register from *ph* anywhere in the IEF scope of *ph*'s creation.

- **next / signal / wait:** The **next** operation has the effect of advancing each phaser on which the task is registered to its next phase, thereby synchronizing with all tasks registered on a common phaser. A **next** operation is equivalent to a **signal** operation followed by a **wait** operation ¹.

¹Phaser's **wait** operation is different from Java Object.wait operation

- **signal operation.** The task signals all phasers that it is registered on with *signal* capability (**signal-only**, **signal-wait** or **signal-wait-single** mode). A phaser advances to its next phase after all registered tasks signal the phaser. Phaser-specific operation, `ph.signal()`, is also supported.
- **wait operation.** The task is blocked until all phasers that it is registered on with *wait* capability (**wait-only**, **signal-wait** or **signal-wait-single** mode) advance to their next phase. Phaser-specific operation, `ph.wait()`, is also supported.

Table 6.1 shows the semantics of phaser operations as a function of registration mode on *ph*. When a task with both *signal* and *wait* capabilities on *ph* performs multiple **signal** operations on *ph* without performing a **wait** operation, only the first **signal** operation is valid and the others become *no-op*. This semantics intends to reduce the complexity of supporting fuzzy [110] or split-phase [111] barrier that allows local work to be performed between the **signal** and **wait/next** operations. On the other hand, multiple **wait** operations by such a task result in an *error* (`PhaserException` at runtime) so as to avoid deadlock.

- **next with single statement:** The **next** $\langle stmt \rangle$ operation has the semantics of a **next** statement as defined above, with the extension of executing *stmt* as a single statement which is guaranteed to be executed exactly once during a phase transition. Here, $\langle stmt \rangle$ can contain multiple statements and are not allowed to perform phaser operations. This operation is only permitted if T_i is registered in **signal-wait-single** mode on the phaser (see Table 6.1). Further, we require all other tasks registered with the phaser in **signal-wait-single**

mode to execute the same static **next** $\langle stmt \rangle$ statements. These constraints are imposed to ensure the integrity of the single statement [81].

At each **wait** operation, a *master* task is selected from the tasks with *wait* capability per phaser. The master task of *ph* handles the process to advance *ph* to next phase, and executes the single statement of **next** $\langle stmt \rangle$ operation on *ph*. The lattice ordering in registration modes is used as priority to select master task so that a task with **signal-wait-single** mode always becomes the master. In a typical implementation, the earliest task to perform **wait** operation becomes the master if multiple tasks have same priority. Therefore, different task can be the master task at each **wait** operation.

6.1.2 Hierarchical Phasers for Tree-based Barriers in HJ

In this section we briefly show the advantage of tree-based barrier synchronization and details of the programming interface. As shown in Figure 6.3, a phaser barrier synchronization is divided into two operations, **gather** and **broadcast**. In the **gather** operation, a master task waits for all signals from worker tasks sequentially, and the waiting time can be proportional to the number of workers. While the single master approach provides an effective solution for modest levels of parallelism, it quickly becomes a scalability bottleneck as the number of threads increases. Thus, **gather** operations are the major scalability bottleneck in single-level phaser operations. On the other hand, the **broadcast** operation is more scalable because each worker just waits for a **broadcast** signal from the master. The tree-based hierarchical barrier synchronization employs multiple sub-masters so that the **gather** operation in the same level (tier) can be executed in parallel by sub-masters (Figure 6.4). Furthermore, the hierarchical structure is amenable to the natural hierarchy in the hardware; each

sub-master can naturally leverage data locality among workers in its sub-group.

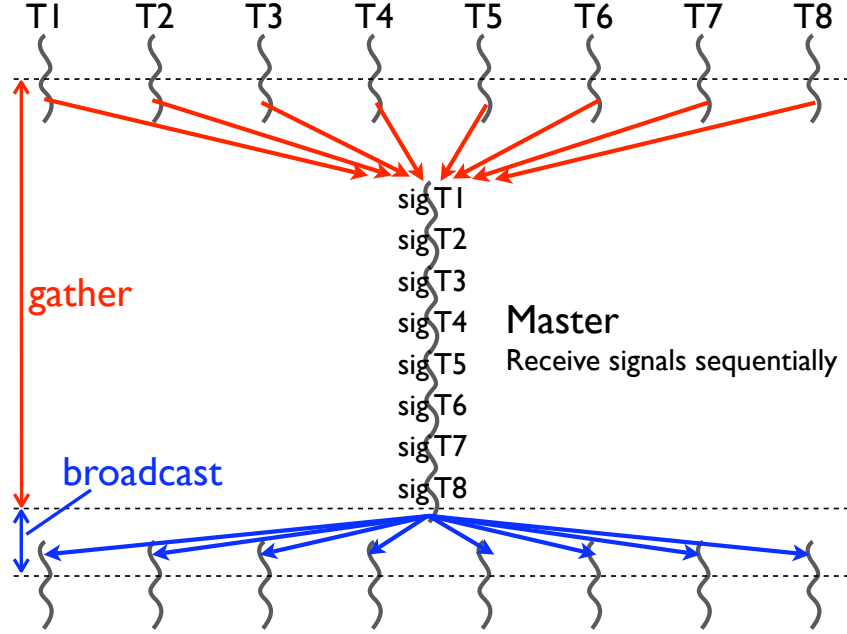


Figure 6.3 : Single-level phaser with single master

As shown in Section 6.1.1, the constructor to allocate a hierarchical phaser takes the number of tiers and degree of the tree as parameters. The `numTiers` parameter ($= T$) specifies the number of tiers to be used by the runtime system's tree-based sub-phaser structure, and `numDegree` ($= D$) is the maximum number of child sub-phasers that can be created on a parent sub-phaser. A hierarchical phaser with `numTiers=1` is equivalent to a single-level phaser. The leaf of a sub-phaser tree has no child sub-phasers, and deals with the tasks that are assigned to the leaf. If there is no tasks on a leaf sub-phaser, the leaf is inactive and does not attend tree-based barriers. Similarly a non-leaf sub-phaser that has no active child sub-phasers is also inactive. Each active leaf sub-phaser must contain at least one task with *wait* capability so that it can be the master task of the leaf sub-phaser. However, programmers have no control over

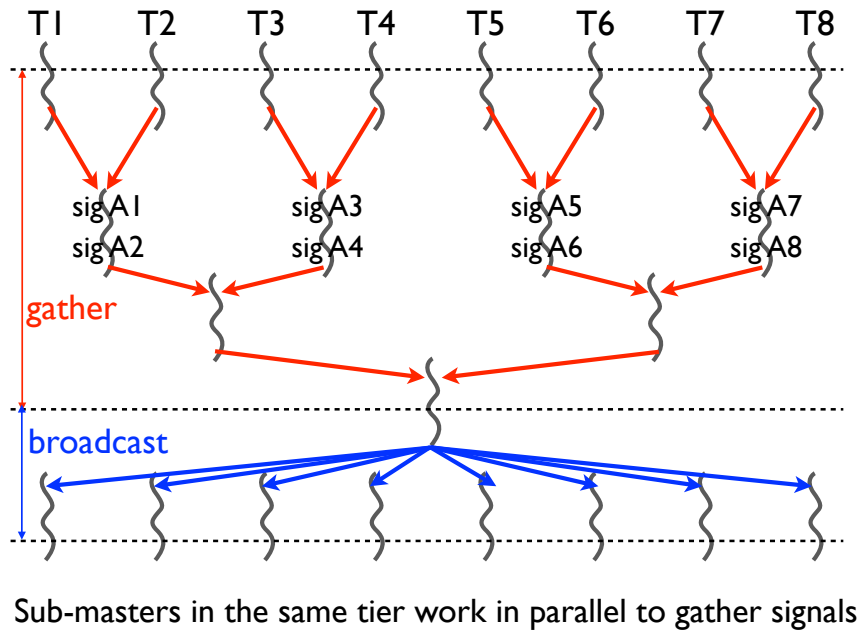


Figure 6.4 : Hierarchical phaser with sub-masters

task assignment to leaf sub-phasers and therefore registration in `signal-only` mode is not allowed for a hierarchical phaser.

Although there is no limit on the number of tasks registered on a phaser, the runtime may run into some scalability bottlenecks if the number exceeds D^T , since that implies that the synchronizations and reductions will need to be serialized within “sub-masters” at the leaves of the phaser tree. Figure 6.4 is the case of `numTiers` = 3 and `numDegree` = 2, and the scalability issue may occur when tasks more than $2^3 = 8$. As with flat phasers, hierarchical phasers support dynamic task parallelism so as to allow the set of tasks synchronized on a phaser to vary dynamically.

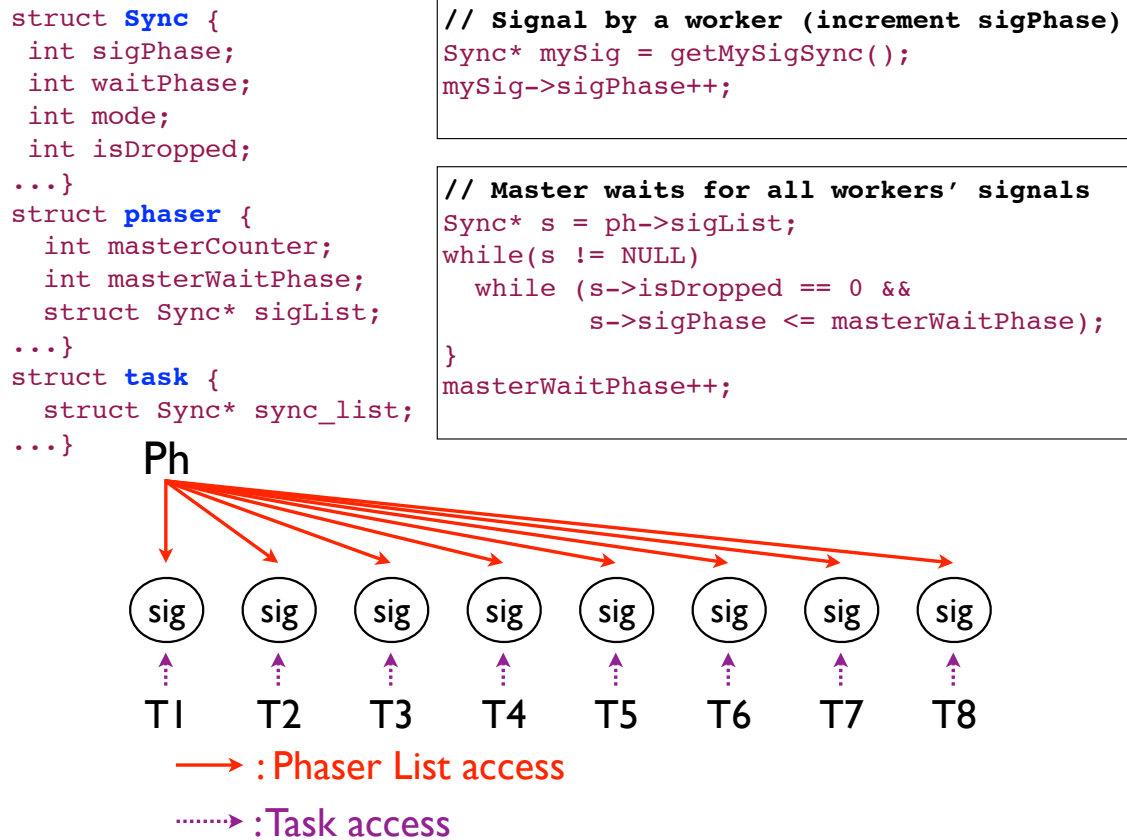


Figure 6.5 : Data structures for flat phaser

6.1.3 Phaser Implementation in HJ

Figure 6.5 shows semantics and data structures for the gather operation of the single-level barrier. Each task registered on a phaser has a **Sync** object corresponding to the phaser, that contains the registration mode and the current signal and wait phase. These **Sync** objects are also included in List **sigList** of the **phaser**, a list of all signalers. All tasks registered on the phaser send a signal to the master task by incrementing its **sigPhase** counter, and the master task waits for all **sigPhase** counters to be incremented by busy-wait loop. A registered task can also spawn another task, or child task, and register the child on the phaser. A new **Sync** object

```

struct SubPhaser {
    Sync* sigList; // Only leaf sub-phaser contains
    int masterSigPhase; // Signal for the higher tier
    int masterWaitPhase; // Wait for the lower tier
    struct SubPhaser* parent; // Parent in the tree
    ...}
struct phaser {
    int masterPhase; // Signal to broadcast
    ...}

```

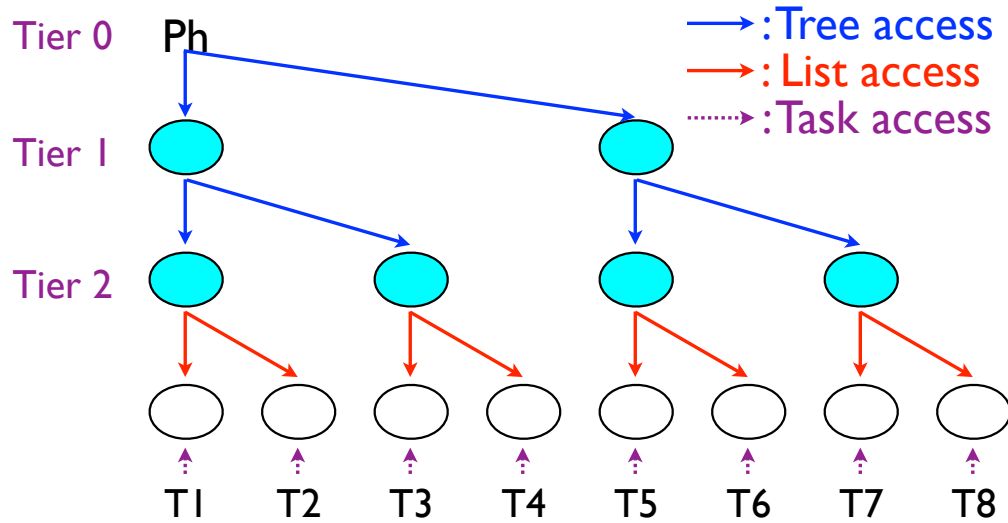


Figure 6.6 : Data structures for tree phaser

corresponding to the child task is appended to `sigList`, and the child task attends to synchronizations on the phaser. Busy-wait loops in phaser runtime have timeout periods that can be specified as a runtime parameter. When a busy-wait loop times out, the task sleeps and the hardware thread switches to another task. Once every signaler has signaled, the master wakes up all suspended workers serially.

We have seen that the hierarchical phaser employs a tree of sub-masters, instead of a single master. When an task spawns a child task, the child is registered on the same leaf sub-phaser as its parent activity until the number of activities on the leaf reaches `numDegree`. If the leaf is full, the child activity is registered on another leaf sub-phaser.

This process continues so long as the total number of levels does not exceed `numTiers`. Since this process needs additional atomic accesses, the initialization (registration) overhead of hierarchical phasers is generally larger than flat phasers. Figure 6.6 shows semantics and data structures for the gather operation of the tree-based barrier. Every sub-phaser has two counters that track the current signal phase and wait phase, named *masterSigPhase* and *masterWaitPhase*. `SubPhaser` contains `List sigList`, `sigPhase` and `masterWaitPhase` counters. The `sigList` of a leaf sub-phaser includes `Sig` objects for tasks that are assigned to the leaf sub-phaser. `phaser` class has a two dimensional `SubPhaser` array and all tasks can access the hierarchical sub-phasers so that any eligible task can be a master task to advance the sub-phaser. In the gather operation, all sub-masters on leaf sub-phasers check their `sigList` and wait for the signals from other tasks in parallel, and increment their `sigPhase` counters after waiting the signals. A sub-master on non-leaf sub-phaser waits for the `sigPhase` increments of its child sub-phasers and also increments its `sigPhase`. Finally, the global master receives the signal from the top level sub-phasers and finishes the hierarchical gather operation. The phaser has a global counter called *masterPhase*. After the gather operation completes, the broadcast is carried out to all waiters by incrementing the `masterPhase` counter.

6.2 Research Contributions

In this work, we present generalized scalable designs for high-performance synchronization with the `phaser` model. We show applicability for extreme-scale systems with implementations for multicore and manycore architectures, and across compute nodes. We also preserve the simple `phaser` programming model to make applications portable across a wide range of systems. The contributions of this thesis in the phaser

synchronization model can be summarized as:

- A generalized tree-based **phaser** synchronization algorithm.
- The design and implementation of the multicore **phaser** synchronization model for dynamic task parallelism in Habanero-C.
- The design and implementation of the manycore **phaser** synchronization model with hardware optimizations for the Cyclops64 manycore processor.
- The design and implementation of a hybrid **phaser** synchronization model for unified shared and distributed memory collective synchronization using the HC-COMM runtime.
- Support for **phaser** accumulators in both intra-node and hybrid **phaser** implementations.

6.3 Phasers for Multicore Synchronization

In this section, we shall look at the **phaser** design for multicore architectures. This model integrates **phaser** into Habanero-C, a dynamic task parallel language. This language integration is similar to the Habanero-Java model. Next, we look at some of the details of the **phaser** data structure in Section 6.3.2. Finally, we describe the details of a novel algorithm for tree-based **phaser** synchronization in Section 6.3.3 that overcomes some of the limitations of the HJ model.

6.3.1 Programming Model for Habanero-C

The **phaser** synchronization model in Habanero-C follows closely to Habanero-Java model described in Section 6.1.1. In Habanero-C, tasks can register on a **phaser**

in one of the 3 *modes*: `SIGNAL_WAIT_MODE`, `SIGNAL_ONLY_MODE`, and `WAIT_ONLY_MODE`. The **phaser** mode signifies its capabilities when performing synchronization operations. The Habanero-C language interface for **phasers** includes:

- *Creation*: `PHASER.CREATE(mode)` creates a **phaser** object and registers the calling task on the **phaser** with the specified *mode*.
- *Registration*: A child task can register on a **phaser** object that was created by the parent using the **phased** clause in the **async** statement. `async phased <stmt>` registers the **async** with all **phasers** created by the parent in the immediate enclosing **finish** scope and asynchronously execute `<stmt>`. `async phased SIGNAL_ONLY(ph1, ...) WAIT_ONLY(ph2, ...) SIGNAL_WAIT(ph3, ...) <stmt>` registers an **async** on specific **phasers** with specific *modes*. The parent should be registered on all the **phasers** in modes that are greater than or equal to the modes of the child as shown in Figure 6.1.
 - `SIGNAL_WAIT > SIGNAL_ONLY`
 - `SIGNAL_WAIT > WAIT_ONLY`
 - `SIGNAL_ONLY = WAIT_ONLY`
- *Synchronization*: The **next** statement executed by a task will synchronize the task on all the **phasers** that it is registered on.

Figure 6.7 shows an example of using **phasers** to implement a barrier among multiple asynchronously created tasks. The **async** statement in line 4 and the **j-for** loop create `ntasks` child tasks, each registering with the **phaser** created in line 2 in the same mode as in the master task. The **next** statement in line 8 is the actual barrier wait; each task waits until all tasks arrive at this point in each iteration of the **i-for**

```

1: finish {
2:   new Phaser(SIGNAL_WAIT);
3:   for (int j=0; j<ntasks; j++)
4:     async phased IN(j) {
5:       for (int i=0; i<innerreps; i++) {
6:         delay(delaylength);
7:         printf("Task %d at step %d!\n", j, i);
8:         next; }
9:   } }

```

Figure 6.7 : Barrier Example

loop. The first `next` operation of each task causes itself to wait for the master task to do `next` operation or to deregister. When the master task reaches the end of the `finish` scope, it deregisters from the phaser so all child tasks continue and synchronize by themselves in each iteration.

6.3.2 Phaser Data Structure

The implementation of hierarchical phasers in Habanero-C is a completely new design that is optimized to take advantage of the runtime's memory management. In this phaser model, the constructor for a hierarchical phaser differs from the HJ version shown in Section 6.1.1 by removing the *numTiers* parameter. All other the programming constructs remain unchanged between flat phasers and hierarchical phasers. Figure 6.8 shows the hierarchical phaser design for Habanero-C. There are three main components to the phaser design: the basic phaser data structure, the tree of sub-phasers and the `phaserSync` objects. The `subphaser` tree is built dynamically at runtime when tasks register on the `phaser` in a signaling mode. These tasks form attach themselves to the leaf nodes of the `subphaser` tree. Tasks registering with `wait-only` mode do not get attached to the tree. During synchronization, signaling tasks increment their local phase counter to indicate a signal. Tasks registered on

the phaser with a wait mode compete to become masters of the **subphaser** nodes in the tree. Let us call a master of a **subphaser** to be a submaster. It is the submaster's responsibility to gather the signals from the children. For leaf **subphaser** nodes, the children are the signaling tasks, while for internal **subphaser** nodes, the children would **subphaser** nodes as well. After a submaster gathers signals from its children, it increments the phase of the **subphaser** node, thereby indicating a signal from that **subphaser** node to the parent **subphaser** node. This way the signals from the tree propagate from the leaves to the root. When the root has gathered signals from its children, it indicates the completion of all signals in that synchronization phase. Following this, the master at the root will increment the overall phase of the phaser to indicate the start of the next phase.

A major performance overhead is the competition amongst waiters to become submasters. Competition is resolved through an atomic *compare-and-swap* (**CAS**) operation, which is typically more expensive than non-atomic operations. Considering n signalers at the leaves of a complete binary **subphaser** tree with $n - 1$ internal nodes, imply at least $n - 1$ **CAS** operations for every synchronization phase. This can be considered as large overhead. To reduce this overhead, we can assign a *fixed* waiter task for a **subphaser** node. In case, that task drops out of the phaser, the **subphaser** node will become *unfixed* and will need to be reassigned to another waiter. This dynamic fixing of the **subphaser** nodes is handled by our algorithm.

Most of the basic phaser data structure derives from the hierarchical phaser design for Habanero-Java 6.1.2. Figure 6.8 shows some of the important member fields of the phaser data structure. There are a few other variables that the runtime maintains which we are going to elaborate on them while describing the algorithm in Section 6.3.3.

phase This counter, as the name suggests, tracks the current phase of this synchronization object.

master This counter helps decide whether the phaser has already selected a master of this phase. As mentioned before, it is the phaser master's responsibility to finally broadcast the phase increment.

leaf This variable always points to the very first **subphaser** structure that gets created. It gets set once and never changes after it is set.

root This variable points to the root of the **subphaser** tree. The root can change dynamically as the tree grows when more tasks register on the phaser. Currently

the implementation does not shrink the overall tree when tasks drop. Instead whole subtrees of the phaser tree have the option of being deactivated.

landing_pad This variable holds a list of signalers who have just registered on the phaser and have not yet completed one phase transition operation. They are taken off the list by the root master before broadcasting the phaser transition. Tasks are added to the list in ascending order of the unique registration identifiers. A task blocks until all lower identifiers are have been added to the list.

unfixed_sph This variable holds a list of **subphaser** objects that do not have a fixed master assigned.

Hierarchical phasers consists of a tree of subphasers inside the main phaser data structure. The subphaser tree node's degree is set as a parameter when the phaser is created. The leaf nodes of the tree contain degree number of tasks while the internal nodes contain degree number of subphasers. In Figure 6.8, the **subphaser** structures are in the circles denoted by S_i . Some of the important components of the **subphaser** are:

subphase This is for the **subphaser** to gather signals from the children and propagate a signal to the parent.

submaster This variable helps to decide the master who gathers the signals of its children in case the master has not been fixed.

fixedwaiter This variable points to the active task which is fixed to be master of the **subphaser** for every synchronization phase.

The **phaserSync** objects act as an interface between the task and the **phaser** object. When a task registers on a **phaser**, it creates the appropriate **phaserSync** objects

according to the mode of registration. In Figure 6.8, the `phaserSync` objects are in the rectangles denoted by T_k . For all signal modes such as `signal-only` or `signal-wait`, a `sigSync` object is created, while for all wait modes, a `waitSync` is created. Both `sigSync` and `waitSync` objects are maintained by the task. References to registered `sigSync` objects are also maintained by the subphaser tree leaves. Every `sigSync` object maintains a *phase* variable to notify the phaser master that the signal has been done. Every `waitSync` object also maintains a *phase* variable which helps in busy waiting on the phaser broadcast. The `sigSync` maintains a *isActive* boolean field to notify the phaser master in case it has dropped off. If a task is a fixed master on a subphaser, then the `waitSync` object maintains a reference to that subphaser with the *fixed_subphaser* variable.

6.3.3 A Generalized Tree-based Phaser Synchronization Algorithm

Past work on hierarchical phaser synchronization [112] suffers from two limitations. Firstly, there is no support for tasks with `signal-only` registration modes. With such a restriction, it is not possible to express point-to-point synchronization patterns. Secondly, the phaser tree size is fixed at the time of phaser creation. The user has to specify the maximum allowed height (T) and degree (D) of the tree as part of constructor. This implies that the user should have prior knowledge of the maximum number of tasks (D^T) that can register on a phaser, which is a restriction for dynamic task parallel computation on extreme-scale systems. In this section, we describe a new generalized tree-based `phaser` synchronization algorithm aiming to overcome these limitations.

The `phaser` synchronization model can be broadly classified into three distinct parts during the lifetime of a task associated with a phaser object. First, the reg-

istration process associates the task and the phaser object. Following registration a task begins the active synchronization operations. Finally, the de-registration or drop step disassociates the task from any further participation in the phaser object's activities.

Registration Phase

There are two phaser registration scenarios. First, when a task creates a phaser, that task is automatically registered on the phaser as part of the phaser creation function. Second, when a task creates a child task, the parent has the option of registering the child on the phaser objects that the parent is registered on and shares the same immediately enclosing finish scope. In either case, the registration process associates the phaser object with the `phaserSync` objects depending on the registration mode. A `phaserSync` object, as described in Section 6.3.2, acts as the interface between a task and the phaser object.

Algorithm 2: PhaserRegistration

Data: phaser ph , mode m

Result: sync objects s and w

if $m \neq \text{signal_only}$ **then**

$w \leftarrow \text{initializeWaitSync}();$

end

if $m \neq \text{wait_only}$ **then**

$s \leftarrow \text{initializeSigSync}();$

$\text{InsertSigIntoPhaserTree}(ph, s);$

end

Algorithm 2 shows the pseudocode for the registration function. If the registration mode has a *wait* component, then a **waitSync** object is created and initialized. Similarly, if the registration mode has a *signal* component, then a **sigSync** object is created and initialized. The function returns these objects to the caller where they would be added to the frame of the task being registered. If a **sigSync** is created, this object is added to the phaser tree, which consists of a tree of subphaser nodes where the leaf subphasers have **sigSync** objects attached.

Algorithm 3 shows the function pseudocode for adding a **sigSync** to the phaser tree. The function first assigns a unique identifier to the new task, using an atomic increment of a shared counter, *sigCounter*. This id tells us the insertion position at the leaf level, the leaf subphaser number and the offset into that subphaser based on the degree of the tree. If the offset is 0, then the task is responsible for setting the phaser tree appropriately. But for a non-zero offset, the insertion busy waits until the subphaser shows up on the tree. The task which gets the responsibility of setting up the subphaser, also busy waits until all the previous leaves have been setup. However, the tree setup function can be concurrent with non-zero offset insertions in previous leaves. The task starts setting up the tree by creating the leaf subphaser and adding more sub-phasers to the tree if required in order to complete the tree. Once the tree has been setup, the *leafCounter* variable is incremented so that other tasks waiting on this leaf subphaser can proceed.

The tree insertion routine also performs two other functions. First, if this task has a *wait* component, then, it may be a good choice to become a fixed master on a subphaser in the tree. Fixed masters have the advantage of not employing an atomic operation to become a master dynamically during a synchronization operation. However, we allow only tasks registered in **signal-wait** mode to become fixed masters

Algorithm 3: InsertSigIntoPhaserTree

Input: phaser ph , sig sync s

```

 $sigId \leftarrow getUniqueSigId(ph.sigCounter);$ 
 $sphId \leftarrow sigId/ph.degree;$                                 /* leaf sub-phaser */
 $sphOff \leftarrow sigId \% ph.degree;$                         /* offset into leaf sub-phaser */
if  $sphOff = 0$  then
    |  $sph \leftarrow subPhaserCreate();$ 
    | if  $sphId = 0$  then
    | |  $ph.leaf \leftarrow sph;$ 
    | else
    | | busy wait until  $ph.leafCounter$  reaches  $sphId$ ;
    | | append  $sph$  to the list of leaves and setup the rest of the tree;
    | end
    |  $sph.sigArray[0] \leftarrow s;$ 
    | atomic increment of  $ph.leafCounter$ 
else
    | busy wait until  $ph.leafCounter$  reaches  $sphId + 1$ ;
    | traverse list of leaves to reach leaf with id  $sphId$ ;
    |  $sph.sigArray[sphOff] \leftarrow s;$ 
end
 $s.leaf \leftarrow sph;$ 
if  $isSigWait(s)$  then
    | if  $FixSubPhaser(s) = false$  then
    | |  $AddSubPhaserToUnfixedList(sph);$ 
    | end
end
 $InsertToLandingPad(ph, s);$ 

```

Algorithm 4: FixSubPhaser

Input: sig sync s

Output: True if a subphaser master gets fixed. False otherwise.

```

 $sph \leftarrow s.leaf;$ 

while  $sph$  do
  | if  $trySynchronizedMasterFix(sph, s) = true$  then
  |   |  $s.wait.fixedsph \leftarrow sph;$ 
  |   | return  $true$ 
  | end
  |  $sph \leftarrow sph.parent;$ 
end

return  $false$ 

```

so that the synchronization phase does not suffer from any delays resulting from **wait-only** tasks. Algorithm 4 shows the pseudocode for this function. The current algorithm fixes a task as master on a subphaser on the path from the leaf to root only to benefit from locality of the gather operation. If the task that is performing a gather operation shares a level of cache with one who needs to signal, then the busy wait basically spins on a cache line getting dirty without going through the system bus. If such a scenario comes about at runtime, it will boost performance and greatly reduces unnecessary memory traffic. We do not try to reshape or rebalance the tree with respect to fixed masters. Fixed masters will depend on dynamic registration order of **signal-wait** tasks. In the worst case, a fixed master may inhibit another **signal-wait** task in its subtree from becoming a fixed master, and may end up gathering signals from a sibling subtree as well. The second function of the registration

phase adds the `sigSync` object to a list on the phaser known as the *landing pad*. The landing pad ensures that there are no racy registrations when the tree root master gathers all signals. A common racy scenario is when one task is waiting at the root of the tree while another task is creating a child whose registration would add an extra level to the tree. As soon as the registration is done, and the parent signals on the tree, the task at the root being unaware of the new registration would erroneously conclude that all tasks have signaled. In fact, the root itself has now changed from before. The landing pad along with a dynamic root check ensures that this situation is averted. This is one of the critical design features for supporting all modes of registration on the phaser tree.

Synchronization Phase

This part of the algorithm deals with the phaser synchronization operation called `next`. The `next` operation comprises of the `signal` and `wait` functions. If a task's registration mode is `signal-only`, then a `next` perform only the `signal`. Similarly when the task is in `wait-only` mode, the `next` does only the `wait`. In all other modes, both `signal` and `wait` are performed.

Algorithm 5 shows the pseudocode for the `signal` operation. In order to signal, the task increments the *phase* counter on the `sigSync` object. The *checkphase* counter keeps track of early signal operations done by the task. If the *checkphase* lags behind the *phase*, then a `signal` done through a `next` become a no-op. Additionally this function checks if there is any requirement for a traversal of the tree to fix this task as the master of an unfixed subphaser. The check is done with one compare operation and so it does not add much overhead for a regular `next` when the check fails. However, when the condition succeeds, then the task has to check if it can

Algorithm 5: PhaserSignal

Input: sig sync s

```

if  $s.phase = s.checkphase$  then
    if  $checkUnfixedSubPhasers() = true$  then
         $FixSubPhaser(s);$ 
    end
     $s.phase ++;$ 
end

 $s.checkphase ++;$ 

```

become the master of an unfixed subphaser. This requirement of this dynamic fixing may arise when a task that was previously a fixed master on a subphaser drops from the phaser, and in the process unfixes the subphaser.

Algorithm 6 shows the **wait** operation. In this function, the task first checks if it is the fixed master of a subphaser, and if that fact is true, then it proceeds to perform a wait operation on that subphaser. This wait operation is shown by the function *doWaitTree* in Algorithm 7. But, if the task is not a fixed master of any subphaser, it tries to become the phaser master. The phaser master has the responsibility of ensuring all the tree signals have arrived before broadcasting the *phase* change to all waiters. This functionality is shown in the *doWaitPhaser* function in Algorithm 9 and is explained later.

The *doWaitTree* function ensures that the master of a subphaser waits for all signals in it's subtree followed by waiting for the parent subphaser's phase change. The master first checks if the subphaser is a leaf, and if so, it gathers the signals from the **sigSync** objects attached to the leaf subphaser. If the subphaser is not a leaf, then

Algorithm 6: PhaserWait

Input: phaser ph , wait sync w

```

if  $w.fixedsph \neq \emptyset$  then
    |  $doWaitTree(w, w.fixedsph, true);$ 
end

while  $w.phase \geq ph.phase$  do
    | if  $ph.master = 0$  then
    | | if  $ph.fixedmaster = w$  then
    | | |  $doWaitPhaser(ph, w);$ 
    | | else
    | | | busy wait for either  $ph.phase$  or  $ph.master$  to change;
    | | end
    | else
    | | if  $isPhaserUnfixedMaster(ph, w) = true$  then
    | | |  $doWaitPhaser(ph, w);$ 
    | | else
    | | | busy wait for either  $ph.phase$  to change;
    | | end
    | end
end

```

Algorithm 7: doWaitTree

Input: wait sync w , subphaser sph , boolean $checkparent$

```

if  $isLeaf(sph)$  then
    | busy wait on array of signaler tasks;
else
    | foreach child subphaser  $c$  do  $doWaitNode(w, c, false)$ ;
end

 $sph.phase++$ ;

if  $sph.parent \neq \emptyset$  &  $checkparent = true$  then
    |  $doWaitNode(w, sph.parent, true)$ ;
end

```

Algorithm 8: doWaitNode

Input: wait sync w , subphaser sph , boolean $checkparent$

```

while  $wait.phase \geq sph.phase$  do
    | if  $sph.fixedwaiter \neq \emptyset$  then
    | | busy wait for  $sph.phase$  to change or  $sph.fixedwaiter$  be inactive;
    | else
    | | if  $isSubPhaserUnfixedMaster(sph, w) = true$  then
    | | |  $doWaitTree(w, sph, checkparent)$ ;
    | | else
    | | | busy wait for either  $sph.phase$  to change;
    | | end
    | end
end

```

Algorithm 9: doWaitPhaser

Input: phaser ph , wait sync w

foreach element s in $ph.landingpad$ **do** busy wait until $s.phase > ph.phase$;

$r \leftarrow \emptyset$;

while $r \neq ph.root$ **do**

$r \leftarrow ph.root$;

$doWaitNode(w, ph.root, 0)$;

end

Remove sub phasers with fixed masters from unfixed list;

$ph.phase++$;

it gathers signals from children subphasers by calling the function *doWaitNode* shown in Algorithm 8. Once all the signals have arrived from the children, the subphaser's phase change is signaled by incrementing the *subphase* variable.

The *doWaitNode* function checks if the subphaser already a fixed master, and if so, then waits for the fixed master to signal the phase change on that subphaser. If the function detects that the fixed master has dropped, or if there was no fixed master in the first place, then it tries to become a temporary master by performing an atomic *compare- and- swap* on the submaster variable. On succeeding it performs a *doWaitTree* function on that subphaser. On failure, it waits for the subphaser to signal a phase change.

Now, the *doWaitTree* function takes a boolean argument called *checkparent*. If the argument is true, then it means that the function cannot complete until the parent has signaled a phase change. The rationale is that even if a fixed master of a subphaser has signaled its phase change, the only way to ensure progress is to ensure that your parent

has gathered all signals in its subtree. So, the fixed master calls a *doWaitNode* on the parent. Consider the scenario when there is only one task registered in **signal-wait** mode on the phaser and all others are in **signal-only** mode. Since, only tasks with **signal-wait** can become fixed masters, this task would basically have to gather the signals from all others. This ensured by the algorithm through checking the parent after collecting signals from its subtree.

The *doWaitPhaser* function is called by the task which is the global master of this phaser. The global master may also have a task fixed as its master in order to reduce the atomics required to be temporary master. This function first waits for all signals from the landing pad list of tasks. Once the signals have arrived, the tasks are removed from the landing pad. Next, the global master performs a *doWaitNode* on the root of the phaser tree. Doing this ensures that the global master has collected all the signals in the subtree under the root. Consider the scenario when all the tasks registered on the phaser tree are in **signal-only** mode. In such a case, the global master will ensure that it gathers all their signals through the *doWaitNode* function. Now, it might be the case during the gather of signals though the root, more tasks get registered on the phaser and the tree grows new levels. This would imply that the root has changed from the time the global master started the *doWaitNode* function. As a result, the algorithm checks for this change and repeats the process if there was indeed a change to the root. After gathering all signals from a stabilized root, the global master removes all subphasers from the `unfixed_sph` list which have found new fixed masters. The final step of this function broadcasts the phase change in the phaser by incrementing the *phase* variable.

Algorithm 10: PhaserDropSig

Input: phaser ph , sig sync s

```

if  $s.wait \neq \emptyset$  then
  | if  $s.wait.fixedsph \neq \emptyset$  then
  |   |  $s.wait.fixedsph.fixedmaster \leftarrow \emptyset$ ;
  |   | Add  $s.wait.fixedsph$  to  $ph.unfixedsubphasers$  list;
  | end
  | if  $ph.fixedmaster = s.wait$  then
  |   |  $ph.fixedmaster \leftarrow \emptyset$ ;
  | end
end

 $s.isActive \leftarrow 0$ 

```

De-registration Phase

The de-registration phase is to drop a task from the phaser. As mentioned earlier in the HJ phaser model, tasks are dropped either on completion or on an explicit drop call. The task simply has to make its `sigSync` object inactive. Additionally, if the task was a fixed master on a subphaser then it has to make that subphaser available for other tasks to become the fixed master. This is done by clearing the `fixedmaster` variable on the subphaser and also adding the subphaser to the `unfixed_sph` list.

In this section, we have seen that the algorithm can handle all kinds of registration modes on a phaser tree and improves performance by managing fixed masters for the subphaser tree. Furthermore, the synchronization algorithm also takes advantage of locality benefits in a fully dynamic task parallel environment. The salient points of this algorithm can be summarized as follows.

- Supports task registration for all the modes.
- Supports an unlimited number of tasks participating in the tree synchronization.
- Dynamic management of fixed masters in the phaser tree thereby greatly reducing system bus contention.
- Locality aware fixed master assignment for improving busy-wait performance.

6.3.4 Results

In our multicore experiments, we compare **phaser** performance for barrier synchronization against OpenMP barrier implementations on various platforms. The barrier microbenchmark was based on the EPCC OpenMP *syncbench* test that was developed for evaluating OpenMP barrier overhead [113]. The benchmark runs a loop with a barrier call in its body. This loop is run for a very large number of iterations. The total running time of the loop is divided by number of iterations to get the average time per iteration. Similar to this method, a reference loop is also run which does not contain the barrier call in its body. The average iteration time of the reference loop is then subtracted from the original loop iteration time to produce the barrier overhead time. This constitutes one sample. After many such samples are collected, the minimum, maximum and average times are obtained and displayed along with the standard deviation. In these results, we present the minimum of all the barrier overhead samples. For OpenMP barrier times, we collected results with `OMP_WAIT_POLICY` set to `ACTIVE` as well as the default configuration. We report the best times achieved from either configuration.

Figure 6.9 compares barrier performance of Phaser against OpenMP implementation by the Intel `icc` and `GCC` compilers. The execution platform was an Intel

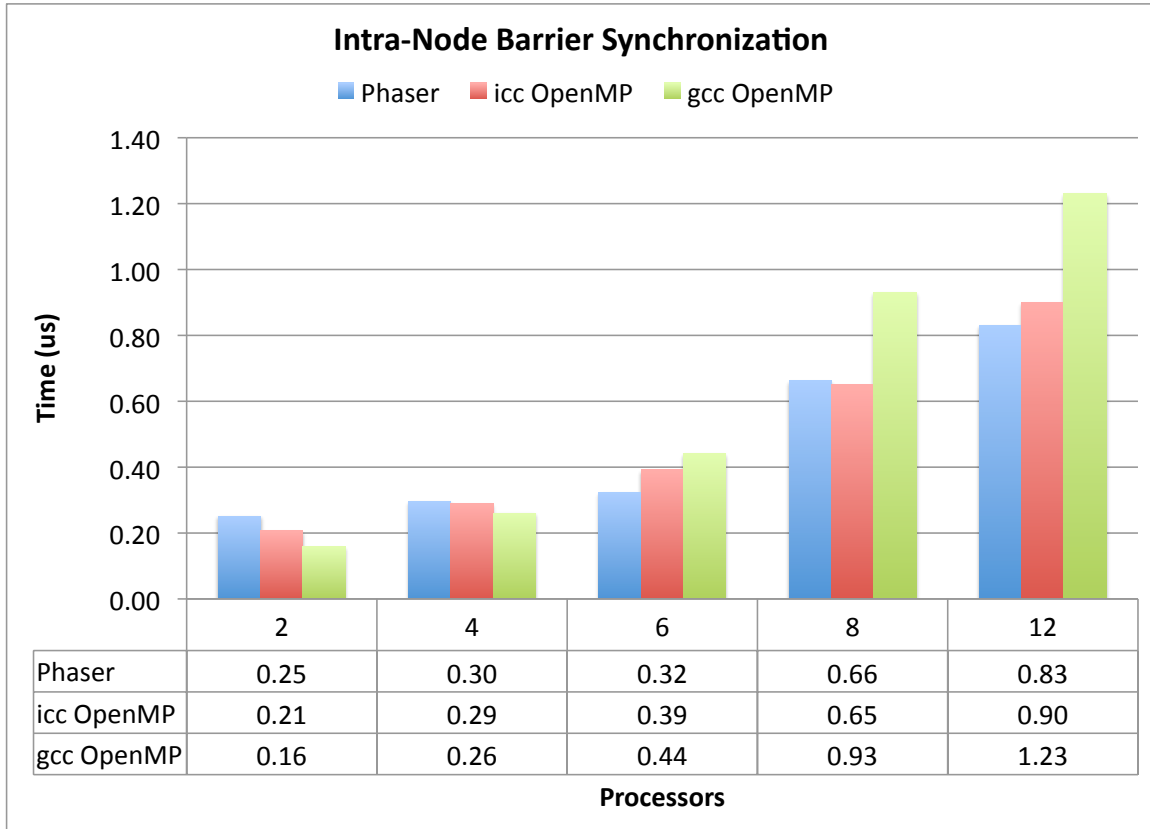


Figure 6.9 : Barrier Synchronization on x86 node

Westmere node with 12 processor cores running at 2.83 GHz. We used Intel `icc` compiler version 12.0.4 and GCC compiler version 4.4.6 and for each case we bound the threads to cores at runtime. The Intel OpenMP implementation by default used the *hyper* algorithm for the barrier operation, a hypercube-embedded tree gather and release algorithm. Two other barrier implementations, namely the *linear* and *tree* algorithms, were also tested by setting the environment variable `KMP_PLAIN_BARRIER_PATTERN`, and the best times are reported. The GCC OpenMP implementation used a counting barrier implementation. The results show that `phaser` outperforms both `icc` and `GCC` as we scale up to 12 cores.

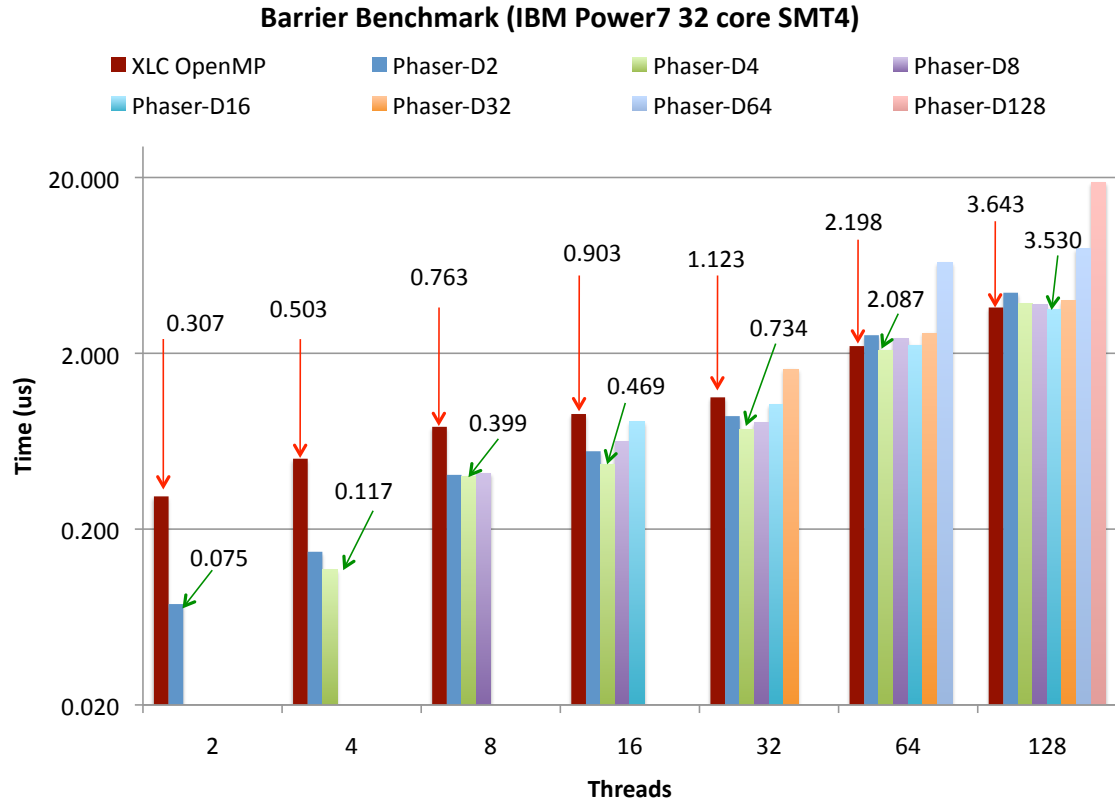


Figure 6.10 : Barrier Synchronization on Power7 node

In Figure 6.10, we compare **phaser** barrier performance on the IBM Power7 platform which provide 128 hardware threads on 32 cores in SMT4 mode. We measure performance for different **phaser** tree degrees and compare against IBM XLC OpenMP barrier performance. The XLC OpenMP configuration is set to active spinning ($XLSMPOPTS = SPINS = 0 : YIELDS = 0 : STARTPROC = 0 : STRIDE = 1$). We vary the number of threads synchronizing on the barrier from 2 to 128. We see that in each case, there exists a **phaser** tree configuration that outperforms the XLC OpenMP barrier performance.

We have also used the dual-CPU Niagara T2 machine for our evaluation. In this

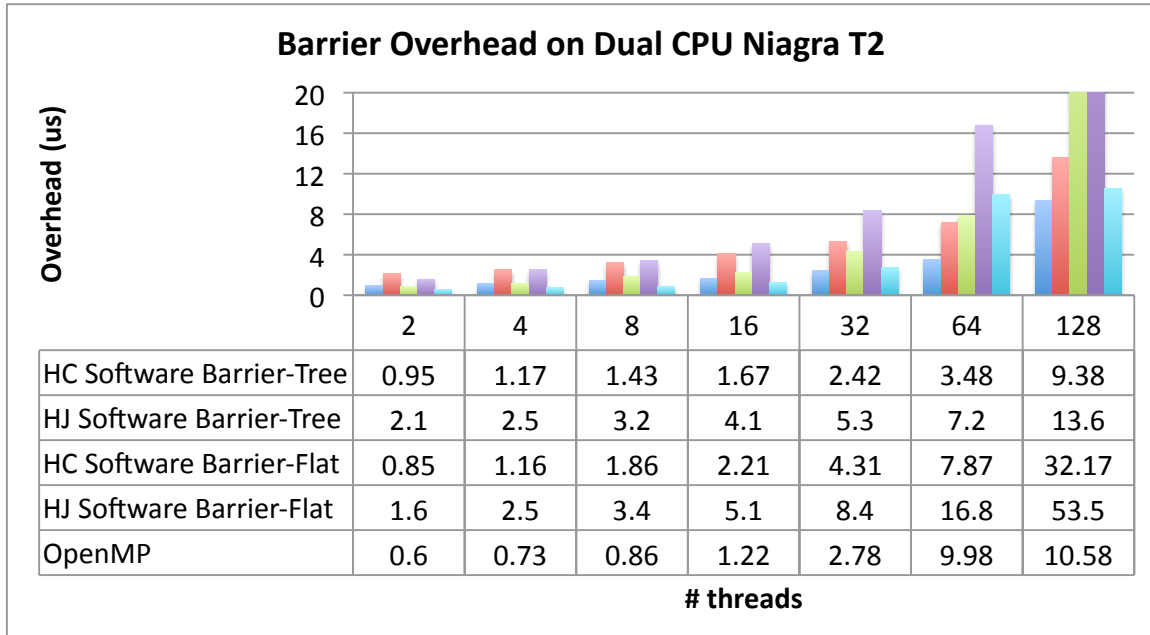


Figure 6.11 : Phaser barrier overhead on a dual-CPU Niagara T2 machine

machine, each Niagara T2 CPU has 8 hardware cores, each of which can sustain 8 SMT (simultaneous multithreading) threads for a total of 128 concurrent threads. The experiments run on the Solaris 10 operating system and they were compiled using the Sun Studio 10 (update 1) OpenMP compiler. Figure 6.11 presents the barrier overhead of our phaser implementation and OpenMP on the 128-thread Niagara T2 machine. For comparison, we also include the results of Habanero-Java phaser implementation. Due to the lack of hardware support for barriers or thread suspend/awake in the Niagara T2 processor, we only evaluate the barrier implementation using the busy-wait approach with and without hierarchical phasers. We can see that hierarchical phasers reduce the barrier overhead by a large margin for both the Habanero-C and Habanero-Java, while the Habanero-C tree implementation outperforms the OpenMP barrier.

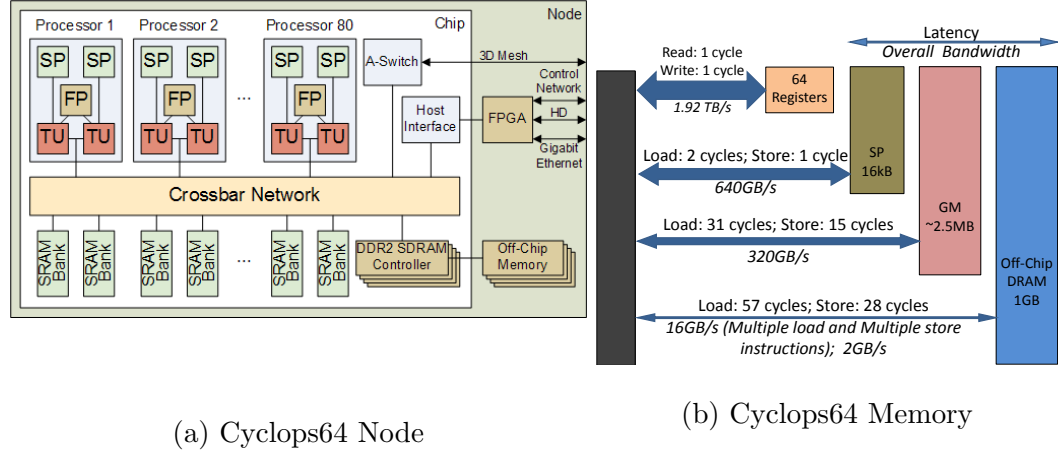


Figure 6.12 : Cyclops64 Architecture Details

6.4 Phasers for Manycore Synchronization

In this Section, we explore a phaser implementation that leverages hardware support for synchronization using the IBM Cyclops64 (C64) manycore chip [114] as our evaluation platform. The IBM Cyclops64 is a massively parallel manycore architecture initially developed by IBM as part of the Blue Gene project. As shown in Figure 6.12, a C64 processor features 80 processing cores on a chip, with two hardware thread units per core that share one 64-bit floating point unit. Each core can issue one double precision floating point Multiply Add instruction per cycle, for a peak performance of 80 GFLOPS per chip when running at 500MHz. The processor chip includes a high-bandwidth on-chip crossbar network with a total bandwidth of 384 GB/s. C64 employs three-levels of software-managed memory hierarchy, with the Scratch-Pad (SP) currently used to hold thread-specific data. Each hardware thread unit has a high-speed on-chip SRAM of 32KB that can be used as a cache.

C64 utilizes a dedicated signal bus (SIGB) that allows thread synchronization without any memory bus interference. The SIGB connecting all threads on a chip

Name	Description
<code>tnt_create(...)</code>	Create a TNT thread; its syntax is similar to <code>pthread_create</code>
<code>tnt_join(...)</code>	Wait for a thread to terminate, similar to <code>pthread_join</code>
<code>tnt_suspend()</code>	Suspend current thread
<code>tnt_awake (const tnt_desc_t)</code>	Awaken a suspended thread
<code>tnt_barrier_include (tnt_barrier_t *)</code>	Join in the next barrier wait operation
<code>tnt_barrier_exclude (tnt_barrier_t *)</code>	Withdraw from the next barrier wait operation
<code>tnt_barrier_wait (tnt_barrier_t *)</code>	Wait until all threads arrive this point

Table 6.2 : Cyclops64 TNT APIs for Hardware Synchronization Primitives

can be used for broadcast operations taking less than 10 clock cycles, enabling efficient barrier operations and mutual exclusion synchronization. Fast point-to-point signal/wait operations are directly supported by hardware interrupts, with costs on the order of tens of cycles. The C64 tool chain includes a highly efficient threading library, named TiNy-Threads (TNT) [114], which uses the C64 hardware support to implement threading primitives. The TNT API is similar to the Pthread API, simplifying porting of pthread-based runtime systems and applications to Cyclops64. Additionally, TNT provides APIs that can be used to access the hardware synchronization primitives to allow for suspension of threads, and including and excluding specific threads from barriers, as shown in Table 6.2.

6.4.1 Optimization Using Hardware Barriers

Phasers can be optimized in manycore architectures that offer direct hardware support for barriers, such as C64. The phaser runtime is able to detect if a phaser operation specified by the user program is equivalent to a barrier operation by checking whether

all phasers are registered in `signal-wait` mode. If so, the underlying hardware support is used directly to perform the barrier operation. Detecting whether or not a particular operation is equivalent to a barrier is straightforward from the phaser model; hardware barriers can be used when all tasks on a phaser are registered in `signal-wait` mode.

Implementing a hardware barrier in a phaser requires threads to include themselves in the barrier by calling `tnt_barrier_include`. This requirement is particularly interesting in a tasking environment due to the fact that the worker thread that executes the task has to include itself in the hardware barrier. The Habanero-C runtime only includes a worker in the hardware barrier when it is ready to execute a task. The C64 chip supports five hardware barriers that can be accessed using the TNT barrier API. If a programmer uses more than five barriers in a program, the extra barriers will execute as software barriers.

6.4.2 Optimization Using Thread Suspend and Awake

The TNT API provides functions to suspend a thread and to awake a sleeping thread. A `suspend` instruction temporarily stops execution in a non-preemptive way, and a `signal` instruction awakes the sleeping task. Using thread suspend and awake mechanism in place of the busy-wait approach reduces memory bandwidth pressure because all waiting tasks can suspend themselves instead of spinning. The master can collect all the signals from waiting tasks and finally signals the suspended tasks to resume the execution.

The C64 chip provides an interesting hardware feature called the “wake-up bit”. When a thread tries to wake up another thread, it sets the “wake-up bit” for that thread. This enables a thread to store a wake-up signal. Hence, if a thread tries to

suspend itself after a wake-up signal is sent, it wakes up immediately and the suspend effectively becomes a no-op. This feature is utilized by phasers to transition from one phase to the next without worrying about a thread that can execute a suspend after a wake up signal.

6.4.3 Adaptive Phasers

Adaptability is one of the main features of our phaser implementation. As explained before, the runtime can directly detect the synchronization operation being performed and make a reasonable decision as to how to execute it. A phaser operation can switch to the optimized versions that utilize hardware primitives. These details of how a phaser operation is executed are hidden from the user.

Phaser operations can be implemented in a number of ways to take advantage of the particular characteristics of the underlying hardware. Even when a phaser has all tasks registered in **signal-wait** mode, it is not guaranteed that a hardware barrier will be used. A task that is registered to support split-phase or fuzzy barriers may signal ahead of its **next** operation. When a task registers as **signal-only** or **wait-only** on a phaser that has been using a hardware barrier, our runtime detects such a scenario and switches to software mode. The runtime chooses the best mode of operation, depending on the current program state and available features. Each implementation alternately exhibits particular traits: maximum portability and reasonable performance is achieved with a *busy-wait* implementation; low bandwidth and low power usage are featured in the *suspend-awake* implementation.

6.4.4 Memory Optimizations

Phaser and `phaserSync` objects contain volatile phase counters, and phaser operations involve frequent read and write of those counters in both software based busy-wait approach and hardware-optimized implementations. So low latency and high bandwidth of the memory system are key to the performance of phasers. The C64's memory hierarchy, as seen in Figure 6.12, is similar to hardware cache in regular commodity CPUs. The power of using it comes from program manageability as our runtime itself can decide which synchronization objects need to reside on or move to the high-speed SRAM. Yet there is a tradeoff in this software-managed caching approach because the DRAM is limited in its sizes and shared with stack in C64. For a simple DRAM-optimization, the runtime allocates on SRAM, synchronization objects that contain spinning counters. More complex optimizations use heuristic or historical information to identify frequently-accessed data and move them to SRAM. Further memory management by the Habanero-C runtime, such as allocating a list of synchronization objects in a dense array, provide another level of memory optimizations on C64.

6.4.5 Results

Results of Memory Optimization on Cyclops64

In Figure 6.13, we show the barrier overhead of using software phasers that reside on either SRAM or DRAM. By allocating the synchronization objects in SRAM, we avoid spinning on flags allocated on the DRAM. Similar to past results [17] that show the benefits of local spinning and avoiding spinning across the network, we achieve better performance by spinning on SRAM allocated flags. This optimization results in dramatic overhead reduction for both flat-phaser and hierarchical-phaser

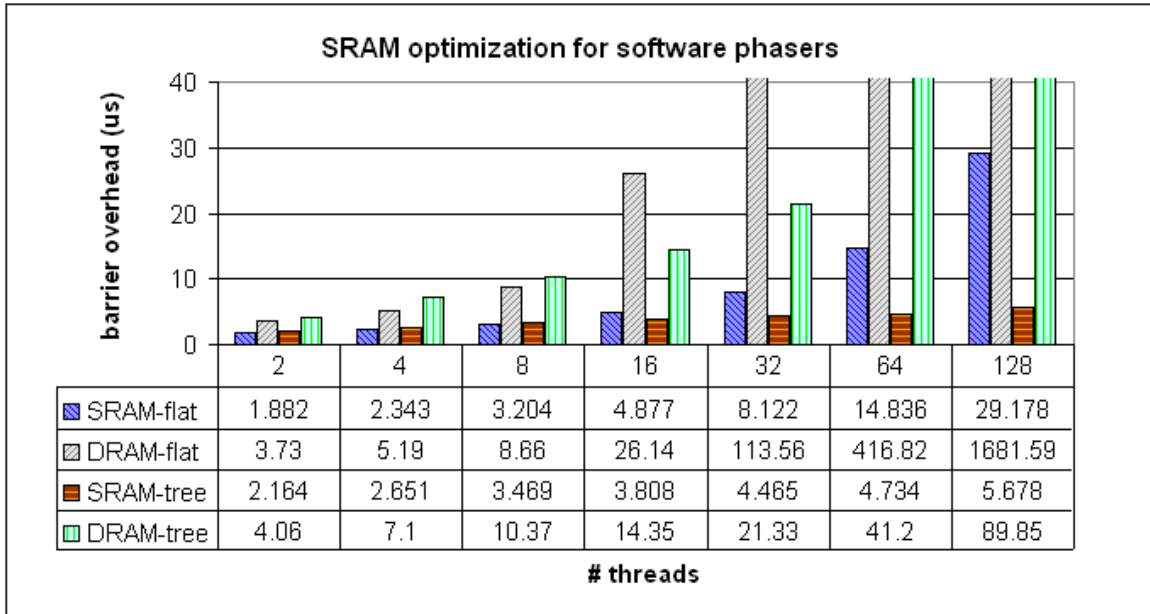


Figure 6.13 : SRAM optimization for phasers on Cyclops64

implementations; two orders of magnitude for flat-phaser and 1 order of magnitude for hierarchical phaser. From now on, we use SRAM hierarchical phaser implementation to represent our software phaser when comparing with other hardware-based implementations.

Results of Barrier and Point-to-Point Microbenchmarks on Cyclops64

The barrier microbenchmark was based on the EPCC OpenMP *syncbench* benchmark. Figure 6.14a shows the barrier overheads using four phaser implementations on C64. The implementation that leverages the C64 hardware barrier incurs much lower overhead than that of the software barrier. The implementation that uses suspend/awake performs worse than software phasers because of the sequentially accumulated cost of hardware interrupt in suspend/awake implementation. For software hierarchical phasers, both signal gathering and wait operations are performed in parallel, thus

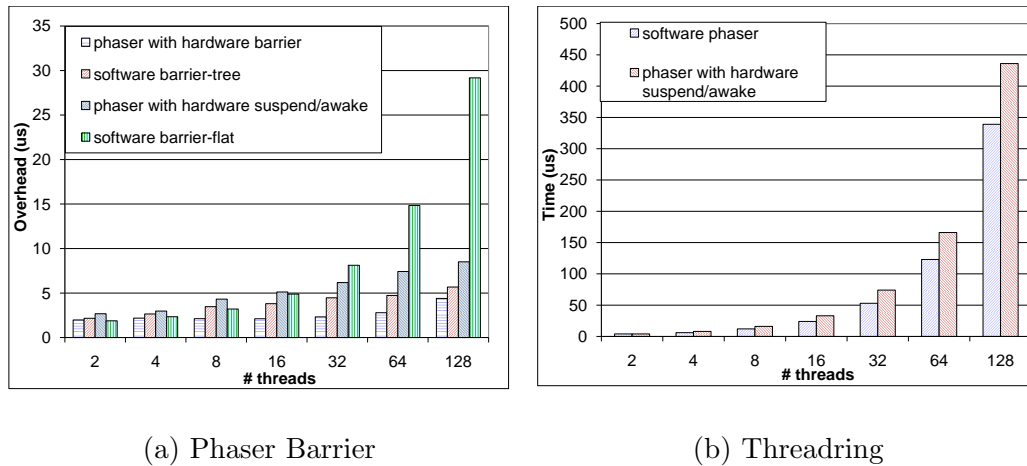


Figure 6.14 : Barrier and Point-to-Point Microbenchmarks

reducing overhead.

The *threadring* microbenchmark evaluates point-to-point signal-wait operation of two tasks. In this program, a group of tasks form a signal ring; each task waits on the signal from the previous task and signals the next task after receiving the signal. As shown in Figure 6.14b, the memory consumption of the software busy-wait approach has little impact on the time required to complete a round of the ring. In fact, the implementation using software phasers performs slightly better than the one using hardware interrupts. These imply the effectiveness of using the portable software-based solution for point-to-point synchronizations. The high performance obtained using the *busy-wait* implementation is due in part to the high bandwidth and low latency of the local on-chip memory in C64. Although the other techniques in our experiments use hardware support, they still suffer from overhead in the supporting software required to use the hardware primitives. In contrast, *busy-wait* uses a very simple polling mechanism that does not require complex software support.

6.5 Phasers for Hybrid Synchronization

Phasers have been extended to support collective operations at inter-node level. We use the HCMPI programming model to create a hybrid synchronization construct, called **hcmapi-phaser**, which uses **phaser** synchronization at intra-node level and MPI collective synchronization at inter-node level. In this model, the synchronization statement **next** provides unified synchronization for tasks registered on a **phaser** across the whole system by using the HC-COMM runtime. In this section, we discuss the HCMPI **phaser** barrier and accumulator models. We believe task based unified collective synchronization operations on distributed systems to be a novel contribution.

Phaser API	Description
<i>ph</i> = HCMPI_PHASER_CREATE(int mode)	hcmapi-phaser create
<i>ph</i> = HCMPI_ACCUM_CREATE(int mode, <i>init_val</i> , HCMPI_Type type, HCMPI_Op oper)	hcmapi-accum create
next	phaser synchronization
accum_next (<i>value</i>)	accumulator synchronization
accum_get (<i>ph</i>)	accumulator result

Table 6.3 : HCMPI PHASER API

The goal of this hybrid synchronization model is to provide clean semantics for system wide collective operations. We combine inter-node MPI collectives with intra-node **phaser** synchronization. An instance of **hcmapi-phaser** is created using the HCMPI_PHASER_CREATE API shown in Table 6.3. Since this hybrid model supports only MPI collectives at inter-node level, an **hcmapi-phaser** can only be created using the **signal-wait** mode. This also implies that the task which creates the **hcmapi-phaser**

instance is registered in `signal-wait` mode. Dynamic registration and deregistration is allowed, as well as arbitrary mode patterns for new tasks created after the `hcmphi-phaser` instance. New tasks can be registered on a `hcmphi-phaser` in one of `signal-wait`, `signal-only` or `wait-only` modes. So, regardless of the registration modes used for tasks within a node, the inter-node synchronization will always be a MPI collective, such as a barrier or a reduction. In a system-wide barrier or reduction operation, all tasks registered on a `hcmphi-phaser` have to be in `signal-wait` mode. Registered tasks can synchronize both within the node and across nodes using the synchronization primitive `next`. The inter-node SPMD model requires that every rank process creates its own `hcmphi-phaser` before participating in the system wide `next` operation. Figure 6.15 shows an example of using the `hcmphi-phaser` as a barrier.

```
finish {
    phaser *ph;
    ph = HCMPI_PHASER_CREATE(SIGNAL_WAIT_MODE);
    for (i = 0; i < n; ++i) {
        async phased(ph) IN(i) {
            ...; next;
            ... //do post-barrier work
        } /*async*/ } /*for*/ } /*finish*/
```

Figure 6.15 : HCMPI Phaser Barrier Model

The HCMPI model integrates intra-node `phaser` accumulators [115] with inter-node MPI reducers using the `hcmphi-accum` construct. An instance of `hcmphi-accum` is created using the `HCMPI_ACCUM_CREATE` API, shown in Table 6.3. The API takes a

HCMPI_MAX	HCMPI_MIN	HCMPI_SUM
HCMPI_PROD	HCMPI_LAND	HCMPI_BAND
HCMPI_LOR	HCMPI_BOR	HCMPI_LXOR
HCMPI_BXOR	HCMPI_MAXLOC	HCMPI_MINLOC

Table 6.4 : HCMPI Ops

registration mode, an initial value for the reduction element, a type of the element and the type of the reduction operation. The registration mode can only be `signal-wait` in the current implementation. Supported reduction operators are shown in Table 6.4. In this model, computation tasks at the intra-node level register on a `hcmapi-accum` instance and participate in the specified global reduction operation via the runtime call `accum_next(value)`, which takes as an argument the individual datum provided by the task for the reduction. Tasks arrive at the synchronization point with a value and participate in all `hcmapi-accum` instances they are registered with. After synchronization completes, `accum_get` will return the globally reduced value. At the inter-node level, we currently only support the `MPI_Allreduce` model. This means that a call to `accum_get()` will return the globally reduced value. Figure 6.16 shows an example of the `hcmapi-accum` model for the SUM operation.

6.5.1 Implementation

HCMPI builds on Habanero-C's tree-based implementation of `phaser` and the `HCCOMM` runtime to integrate inter-node MPI collectives and intra-node `phaser` synchronization. Tree based phasers have been shown to scale much better than flat phasers [112, 116]. `HCMPI_PHASER_CREATE` creates a phaser barrier, while `HCMPI_`

```

finish {

    phaser *ph;

    ph = HCMPI_ACCUM_CREATE(HCMPI_SUM,HCMPI_INT);

    for (i = 0; i < n; ++i) {

        async phased IN(...) {

            int* my_val = get_my_val();

            accum_next(my_val);

            ...; } /*async*/ } /*for*/ } /*finish*/

    int* result = (int*)accum_get(ph);

```

Figure 6.16 : HCMPI Phaser Accumulator Model

`ACCUM_CREATE` creates an accumulator object. Tasks can dynamically register to and drop from a `hcmapi-phaser`. The `next` statement and the `accum_next` APIs act as the global synchronization points for barriers and accumulators. Figure 6.17 illustrates the synchronization process for HCMPI phaser barrier and accumulator operations. In the case of a barrier, tasks, T0 to T7, arrive at the `next` statement and signal the phaser. Then they start the wait phase. These tasks traverse the internal nodes of the phaser tree to see if they can become sub-masters at any of the sub-phaser nodes S0 to S6. The first task to arrive at a sub-phaser becomes the sub-master for that node. The sub-master collects the signals from its sub-tree and then signals its parent. This way, signals on the phaser tree propagate up to the root node. The first task to arrive at the root node becomes the phaser master. Others wait for the phaser master to signal the start of the next phase. The `MPI_Barrier` operation is started only after the phaser master at the root sub-phaser receives all signals in the phaser tree. The phaser master waits on a notification from the communication task that

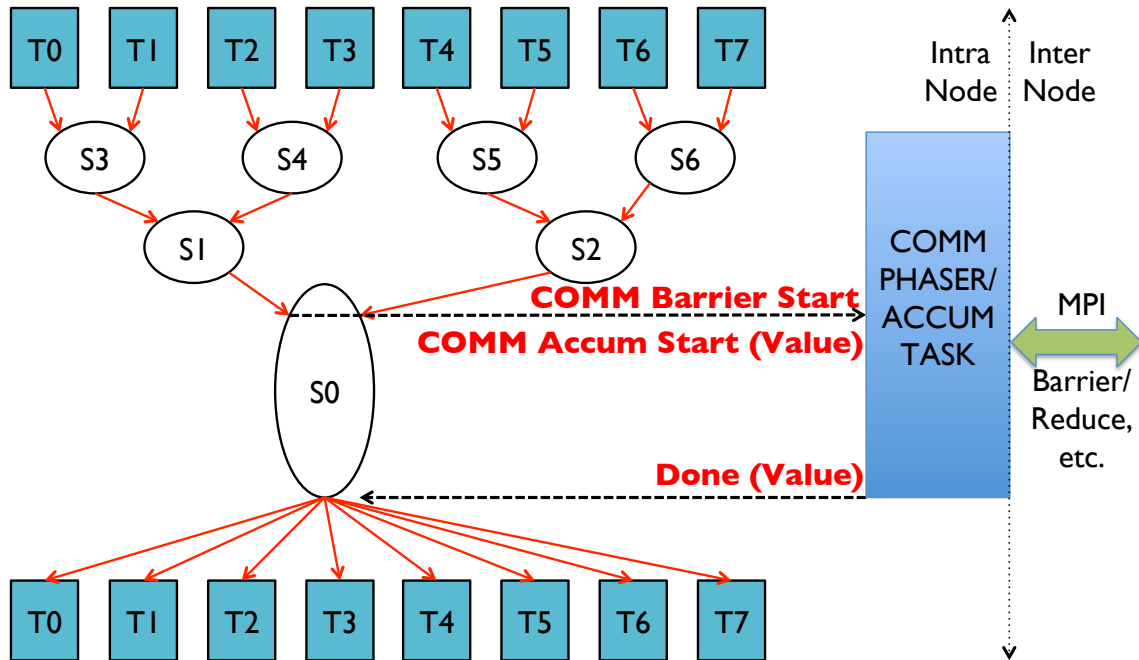


Figure 6.17 : HCMPI Phaser Barrier

the `MPI_Barrier` operation is completed. Once the notification arrives, the phaser master signals all the intra-node tasks to start their next phase. In case of phaser accumulators, each task arrives at the `accum_next` synchronization point with a value in addition to the signal. The value gets reduced to a single element at the root of the phaser tree and then the phaser master signals the hcmpti phaser communication task to start the `MPI_Allreduce` operation. The globally reduced value is saved in the phaser data structure and can be retrieved by the `accum_get` call on that phaser object.

6.5.2 Results

We measure the performance of HCMPI phaser barriers and accumulators. We compare against MPI-only and hybrid MPI+OpenMP performance. We used a modified

version of the EPCC Syncbench [113] for barrier and reduction (accumulator) tests. The benchmarks run a loop containing a barrier or reduction operation for a large number of times. The cost of synchronization is estimated by subtracting the loop overhead from the iterations. We measure synchronization performance on 2 to 64 nodes while using 2 to 8 cores per node. In our experiment, the MPI-only version uses `MPI_THREAD_SINGLE`, while the hybrid MPI+OpenMP version uses `MPI_THREAD_MULTIPLE`. Both the HCMPI and hybrid versions use one process per node and use threads for the number of cores used inside a node. The MPI-only version uses one process for every core used in the experiment to perform distributed collective operations. The HCMPI test creates the number of tasks and computation workers equal to the number of cores used per node in the experiment. Together they perform the integrated synchronization at the intra-node and inter-node level for both barriers and accumulators. We measure HCMPI phaser barrier performance. The MPI+OpenMP hybrid version creates a parallel region of number of threads equal to the number of cores. Threads first synchronize using a OpenMP barrier, then the `MPI_Barrier` is called by a **single** thread while the others wait at subsequent OpenMP barrier. The hybrid reduction test completes a global reduction by first performing an OpenMP for loop reduction over the number of threads followed by `MPI_Allreduce` by a **single** thread. Remaining threads wait at a OpenMP barrier.

The results in Table 6.5 clearly demonstrate that MPI and hybrid times increase at a faster rate compared to HCMPI with increasing number of cores per node, for both barriers and accumulators. HCMPI depends on MPI performance for inter-node synchronization. When scaling up the number of cores within a node, HCMPI is able to use intra-node phaser synchronization, while MPI depends on `MPI_Barrier` and `MPI_Allreduce` over all cores. Overall, hybrid MPI+OpenMP outperforms MPI while

Collective Synchronization Times in micro-seconds									
Nodes	2			4			8		
Cores	2	4	8	2	4	8	2	4	8
MPI Barrier	3.0	4.1	5.1	5.8	6.7	7.6	9.1	9.8	11.1
MPI+OMP Barrier	2.5	2.8	3.9	5.0	5.8	6.7	8.2	9.1	10.0
HCMPI Phaser	2.1	2.2	2.7	4.8	4.8	5.4	7.7	7.7	8.6
MPI Reduction	3.8	4.6	5.2	6.3	7.2	7.9	9.5	10.7	12.1
MPI+OMP Reduction	3.1	3.6	4.9	5.4	5.9	7.2	8.2	9.1	10.5
HCMPI Accumulator	2.6	2.8	3.5	4.9	5.0	5.8	7.7	7.8	9.4
Nodes	16			32			64		
Cores	2	4	8	2	4	8	2	4	8
MPI Barrier	12.6	13.4	14.7	20.0	19.9	21.6	25.3	25.7	26.2
MPI+OMP Barrier	11.6	12.6	14.2	17.2	19.0	20.8	21.8	24.7	26.2
HCMPI Phaser	11.3	11.2	12.1	17.2	17.8	18.0	22.0	21.7	23.6
MPI Reduction	12.8	14.3	15.3	17.7	18.7	19.8	25.0	25.7	26.7
MPI+OMP Reduction	11.1	12.4	14.1	15.1	16.9	18.9	20.8	23.4	25.8
HCMPI Accumulator	10.7	10.5	12.3	14.7	15.4	16.9	20.8	20.6	23.5

Table 6.5 : EPCC Syncbench with MVAPICH2 on Infiniband

HCMPI outperforms both. These experiments were performed using MVAPICH2 on the DAVinCI cluster. We have not included the results for Jaguar because we discovered inconsistent `MPI_Barrier` performance with MPICH2.

6.6 Summary

In this chapter we presented a new algorithm that enables generalized tree-based synchronization for the `phaser` model. We integrated the `phaser` model into the

Habanero-C task parallel language. We presented the design of the **phaser** model on the manycore Cyclops64 processor. We have shown different techniques for phaser synchronization on Cyclops64 that use a combination of software-based busy-wait approach, hardware barriers, and hardware support for thread suspend/awake. Our experiments show that phasers are able to take advantage of hardware primitives on manycore architectures and optimizations for their memory subsystems to provide superior performance to portable software approaches. We have also extended the phaser construct for integrated hybrid synchronization within and across nodes. Our experiments have shown phasers can outperform standard implementations for barriers, while at the same time provide the flexibility of unified collective and point-to-point synchronization.

Chapter 7

Conclusions

In this dissertation, we addressed the software challenges for programming on extreme-scale systems described in the thesis statement in Section 1.1. This research focussed on the role of a software runtime system in three key areas. The first focus area addressed scalability challenges for a dynamic task parallel system when interfaced with a communication system. The second area of research was related to controlling affinities of compute and data. The third research area dealt with task synchronization issues for extreme-scale systems.

In chapter 4, we presented the **HC-COMM** runtime communication system and **HCMPI** programming model. The **HC-COMM** runtime design is a novel scalable runtime system consisting of a dedicated communication worker and a number of computation workers. The **HCMPI** programming model unifies asynchronous task parallelism at intra-node level with MPI’s message passing model at the inter-node level. The combination of asynchronous message passing and computation tasks enable programmers to easily implement techniques for latency hiding, communication/computation overlap and event driven tasks. With **HCMPI**’s task parallel model, users can benefit from MPI integration with structured task parallelism and data-flow programming. Constructs such as `async`, `finish`, and `await` have been seamlessly integrated with the MPI message passing model. Computation tasks can create new communication tasks, wait for their completion and start execution based on message events.

Our experimental microbenchmark results show that a dedicated communication worker manages contention on the communication sub-system better than multithreaded MPI when increasing the number of communicating resources inside a node. For the UTS benchmark on the ORNL Jaguar machine with 1024 nodes and 16 cores/node, **HC MPI** performed $22.3\times$ faster than MPI for input size T1XXL and $18.5\times$ faster than MPI for input size T3XXL (using the best chunking and polling parameters for both **HC MPI** and MPI). This result demonstrated the importance of a dedicated communication worker for distributed work-stealing. The communication worker responded to steal requests faster without interrupting any computation workers. This overlapping the inter-process steals with intra-process computation proved essential for scalable performance.

In chapter 5, we describe our approach to manage affinities of computation and data at inter-node and intra-node levels. We presented a distributed macro dataflow programming model, called **HAPGNS**, as a simple extension to the shared-memory DDF model. This programming model does not require any knowledge of MPI. User provided data distribution functions act as locality directives. Scalability results for the Smith-Waterman benchmark show the practicality of this approach, which offers high programmability.

Our intra-node locality optimizations are driven by a tuning framework geared towards its use by experts with detailed system knowledge. The tuning framework allows the user to express affinities between task computations and associated data through hierarchical affinity *groups*. The runtime uses **HPT**, a hierarchical place tree construct, used to model the memory hierarchy of a system. The tuning optimizations demonstrate benefit from spatial and temporal task locality using runtime co-scheduling of tasks. We showed performance improvements over an already parallel,

optimally tiled and load balanced execution on a fairly small system with today’s data movement costs. We believe that improvements on future systems with pronounced data movement costs will be much greater.

In chapter 6, we presented a design for the **phaser** synchronization model with applicability to extreme-scale systems. We showed scalable **phaser** designs for multicore compute nodes, manycore compute nodes and inter-node systems. We presented a new algorithm for tree-based synchronization that has general applicability without sacrificing performance. Our results showed that the **phaser** barrier performance was at par with Intel ICC OpenMP and IBM XLC OpenMP barrier performance, and in some cases even outperforming them. We also showed that a **phaser** is able to take advantage of hardware primitives on manycore architectures.

In this dissertation, we have shown that programming on extreme-scale systems will be aided by a combination of novel programming models and a scalable runtime design. Novel programming models need provisions for forward scalability and programmability for existing and future applications. We showed that the **HCMP** programming model can help existing MPI applications embrace task parallelism. The **HAPGNS** programming model is suitable for designing future applications in the data-flow paradigm without requiring any knowledge of MPI. The **HC-COMM** runtime system unified inter-node communication with intra-node computation and provided scalable performance for task parallel applications. The *tuning* framework extended a work-stealing scheduler to guide dynamic execution of tasks according to affinity directives from the user. It used a two-level task scheduling model, a tuning tree and a **HPT**, to co-schedule tasks for spatial and temporal locality benefits. The **phaser** construct enabled task synchronization for long running iterative computation at both intra-node and inter-node levels. At intra-node level, a **phaser** can work for

both barrier and point-to-point synchronization patterns, while at inter-node level it can integrate with MPI collectives for scalable performance. By addressing these challenges, this dissertation makes concrete contributions towards addressing some of the key software challenges for extreme-scale systems. Many more challenges await us on our path to exascale and beyond.

Bibliography

- [1] S. Amarasinghe, D. Campbell, W. Carlson, A. Chien, W. Dally, E. Elnohazy, M. Hall, R. Harrison, W. Harrod, K. Hill, J. Hiller, S. Karp, C. Koebel, D. Koester, P. Kogge, J. Levesque, D. Reed, V. Sarkar, R. Schreiber, M. Richards, A. Scarpelli, J. Shalf, A. Snavely, and T. Sterling, “ExaScale Computing Software Study: Software Challenges in Extreme Scale Systems, Vivek Sarkar, Editor & Study Lead.” DARPA IPTO ExaScale Computing Study, September 2009. <http://users.ece.gatech.edu/~mrichard/ExascaleComputingStudyReports/ECSS%20report%20101909.pdf>.
- [2] K. Bergman, S. Borkar, D. Campbell, W. Carlson, W. Dally, M. Denneau, P. Franzon, W. Harrod, K. Hill, J. Hiller, S. Karp, S. Keckler, D. Klein, P. Kogge, R. Lucas, M. Richards, A. Scarpelli, S. Scott, A. Snavely, T. Sterling, R. S. Williams, and K. Yelick, “ExaScale Computing Study: Technology Challenges in Achieving Exascale Systems, Peter Kogge, Editor & Study Lead.” DARPA IPTO ExaScale Computing Study, September 2008. http://users.ece.gatech.edu/~mrichard/ExascaleComputingStudyReports/exascale_final_report_100208.pdf.
- [3] W. Carlson, T. El-Ghazawi, B. Numrich, and K. Yellick, “Programming in the Partitioned Global Address Space Model.” Tutorial at Supercomputing 2003, November 2003. http://upc.gwu.edu/tutorials/tutorials_sc2003.pdf.

- [4] B. Chamberlain, D. Callahan, and H. Zima, “Parallel Programmability and the Chapel Language,” *Int. J. High Perform. Comput. Appl.*, vol. 21, pp. 291–312, Aug. 2007.
- [5] P. Charles, C. Grothoff, V. Saraswat, C. Donawa, A. Kielstra, K. Ebcioglu, C. von Praun, and V. Sarkar, “X10: An Object-oriented Approach to Non-uniform Cluster Computing,” in *Proceedings of the 20th Annual ACM SIGPLAN Conference on Object-oriented Programming, Systems, Languages, and Applications*, OOPSLA ’05, (New York, NY, USA), pp. 519–538, ACM, 2005.
- [6] W. W. Carlson, J. M. Draper, D. E. Culler, K. Yelick, E. Brooks, and K. Warren, “Introduction to UPC and Language Specication,” Tech. Rep. CCS-TR-99-157, Center for Computing Sciences, Institute for Defense Analyses, May 1999. <http://upc.lbl.gov/publications/upctr.pdf>.
- [7] R. W. Numrich and J. Reid, “Co-Array Fortran for parallel programming,” *ACM SIGPLAN Fortran Forum Archive*, vol. 17, pp. 1–31, Aug. 1998.
- [8] Message Passing Interface Forum, *MPI: A Message-Passing Interface Standard, Version 3.0*, September 2012. <http://www.mpi-forum.org/docs/mpi-3.0/mpi30-report.pdf>.
- [9] Habanero Multicore Software Research Group, Rice University, “The Habanero-C Programming System.” <https://wiki.rice.edu/confluence/display/HABANERO/Habanero-C>.

- [10] M. Frigo, C. E. Leiserson, and K. H. Randall, “The Implementation of the Cilk-5 Multithreaded Language,” in *Proceedings of the ACM SIGPLAN 1998 Conference on Programming Language Design and Implementation*, PLDI '98, (New York, NY, USA), pp. 212–223, ACM, 1998.
- [11] S. Chatterjee, S. Tasirlar, Z. Budimlic, V. Cave, M. Chabbi, M. Grossman, V. Sarkar, and Y. Yan, “Integrating Asynchronous Task Parallelism with MPI,” in *Proceedings of the 2013 IEEE 27th International Symposium on Parallel and Distributed Processing*, IPDPS '13, (Washington, DC, USA), pp. 712–725, IEEE Computer Society, 2013.
- [12] J. Shirako, D. M. Peixotto, V. Sarkar, and W. N. Scherer, “Phasers: a unified deadlock-free construct for collective and point-to-point synchronization,” in *ICS '08: Proceedings of the 22nd annual international conference on Supercomputing*, (New York, NY, USA), pp. 277–288, ACM, 2008.
- [13] Y. Yan, J. Zhao, Y. Guo, and V. Sarkar, “Hierarchical Place Trees: A Portable Abstraction for Task Parallelism and Data Movement,” in *LCPC'09: Proceedings of the 22nd International Workshop on Languages and Compilers for Parallel Computing*, vol. 5898 of *Lecture Notes in Computer Science*, Springer, 2009.
- [14] I. Brooks, Eugene D., “The Butterfly Barrier,” *International Journal of Parallel Programming*, vol. 15, no. 4, pp. 295–307, 1986.
- [15] D. Hensgen, R. Finkel, and U. Manber, “Two Algorithms for Barrier Synchronization,” *Int. J. Parallel Program.*, vol. 17, pp. 1–17, Feb. 1988.

- [16] B. D. Lubachevsky, “Synchronization Barrier and Related Tools for Shared Memory Parallel Programming,” *Int. J. Parallel Program.*, vol. 19, pp. 225–250, Mar. 1991.
- [17] J. M. Mellor-Crummey and M. L. Scott, “Algorithms for Scalable Synchronization on Shared-memory Multiprocessors,” *ACM Trans. Comput. Syst.*, vol. 9, pp. 21–65, Feb. 1991.
- [18] G. E. Blelloch, *Vector Models for Data-parallel Computing*. Cambridge, MA, USA: MIT Press, 1990.
- [19] E. W. Dijkstra, “The Origin of Concurrent Programming,” ch. Cooperating Sequential Processes, pp. 65–138, New York, NY, USA: Springer-Verlag New York, Inc., 2002.
- [20] Arvind, R. S. Nikhil, and K. K. Pingali, “I-structures: Data Structures for Parallel Computing,” *ACM Trans. Program. Lang. Syst.*, vol. 11, pp. 598–632, Oct. 1989.
- [21] P. S. Barth, R. S. Nikhil, and Arvind, “M-Structures: Extending a Parallel, Non-strict, Functional Language with State,” in *Proceedings of the 5th ACM Conference on Functional Programming Languages and Computer Architecture*, (London, UK, UK), pp. 538–568, Springer-Verlag, 1991.
- [22] H. C. Baker, Jr. and C. Hewitt, “The incremental garbage collection of processes,” in *Proceedings of the 1977 symposium on Artificial intelligence and programming languages*, (New York, NY, USA), pp. 55–59, ACM, 1977.

- [23] R. H. Halstead, Jr., “Implementation of Multilisp: Lisp on a Multiprocessor,” in *Proceedings of the 1984 ACM Symposium on LISP and Functional Programming*, LFP '84, (New York, NY, USA), pp. 9–17, ACM, 1984.
- [24] V. Saraswat, B. Bloom, I. Peshansky, O. Tardieu, and D. Grove, “X10 Language Specication Version 2.4,” September 2013. <http://x10.sourceforge.net/documentation/languagespec/x10-latest.pdf>.
- [25] Cray Inc., 901 Fifth Avenue, Suite 1000, Seattle, WA 98164, *Chapel Language Specication Version 0.94*, October 2013. <http://chapel.cray.com/spec/spec-0.94.pdf>.
- [26] J. C. Reynolds, “The discoveries of continuations,” *Lisp Symb. Comput.*, vol. 6, pp. 233–248, Nov. 1993.
- [27] M. Snir, S. W. Otto, D. W. Walker, J. Dongarra, and S. Huss-Lederman, *MPI: The Complete Reference*. Cambridge, MA, USA: MIT Press, 1995.
- [28] M. J. Rashti, J. Green, P. Balaji, A. Afsahi, and W. Gropp, “Multi-core and network aware MPI topology functions,” in *Proceedings of the 18th European MPI Users' Group conference on Recent advances in the message passing interface*, EuroMPI'11, (Berlin, Heidelberg), pp. 50–60, Springer-Verlag, 2011.
- [29] E. Jeannot and G. Mercier, “Near-optimal placement of MPI processes on hierarchical NUMA architectures,” in *Proceedings of the 16th international Euro-Par conference on Parallel processing: Part II*, Euro-Par'10, (Berlin, Heidelberg), pp. 199–210, Springer-Verlag, 2010.

- [30] Y. Cui, K. B. Olsen, T. H. Jordan, K. Lee, J. Zhou, P. Small, D. Roten, G. Ely, D. K. Panda, A. Chourasia, J. Levesque, S. M. Day, and P. Maechling, “Scalable Earthquake Simulation on Petascale Supercomputers,” in *Proceedings of the 2010 ACM/IEEE International Conference for High Performance Computing, Networking, Storage and Analysis*, SC ’10, (Washington, DC, USA), pp. 1–20, IEEE Computer Society, 2010.
- [31] K. Hotta, “Programming on K computer.” Fujitsu presentation at Supercomputing 2010, November 2010. <http://www.fujitsu.com/downloads/TC/sc10/programming-on-k-computer.pdf>.
- [32] Advanced Simulation and Computing Program, (LLNL), “ASC Sequoia Benchmark Codes.” Available at <https://asc.llnl.gov/sequoia/benchmarks/>.
- [33] M. C. Cera, J. V. F. Lima, N. Maillard, and P. O. A. Navaux, “Challenges and Issues of Supporting Task Parallelism in MPI,” in *Proceedings of the 17th European MPI Users’ Group Meeting Conference on Recent Advances in the Message Passing Interface*, EuroMPI’10, (Berlin, Heidelberg), pp. 302–305, Springer-Verlag, 2010.
- [34] D. Buntinas, G. Mercier, and W. Gropp, “Design and Evaluation of Nemesis, a Scalable, Low-Latency, Message-Passing Communication Subsystem,” in *Proceedings of the Sixth IEEE International Symposium on Cluster Computing and the Grid*, CCGRID ’06, (Washington, DC, USA), pp. 521–530, IEEE Computer Society, 2006.

- [35] R. Brightwell, B. Lawry, A. B. MacCabe, and R. Riesen, “Portals 3.0: Protocol Building Blocks for Low Overhead Communication,” in *Proceedings of the 16th International Parallel and Distributed Processing Symposium*, IPDPS ’02, (Washington, DC, USA), pp. 268–, IEEE Computer Society, 2002.
- [36] L. Dagum and R. Menon, “OpenMP: An Industry-Standard API for Shared-Memory Programming,” *IEEE Comput. Sci. Eng.*, vol. 5, pp. 46–55, Jan. 1998.
- [37] OpenMP Architecture Review Board, *OpenMP Application Program Interface, Version 4.0*, July 2013. <http://www.openmp.org/mp-documents/OpenMP4.0.0.pdf>.
- [38] R. Rabenseifner, G. Hager, G. Jost, and R. Keller, “Hybrid MPI and OpenMP Parallel Programming,” in *Recent Advances in Parallel Virtual Machine and Message Passing Interface* (B. Mohr, J. Trff, J. Worringer, and J. Dongarra, eds.), vol. 4192 of *Lecture Notes in Computer Science*, pp. 11–11, Springer Berlin Heidelberg, 2006.
- [39] H. Jin and R. F. Van der Wijngaart, “Performance Characteristics of the Multi-zone NAS Parallel Benchmarks,” *J. Parallel Distrib. Comput.*, vol. 66, pp. 674–685, May 2006.
- [40] M. F. Su, I. El-Kady, D. A. Bader, and S.-Y. Lin, “A Novel FDTD Application Featuring OpenMP-MPI Hybrid Parallelization,” in *Proceedings of the 2004 International Conference on Parallel Processing*, ICPP ’04, (Washington, DC, USA), pp. 373–379, IEEE Computer Society, 2004.

- [41] E. Yilmaz, R. Payli, H. Akay, and A. Ecer, “Hybrid Parallelism for CFD Simulations: Combining MPI with OpenMP,” in *Parallel Computational Fluid Dynamics 2007*, vol. 67 of *Lecture Notes in Computational Science and Engineering*, pp. 401–408, Springer Berlin Heidelberg, 2009.
- [42] W. Pfeiffer and A. Stamatakis, “Hybrid MPI/Pthreads parallelization of the RAxML phylogenetics code,” in *Parallel Distributed Processing, Workshops and Phd Forum (IPDPSW), 2010 IEEE International Symposium on*, pp. 1–8, 2010.
- [43] UPC Consortium, “UPC Language Specifications, Version 1.2,” Tech. Rep. LBNL-59208, Lawrence Berkeley National Lab, May 2005. <http://www.gwu.edu/~upc/publications/LBNL-59208.pdf>.
- [44] The Berkeley UPC Project (joint project of LBNL and UC Berkeley), “Berkeley UPC version 2.18.0,” October 2013. <http://upc.lbl.gov/>.
- [45] D. Bonachea, “GASNet Specification, v1.1,” Tech. Rep. UCB/CSD-02-1207, U.C. Berkeley, October 2002. <http://digitalassets.lib.berkeley.edu/techreports/ucb/text/CSD-02-1207.pdf> (newer versions also available at <http://gasnet.lbl.gov>).
- [46] F. Blagojević, P. Hargrove, C. Iancu, and K. Yelick, “Hybrid PGAS Runtime Support for Multicore Nodes,” in *Proceedings of the Fourth Conference on Partitioned Global Address Space Programming Model, PGAS ’10*, (New York, NY, USA), pp. 3:1–3:10, ACM, 2010.

- [47] J. Mellor-Crummey, L. Adhianto, W. N. Scherer, III, and G. Jin, “A New Vision for Coarray Fortran,” in *Proceedings of the Third Conference on Partitioned Global Address Space Programming Models*, PGAS '09, (New York, NY, USA), pp. 5:1–5:9, ACM, 2009.
- [48] K. Yelick, L. Semenzato, G. Pike, C. Miyamoto, B. Liblit, A. Krishnamurthy, P. Hilfinger, S. Graham, D. Gay, P. Colella, and A. Aiken, “Titanium: a high-performance Java dialect,” *Concurrency: Practice and Experience*, vol. 10, no. 11-13, pp. 825–836, 1998.
- [49] P. N. Hilfinger, D. O. Bonachea, K. Datta, D. Gay, S. L. Graham, B. R. Liblit, G. Pike, J. Z. Su, and K. A. Yelick, “Titanium Language Reference Manual,” Technical Report UCB/EECS-2005-15, University of California at Berkeley, Berkeley, CA, USA, 2005.
- [50] K. Fatahalian, D. R. Horn, T. J. Knight, L. Leem, M. Houston, J. Y. Park, M. Erez, M. Ren, A. Aiken, W. J. Dally, and P. Hanrahan, “Sequoia: Programming the Memory Hierarchy,” in *Proceedings of the 2006 ACM/IEEE Conference on Supercomputing*, SC '06, (New York, NY, USA), ACM, 2006.
- [51] B. Alpern, L. Carter, and J. Ferrante, “Modeling parallel computers as memory hierarchies,” in *Programming Models for Massively Parallel Computers, 1993. Proceedings*, pp. 116–123, 1993.

- [52] G. Bikshandi, J. Guo, D. Hoefflinger, G. Almasi, B. B. Fraguera, M. J. Garzarán, D. Padua, and C. von Praun, “Programming for Parallelism and Locality with Hierarchically Tiled Arrays,” in *Proceedings of the Eleventh ACM SIGPLAN Symposium on Principles and Practice of Parallel Programming*, PPOPP ’06, (New York, NY, USA), pp. 48–57, ACM, 2006.
- [53] R. Chandra, A. Gupta, and J. L. Hennessy, “COOL: An Object-Based Language for Parallel Programming,” *Computer*, vol. 27, pp. 13–26, Aug. 1994.
- [54] L. V. Kale and S. Krishnan, “CHARM++: a portable concurrent object oriented system based on C++,” in *Proceedings of the eighth annual conference on Object-oriented programming systems, languages, and applications*, OOPSLA ’93, (New York, NY, USA), pp. 91–108, ACM, 1993.
- [55] J. Labarta, “StarSs: a Programming Model for the Multicore Era.” In PRACE Workshop ‘New Languages & Future Technology Prototypes’ at the Leibniz Supercomputing Centre in Garching (Germany), March 2010. http://www.prace-project.eu/IMG/pdf/08_starss_jl.pdf.
- [56] A. Duran, E. Ayguad, R. M. Badia, J. Labarta, L. Martinell, X. Martorell, and J. Planas, “OmpSs: A proposal for programming heterogeneous multi-core architectures,” *Parallel Processing Letters*, vol. 21, no. 02, pp. 173–193, 2011.
- [57] J. Bueno, L. Martinell, A. Duran, M. Farreras, X. Martorell, R. M. Badia, E. Ayguade, and J. Labarta, “Productive cluster programming with OmpSs,” in *Proceedings of the 17th international conference on Parallel processing - Volume Part I*, Euro-Par’11, (Berlin, Heidelberg), pp. 555–566, Springer-Verlag, 2011.

- [58] M. Bauer, S. Treichler, E. Slaughter, and A. Aiken, “Legion: Expressing Locality and Independence with Logical Regions,” in *Proceedings of the International Conference on High Performance Computing, Networking, Storage and Analysis*, SC ’12, (Los Alamitos, CA, USA), pp. 66:1–66:11, IEEE Computer Society Press, 2012.
- [59] H. Kaiser, M. Brodowicz, and T. Sterling, “ParalleX An Advanced Parallel Execution Model for Scaling-Impaired Applications,” in *Proceedings of the 2009 International Conference on Parallel Processing Workshops*, ICPPW ’09, (Washington, DC, USA), pp. 394–401, IEEE Computer Society, 2009.
- [60] J. Lifflander, S. Krishnamoorthy, and L. V. Kale, “Work Stealing and Persistence-based Load Balancers for Iterative Overdecomposed Applications,” in *Proceedings of the 21st International Symposium on High-Performance Parallel and Distributed Computing*, HPDC ’12, (New York, NY, USA), pp. 137–148, ACM, 2012.
- [61] ETI Inc., “SWARM (SWift Adaptive Runtime Machine): Scalable Performance Optimization For Multi-Core/Multi-Node.” <http://www.etinternational.com/index.php/products/swarmbeta>.
- [62] G. Aupy, M. Faverge, Y. Robert, J. Kurzak, P. Luszczek, and J. Dongarra, “Implementing a systolic algorithm for QR factorization on multicore clusters with PaRSEC,” in *PROPER 2013 - 6th Workshop on Productivity and Performance*, (Aachen, Germany), Aug. 2013.
- [63] F. Schlimbach, “Distributed CnC for C++,” in *2nd Annual Workshop for Concurrent Collections*, (Houston, TX), 2010.

- [64] C. Fu and T. Yang, “Run-time Techniques for Exploiting Irregular Task Parallelism on Distributed Memory Architectures,” *Journal of Parallel and Distributed Computing*, vol. 42, pp. 143–156, 1997.
- [65] Y. Jégou, “Task migration and fine grain parallelism on distributed memory architectures,” in *Parallel Computing Technologies* (V. Malyskin, ed.), vol. 1277 of *Lecture Notes in Computer Science*, pp. 226–240, Springer Berlin / Heidelberg, 1997.
- [66] S. Ramaswamy, S. Sapatnekar, and P. Banerjee, “A framework for exploiting task and data parallelism on distributed memory multicomputers,” *Parallel and Distributed Systems, IEEE Transactions on*, vol. 8, pp. 1098 –1116, nov 1997.
- [67] E. Allan, D. Chase, J. Hallett, V. Luchangco, J.-W. Maessen, S. Ryu, G. L. S. Jr., and S. Tobin-Hochstadt, “The Fortress Language Specification Version 1.0,” technical report, Sun Microsystems, 2008.
- [68] R. Chandra, L. Dagum, D. Kohr, D. Maydan, J. McDonald, and R. Menon, *Parallel Programming in OpenMP*. San Francisco, CA, USA: Morgan Kaufmann Publishers Inc., 2001.
- [69] B. Chapman, G. Jost, and R. v. d. Pas, *Using OpenMP: Portable Shared Memory Parallel Programming (Scientific and Engineering Computation)*. The MIT Press, 2007.
- [70] J. Reinders, *Intel Threading Building Blocks*. Sebastopol, CA, USA: O’Reilly & Associates, Inc., first ed., 2007.

- [71] V. Cavé, Z. Budimlić, and V. Sarkar, “Comparing the usability of library vs. language approaches to task parallelism,” in *Evaluation and Usability of Programming Languages and Tools*, PLATEAU ’10, pp. 9:1–9:6, 2010.
- [72] Arch D. Robison, “Parallel Programming with Cilk Plus.” Tutorial at International Supercomputing Conference 2012, June 2012. http://parallelbook.com/sites/parallelbook.com/files/ISC2012_Tutorial_9_CilkPlus_Robison_final.pdf (source code available at <https://www.cilkplus.org/>).
- [73] R. D. Blumofe and C. E. Leiserson, “Scheduling Multithreaded Computations by Work Stealing,” in *Proceedings of the 35th Annual Symposium on Foundations of Computer Science*, SFCs ’94, (Washington, DC, USA), pp. 356–368, IEEE Computer Society, 1994.
- [74] OpenMP Architecture Review Board, “OpenMP Application Program Interface, Version 3.0,” May 2008. <http://www.openmp.org/mp-documents/spec30.pdf>.
- [75] V. Cavé, J. Zhao, J. Shirako, and V. Sarkar, “Habanero-Java: The New Adventures of Old X10,” in *Proceedings of the 9th International Conference on Principles and Practice of Programming in Java*, PPPJ ’11, (New York, NY, USA), pp. 51–61, ACM, 2011.
- [76] Y. Guo, R. Barik, R. Raman, and V. Sarkar, “Work-first and help-first scheduling policies for async-finish task parallelism,” in *Proceedings of the 2009 IEEE International Symposium on Parallel&Distributed Processing*, IPDPS ’09, (Washington, DC, USA), pp. 1–12, IEEE Computer Society, 2009.

- [77] S. Tasirlar and V. Sarkar, “Data-Driven Tasks and Their Implementation,” in *Proceedings of the 2011 International Conference on Parallel Processing, ICPP '11*, (Washington, DC, USA), pp. 652–661, IEEE Computer Society, 2011.
- [78] D. Chase and Y. Lev, “Dynamic circular work-stealing deque,” in *Proceedings of the seventeenth annual ACM symposium on Parallelism in algorithms and architectures, SPAA '05*, (New York, NY, USA), pp. 21–28, ACM, 2005.
- [79] R. Thakur, P. Balaji, D. Buntinas, D. Goodell, W. Gropp, T. Hoefler, S. Kumar, E. Lusk, and J. L. Traeff, “MPI at Exascale,” in *Proceedings of SciDAC 2010*, Jun. 2010.
- [80] F. Cappello and O. Richard, “Performance Characteristics of a Network of Commodity Multiprocessors for the NAS Benchmarks Using a Hybrid Memory Model,” in *Proceedings of the 1999 International Conference on Parallel Architectures and Compilation Techniques, PACT '99*, (Washington, DC, USA), pp. 108–, IEEE Computer Society, 1999.
- [81] K. Yelick, D. Bonachea, W.-Y. Chen, P. Colella, K. Datta, J. Duell, S. L. Graham, P. Hargrove, P. Hilfinger, P. Husbands, C. Iancu, A. Kamil, R. Nishtala, J. Su, M. Welcome, and T. Wen, “Productivity and performance using partitioned global address space languages,” in *Proceedings of the 2007 international workshop on Parallel symbolic computation, PASCO '07*, (New York, NY, USA), pp. 24–32, ACM, 2007.

- [82] F. Cappello and D. Etiemble, “MPI versus MPI+OpenMP on IBM SP for the NAS benchmarks,” in *Proceedings of the 2000 ACM/IEEE conference on Supercomputing*, Supercomputing ’00, (Washington, DC, USA), IEEE Computer Society, 2000.
- [83] D. Scales, K. Gharachorloo, and A. Aggarwal, “Fine-Grain Software Distributed Shared Memory on SMP Clusters,” in *Proceedings of the 4th International Symposium on High-Performance Computer Architecture*, HPCA ’98, (Washington, DC, USA), pp. 125–, IEEE Computer Society, 1998.
- [84] C. Bell, D. Bonachea, R. Nishtala, and K. Yelick, “Optimizing bandwidth limited problems using one-sided communication and overlap,” in *Proceedings of the 20th international conference on Parallel and distributed processing*, IPDPS’06, (Washington, DC, USA), pp. 84–84, IEEE Computer Society, 2006.
- [85] V. Marjanović, J. Labarta, E. Ayguadé, and M. Valero, “Overlapping communication and computation by using a hybrid MPI/SMPSs approach,” in *Proceedings of the 24th ACM International Conference on Supercomputing*, (New York, NY, USA), pp. 5–16, 2010.
- [86] R. Rabenseifner, G. Hager, and G. Jost, “Hybrid MPI/OpenMP Parallel Programming on Clusters of Multi-Core SMP Nodes,” in *Proceedings of the 2009 17th Euromicro International Conference on Parallel, Distributed and Network-based Processing*, PDP ’09, (Washington, DC, USA), pp. 427–436, IEEE Computer Society, 2009.

- [87] G. Pike and P. N. Hilfinger, “Better tiling and array contraction for compiling scientific programs,” in *Proceedings of the 2002 ACM/IEEE conference on Supercomputing*, Supercomputing ’02, (Los Alamitos, CA, USA), pp. 1–12, IEEE Computer Society Press, 2002.
- [88] D. Li, B. De Supinski, M. Schulz, K. Cameron, and D. Nikolopoulos, “Hybrid MPI/OpenMP power-aware computing,” in *Parallel Distributed Processing (IPDPS), 2010 IEEE International Symposium on*, pp. 1–12, 2010.
- [89] A. M. Aji, L. S. Panwar, F. Ji, M. Chabbi, K. Murthy, P. Balaji, K. R. Bisset, J. Dinan, W.-c. Feng, J. Mellor-Crummey, X. Ma, and R. Thakur, “On the efficacy of GPU-integrated MPI for scientific applications,” in *Proceedings of the 22nd international symposium on High-performance parallel and distributed computing*, HPDC ’13, (New York, NY, USA), pp. 191–202, ACM, 2013.
- [90] S. J. Pennycook, S. D. Hammond, S. A. Jarvis, and G. R. Mudalige, “Performance analysis of a hybrid MPI/CUDA implementation of the NASLU benchmark,” *SIGMETRICS Perform. Eval. Rev.*, vol. 38, pp. 23–29, Mar. 2011.
- [91] L. Chen, L. Liu, S. Tang, L. Huang, Z. Jing, S. Xu, D. Zhang, and B. Shou, “Unified parallel C for GPU clusters: language extensions and compiler implementation,” in *Proceedings of the 23rd international conference on Languages and compilers for parallel computing*, LCPC’10, (Berlin, Heidelberg), pp. 151–165, Springer-Verlag, 2011.
- [92] S. Potluri, D. Bureddy, H. Wang, H. Subramoni, and D. Panda, “Extending OpenSHMEM for GPU Computing,” *Parallel and Distributed Processing Symposium, International*, vol. 0, pp. 1001–1012, 2013.

- [93] J. Jose, M. Luo, S. Sur, and D. K. Panda, “Unifying UPC and MPI runtimes: experience with MVAPICH,” in *Proceedings of the Fourth Conference on Partitioned Global Address Space Programming Model*, PGAS ’10, (New York, NY, USA), pp. 5:1–5:10, ACM, 2010.
- [94] M. J. Koop, T. Jones, and D. K. Panda, “MVAPICH-Aptus: Scalable high-performance multi-transport MPI over InfiniBand,” *Parallel and Distributed Processing Symposium, International*, vol. 0, pp. 1–12, 2008.
- [95] R. Barik, J. Zhao, D. Grove, I. Peshansky, Z. Budimlić, and V. Sarkar, “Communication Optimizations for Distributed-Memory X10 Programs,” in *IPDPS’11: Proceedings of the 2011 IEEE International Symposium on Parallel&Distributed Processing*, pp. 1101–1113, IEEE, 2011.
- [96] D. J. Quinlan *et al.*, “ROSE compiler framework.” <http://www.rosecompiler.org>.
- [97] C. Huang, O. Lawlor, and L. V. Kalé, “Adaptive MPI,” in *Proceedings of the 16th International Workshop on Languages and Compilers for Parallel Computing (LCPC 2003)*, LNCS 2958, (College Station, Texas), pp. 306–322, October 2003.
- [98] R. Thakur and W. Gropp, “Test Suite for Evaluating Performance of Multi-threaded MPI Communication,” *Parallel Comput.*, vol. 35, pp. 608–617, Dec. 2009.

- [99] S. Olivier, J. Huan, J. Liu, J. Prins, J. Dinan, P. Sadayappan, and C.-W. Tseng, “UTS: An Unbalanced Tree Search Benchmark,” in *Proceedings of the 19th International Conference on Languages and Compilers for Parallel Computing*, LCPC’06, (Berlin, Heidelberg), pp. 235–250, Springer-Verlag, 2007.
- [100] J. Dinan, S. Olivier, G. Sabin, J. Prins, P. Sadayappan, and C.-W. Tseng, “Dynamic Load Balancing of Unbalanced Computations Using Message Passing,” *International Parallel and Distributed Processing Symposium*, vol. 0, p. 391, 2007.
- [101] P. Sadayappan, J. Dinan, G. Sabin, *et al.*, “The Unbalanced Tree Search Benchmark.” <http://sourceforge.net/p/uts-benchmark/home/Home/>.
- [102] S. Ahuja, N. Carriero, and D. Gelernter, “Linda and Friends,” *Computer*, vol. 19, pp. 26–34, Aug. 1986.
- [103] P. Husbands and K. Yelick, “Multi-threading and One-sided Communication in Parallel LU Factorization,” in *Proceedings of the 2007 ACM/IEEE Conference on Supercomputing*, SC ’07, (New York, NY, USA), pp. 31:1–31:10, ACM, 2007.
- [104] M. Frigo and V. Strumpen, “Cache Oblivious Stencil Computations,” in *Proceedings of the 19th Annual International Conference on Supercomputing*, ICS ’05, (New York, NY, USA), pp. 361–366, ACM, 2005.
- [105] K. Datta, *Auto-tuning Stencil Codes for Cache-Based Multicore Platforms*. PhD thesis, EECS Department, University of California, Berkeley, Dec 2009.

- [106] Y. Tang, R. A. Chowdhury, B. C. Kuszmaul, C.-K. Luk, and C. E. Leiserson, “The Pochoir Stencil Compiler,” in *Proceedings of the 23rd ACM Symposium on Parallelism in Algorithms and Architectures*, SPAA ’11, (New York, NY, USA), pp. 117–128, ACM, 2011.
- [107] V. Sarkar, “Synchronization Using Counting Semaphores,” in *Proceedings of the 2nd International Conference on Supercomputing*, ICS ’88, (New York, NY, USA), pp. 627–637, ACM, 1988.
- [108] N. Vasudevan, O. Tardieu, J. Dolby, and S. A. Edwards, “Compile-Time Analysis and Specialization of Clocks in Concurrent Programs,” in *Proceedings of the 18th International Conference on Compiler Construction: Held As Part of the Joint European Conferences on Theory and Practice of Software, ETAPS 2009*, CC ’09, (Berlin, Heidelberg), pp. 48–62, Springer-Verlag, 2009.
- [109] Java Community Process, “Java 7 Phaser (Java Platform, Standard Edition 7 API Specification).” <http://docs.oracle.com/javase/7/docs/api/java/util/concurrent/Phaser.html>.
- [110] M. L. Scott and J. M. Mellor-Crummey, “Fast, contention-free combining tree barriers for shared-memory multiprocessors,” *Int. J. Parallel Program.*, vol. 22, pp. 449–481, Aug. 1994.
- [111] A. Krishnamurthy, D. E. Culler, A. Dusseau, S. C. Goldstein, S. Lumetta, T. von Eicken, and K. Yelick, “Parallel programming in Split-C,” in *Proceedings of the 1993 ACM/IEEE Conference on Supercomputing*, pp. 262 – 273, 1993.

- [112] J. Shirako and V. Sarkar, “Hierarchical Phasers for Scalable Synchronization and Reduction,” in *IPDPS '10: Proceedings of the 2010 IEEE International Symposium on Parallel&Distributed Processing*, (Washington, DC, USA), pp. 1–12, IEEE Computer Society, 2010.
- [113] J. M. Bull, F. Reid, and N. McDonnell, “A Microbenchmark Suite for OpenMP Tasks,” in *Proceedings of the 8th International Conference on OpenMP in a Heterogeneous World, IWOMP'12*, (Berlin, Heidelberg), pp. 271–274, Springer-Verlag, 2012. (Available at <http://www.epcc.ed.ac.uk/research/computing/performance-characterisation-and-benchmarking/epcc-openmp-micro-benchmark-suite>).
- [114] J. D. Cuvillo, W. Zhu, Z. Hu, and G. R. Gao, “TiNy Threads: A Thread Virtual Machine for the Cyclops64 Cellular Architecture,” in *IPDPS '05: Proceedings of the 19th IEEE International Parallel and Distributed Processing Symposium (IPDPS'05)*, (Washington, DC, USA), p. 265.2, IEEE Computer Society, 2005.
- [115] J. Shirako, D. M. Peixotto, V. Sarkar, and W. N. Scherer, “Phaser Accumulators: A New Reduction Construct for Dynamic Parallelism,” in *Proceedings of the 2009 IEEE International Symposium on Parallel&Distributed Processing, IPDPS '09*, (Washington, DC, USA), pp. 1–12, IEEE Computer Society, 2009.
- [116] Y. Yan, S. Chatterjee, D. A. Orozco, E. Garcia, Z. Budimlić, J. Shirako, R. S. Pavel, G. R. Gao, and V. Sarkar, “Hardware and Software Tradeoffs for Task Synchronization on Manycore Architectures,” in *Proceedings of the 17th International Conference on Parallel Processing - Volume Part II, Euro-Par'11*, (Berlin, Heidelberg), pp. 112–123, Springer-Verlag, 2011.